



PONTIFICIA UNIVERSIDAD CATOLICA DE CHILE
SCHOOL OF ENGINEERING

SALT REDUCTION IN FOODS: EFFECT OF CRYSTAL MICROSTRUCTURE ON THE DISSOLUTION KINETICS

MARCELA CRISTINA QUILAQUEO GUTIÉRREZ

Thesis submitted to the Office of Graduate Studies in partial fulfillment of
the requirements for the Degree of Doctor in Engineering Sciences

Advisor:

JOSÉ MIGUEL AGUILERA

Santiago de Chile, August, 2016

© 2016, Marcela Quilaqueo Gutiérrez



PONTIFICIA UNIVERSIDAD CATOLICA DE CHILE
SCHOOL OF ENGINEERING

SALT REDUCTION IN FOODS: EFFECT OF CRYSTAL MICROSTRUCTURE ON THE DISSOLUTION KINETICS

MARCELA CRISTINA QUILAQUEO GUTIÉRREZ

Members of the Committee:

JOSÉ MIGUEL AGUILERA R.

FRANCO PEDRESCHI P.

CÉSAR SÁEZ N.

VALERIO BIFANI C.

LISA DUIZER

CRISTIÁN VIAL E.

Thesis submitted to the Office of Graduate Studies in partial fulfillment of
the requirements for the Degree of Doctor in Engineering Sciences

Santiago de Chile, August, 2016

© 2016, Marcela Quilaqueo Gutiérrez

Dedicado a mi amado Yeison, a mi madre y a mi hermana, quienes son mi apoyo y motor en la vida.

AGRADECIMIENTOS

Quisiera agradecer a todos quienes han estado conmigo y han contribuido con su granito de arena para poder llegar al final de esta etapa. Primero que todo agradezco a Dios, quien ha guiado mi camino todo este tiempo y me ha acompañado.

A mi madre Anita, a mi hermana María Paz y a mi tía Ruth por apoyarme siempre en todos mis planes, por darme ánimo cuando lo necesité, por confiar en mí, por acompañarme aunque estuviera lejos y por ser la motivación de avanzar en la vida. A mi compañero de vida Yeison, por haberme apoyado desde el principio, aun cuando ningún plan era seguro, por tener la paciencia de escuchar de las buenas y malas experiencias, y por esperarme.

A quienes han sido mi familia Santiaguina, Genoveva, Ricardo, Kathy, Jonatan, Paula, Cristóbal, Toven, Gabriel, Juanito, por haberme dado su amistad, compañía y momentos inolvidables. A mis amigas que desde la semi-distancia siempre estuvieron presente con su amistad y apoyo, Lorena y Romina.

A mis compañeros de laboratorio, Catalina, Loreto, Javiera, Gabriel, Ross, con quienes más que ser colegas fuimos amigos, por haber tenido siempre la voluntad de escuchar y orientar mis teorías científicas y de la vida. A Mane quien siempre ha estado dispuesta a solucionar los problemas de gestión académica.

Al profesor José Miguel, por haberme dado la oportunidad de formar parte de su equipo, por su tiempo en las correcciones y por todo lo que me ha enseñado. Al profesor Valerio, porque desde antes de comenzar esta etapa ya me apoyaba, junto con la profesora Mónica, y lo ha seguido haciendo hasta ahora. A la profesora Lisa, quien me recibió en

su laboratorio para trabajar con ella. Sin duda me permitió crecer mucho en el ámbito profesional y personal. A los profesores que integran la comisión de evaluación, César, Franco y Cristián, por su tiempo y dedicación.

Finalmente agradezco a CONICYT que me dio el apoyo financiero para la realización del presente trabajo, a través de la Beca de Doctorado Nacional, de la Beca de Gastos Operacionales y de la Beca de Apoyo para la Realización de Pasantías Doctorales.

TABLE OF CONTENTS

DEDICATORIA.....	iii
AGRADECIMIENTOS	iv
LIST OF TABLES	x
LIST OF FIGURES.....	xii
ABSTRACT	xiv
RESUMEN	xvii
LIST OF PAPERS.....	xx
1. INTRODUCTION: ADVANCES IN REDUCTION OF SODIUM ADDED TO FOODS	1
1.1. Introduction.....	1
1.2. Why is it necessary to reduce the dietary sodium?.....	7
1.3. Salt in foods	7
1.3.1 Effect of salt in food preservation	8
1.3.2 Effect of salt in saltiness.....	9
1.3.3 Salt as functional ingredient.....	10
1.4. Strategies for sodium reduction in foods	11
1.4.1 Cognitive mechanisms	11
1.4.2 Chemical mechanisms.....	13
1.4.3 Product structure design	15
1.4.3.1. Interaction of sodium with the food matrix.....	16
1.4.3.2. Distribution of salt across the food matrix.....	17
1.4.3.3. Dissolution of salt crystals	18
1.5. Advances in sodium reduction in different food products.....	23
1.5.1. Bread	23
1.5.2. Meat products.....	24
1.5.3 Cheese	25
1.5.4 Soups	26

1.5.5 Snacks.....	27
1.6. Perspectives	28
1.7. Hypothesis and objectives of this thesis	28
1.8. Outline	29
References.....	31
2. DISSOLUTION OF NaCl CRYSTALS IN ARTIFICIAL SALIVA AND WATER BY VIDEO-MICROSCOPY	39
2.1. Introduction.....	39
2.2. Materials and methods	42
2.2.1. Samples	42
2.2.2. Elaboration of artificial saliva	43
2.2.3. Viscosity of artificial saliva.....	43
2.2.4. Determination of moisture content.....	44
2.2.5 Determination of insoluble material.....	44
2.2.6. Scanning electron microscopy (SEM) and energy dispersive spectroscopy (EDS)	44
2.2.7. Porosity.....	44
2.2.8. Kinetics of dissolution of single crystals.....	45
2.2.9. Statistical analysis	47
2.3. Results.....	47
2.3.1 Viscosity of artificial saliva.....	47
2.3.2. Chemical and physical characterization of crystals	48
2.3.3. Dissolution kinetics of single crystals	52
2.4. Conclusions.....	59
Acknowledgments	60
References.....	61
3. THE MORPHOLOGY OF SALT CRYSTALS AFFECTS THE PERCEPTION OF SALTINESS	65
3.1. Introduction.....	65
3.2. Materials and methods	67
3.2.1 Materials.....	67
3.2.2 Salt characterization	67
3.2.2.1 Mineral analysis	67

3.2.2.2	Moisture content.....	68
3.2.2.3	Apparent density	68
3.2.2.4	Scanning electron microscopy and micro computed tomography	68
3.2.2.5	Optical microscopy	69
3.2.3	Crystal dissolution in artificial saliva by video-microscopy	69
3.2.4	Sensory evaluation	70
3.2.5	Statistical analysis	72
3.3.	Results and discussion	73
3.3.1	Salt characterization	73
3.3.2	Crystal dissolution in artificial saliva through video-microscopy ..	78
3.3.3	Sensory evaluation	80
3.4.	Conclusions.....	85
	Acknowledgments	86
	References.....	87
4.	CRYSTALLIZATION OF NaCl BY FAST EVAPORATION OF WATER IN DROPLETS OF NaCl SOLUTIONS	89
4.1.	Introduction.....	89
4.2.	Materials and methods	91
4.2.1.	Materials.....	91
4.2.2.	Crystallization process	91
4.2.3.	Salt characterization	93
4.2.3.1.	Size and shape measurements	93
4.2.3.2.	Scanning electron microscopy (SEM).....	94
4.2.3.3.	Color determination.....	94
4.2.3.4.	Thermogravimetric analysis	94
4.2.3.5.	X-ray diffraction (XRD).....	95
4.2.3.6.	Moisture content.....	95
4.2.3.7.	Salt dissolution in artificial saliva	95
4.2.4.	Statistical analysis	96
4.3.	Results and discussion	96
4.3.1.	Size and shape of crystals.....	97
4.3.2.	Color of crystals	102
4.3.3.	Thermogravimetric measurements, X-ray diffraction and moisture content of crystals of two selected fast drying conditions	104

4.3.4. Salt dissolution in artificial saliva of crystals of two selected fast drying conditions	107
4.4. Conclusions.....	110
Acknowledgments	110
References.....	111
5. CONCLUSIONS AND FUTURE PROSPECTS.....	114

LIST OF TABLES

Table 1.1. Differences of sodium content between some natural foods and their processed counterparts.....	4
Table 1.2. Sodium content of some of processed foods and target values	6
Table 2.1. Description and nomenclature of commercial salts.....	42
Table 2.2. Characteristics of salt particles studied	48
Table 2.3. Area and shape parameters for single crystals before dissolution.....	52
Table 2.4. Rate constants of dissolution kinetics ($K \cdot 10^{-4}$ values in s^{-1}) of the different commercial salts. K_0 were calculated for samples RSA, RSB, RSC and SSA, while K_1 was calculated for samples of SSB salt after fitting data to a zero and first order kinetic models, respectively	54
Table 3.1. Description of commercial salts analyzed and amount of salt containing 20 mg of sodium (used for sensory testing).....	67
Table 3.2. Mean values of minerals present in salts studied	74
Table 3.3. Characteristics of salt particles studied	75
Table 3.4. Projected area and shape parameters for salt crystals	78
Table 3.5. Model adjusted to area reduction, rate constants (K values in s^{-1}), coefficient of determination ranges (R^2), and total dissolution time (s) of crystals analyzed.....	79
Table 3.6. Mean values of time intensity curve parameters of salts studied	82
Table 4.1. Equivalent diameter (μm) and circularity of microcrystals.....	98

Table 4.2. Color values of salt microcrystals	103
Table 4.3. Characteristics of LC and SC microcrystals, and original pure salt	105

LIST OF FIGURES

Figure 1.1. Morphologies of salt crystals obtained by different crystallization conditions: (a) SEM and optical microscopy images of crystals, and (b) photo images and their respective X-ray diffraction pattern	22
Figure 2.1. System for the <i>in situ</i> observation of dissolution of each salt crystal	46
Figure 2.2. Scanning electron photomicrographs of representative crystals: (a) RSA, (b) RSB, (c) RSC, (d) SSA, and (e) SSB	50
Figure 2.3. (a) Representative dissolution curves of single salt crystals of different samples dissolved at 36 °C in AS-Mu, and; (b) microscopy images for the sequence of the dissolution	53
Figure 2.4. Behavior of crystals during dissolution. (a) Percentage of fractionated crystals of different salts (n = 60 per salt type). (b) Representative image sequences of dissolution of a salt crystal in water at 25 °C, that is not fragmented (RSA) and another that is fragmented (SSB).....	56
Figure 2.5. Average dissolution time (pooled values of all data) of salt crystals from different commercial salts and effect of solution type and temperature	58
Figure 3.1. Time-intensity parameters extracted for curve	72
Figure 3.2. SEM images and micro-CT images of cross-section (last column) of crystals	77
Figure 3.3. Area reduction (%) of one representative crystal of each salt type	79
Figure 3.4. Average time-intensity curves of different salts	81
Figure 4.1. Scheme of the experimental set-up used to form salt microcrystals. The brine droplets were added to the beaker with olive oil using a syringe. The beaker was maintained inside the thermoregulated bath filled with silicone oil to control the temperature	92
Figure 4.2. Size distribution of salt microcrystals at different oil temperatures	99

Figure 4.3. SEM images of microcrystals obtained by fast water evaporation from droplets of salt solutions as a function of oil temperature, salt concentration and droplet size (S, small; L, large).....	100
Figure 4.4. Thermograms from the TGA measurements of LC and SC microcrystals, original NaCl, and olive oil.....	104
Figure 4.5. Dissolution in artificial saliva (20 °C) of LC and SC microcrystals and original salt	108
Figure 4.6. Original salt crystals: (a) SEM image, and (b) size distribution obtained from image analysis of 100 crystals	108

PONTIFICIA UNIVERSIDAD CATOLICA DE CHILE
SCHOOL OF ENGINEERING

**SALT REDUCTION IN FOODS: EFFECT OF CRYSTAL
MICROSTRUCTURE ON THE DISSOLUTION KINETICS**

Thesis submitted to the Office of Research and Graduate Studies in partial fulfillment
of the requirements for the Degree of Doctor in Engineering Sciences by

MARCELA C. QUILAQUEO

ABSTRACT

A high sodium intake through table salt (NaCl) added to foods has been linked with the risk of several diseases, such as hypertension and cardiovascular diseases. The main source of sodium in the diet comes from processed foods, hence several strategies for reducing salt in foods are being developed by industry. Among these strategies, the optimization of delivery salt ions in the mouth has been less studied. The aim of this thesis was to determine the influence of the microstructure of salt crystals on their dissolution rate in water and artificial saliva and its correlation with saltiness perception.

In the first part, it compares the dissolution of five commercial salts in deionized water and two formulations of artificial saliva, at four temperatures and in the absence of agitation. Salt dissolution was quantified *in vitro* by analysis of video-microscopy images taken at different times. Higher dissolution rates of salt crystals were found in water than in artificial saliva, and at higher temperatures. Video-microscopy was instrumental to reveal that some crystals were fragmented during dissolution while others remained as a unit of diminishing size until complete solubilization. Increased surface area after fragmentation led to pyramid-shape crystals having the highest dissolution rates. Hence, significant changes can be achieved in the dissolution of salt depending on the crystal structure and its dissolution pattern.

In the second part, the aim was to study the dissolution of salt crystals with different morphologies in artificial saliva and to correlate the findings with the perception of saltiness over time. The morphology of five commercial salts was analyzed by scanning electron microscopy and micro computed tomography (micro-CT) studies. Shape parameters of crystals were determined using images from optical microscope. Crystal dissolution in artificial saliva was evaluated using video-microscopy and the perception of saltiness was evaluated using sensorial test of time-intensity at standardized sodium content. Salt morphology was correlated well with dissolution rate and certain time-intensity parameters (time to maximum intensity, intensity at maximum and increase angle). Non-cubic and agglomerated crystals, such as Kosher and Maldon salts, were dissolved faster (dissolution rate up to 3.8 times higher) and experienced maximum saltiness (up to 17 % more) at shorter times (up to 40% less). Crystal morphology may be a variable to consider to achieve sodium reduction while maintaining salt intensity.

In the final part, a new methodology to obtain salt as microcrystals was developed. The crystallization of salt by fast water evaporation from droplets of saline solutions within a hot oil phase was evaluated. The effects of the oil temperature (150; 165 and 180°C), droplet volume (17 and 42 μL) and brine concentration (15 and 26% w/v) were studied. Highly crystalline particles with mean sizes between 9 and 23 μm , and containing about 2% of remaining oil were obtained. The crystal size decreased by increasing the oil temperature, solution concentration and volume of the droplets. The dissolution rate of these microcrystals was more than 2 times faster than that of the original crystals. In conclusion, agglomerated, flat or pyramidal structures and microcrystals have a high superficial area allowing a fast dissolution in saliva, hence a high saltiness perception. These types of salt crystals could be preferentially exploited in surface-salted or coated foods, i.e., snacks, salads, etc.

Members of the Doctoral Thesis Committee:

José Miguel Aguilera R.

Franco Pedreschi P.

César Sáez N.

Valerio Bifani C.

Lisa Duizer

Cristián Vial E.

Santiago, August, 2016

PONTIFICIA UNIVERSIDAD CATOLICA DE CHILE
ESCUELA DE INGENIERIA

**REDUCCIÓN DE SAL EN ALIMENTOS: EFECTO DE LA
MICROESTRUCTURA DEL CRISTAL EN LA CINÉTICA DE DISOLUCIÓN**

Tesis enviada a la Dirección de Investigación y Postgrado en cumplimiento parcial de los requisitos para el grado de Doctor en Ciencias de la Ingeniería.

MARCELA CRISTINA QUILAQUEO GUTIÉRREZ

RESUMEN

Un alto consumo de sodio, a través de la sal (NaCl) agregada a los alimentos ha sido relacionado con el riesgo de desarrollar diversas enfermedades incluyendo hipertensión y enfermedades cardiovasculares. La principal fuente de sodio en la dieta es la que viene en los alimentos procesados, por lo que diversas estrategias para la reducción de sal en alimentos han sido desarrolladas por la industria. Entre estas estrategias, la optimización de la liberación de los iones de sal en la boca ha sido poco estudiada. El objetivo de la presente tesis fue determinar la influencia de la microestructura de los cristales de sal en su índice de disolución en agua y saliva artificial y su correlación con la percepción de salinidad.

Esta tesis está dividida en tres partes. En la primera parte se compara la disolución de cinco sales comerciales en agua desionizada y dos formulaciones de saliva artificial, a cuatro temperaturas y en ausencia de agitación. La disolución de la sal fue cuantificada *in vitro* mediante el análisis de imágenes obtenidas por video-microscopía a diferentes tiempos. Los índices de disolución fueron mayores en agua que en saliva artificial y, a mayores temperaturas. La video-microscopía fue un instrumento que reveló que algunos cristales se fragmentaron durante su disolución, mientras otros permanecieron como una unidad que disminuyó su tamaño hasta su completa solubilización. El aumento del área superficial dio lugar a que los cristales de forma piramidal tuviesen los mayores índices de disolución. Por consiguiente, cambios significativos pueden ser

logrados en la disolución de la sal dependiendo de la estructura del cristal y su patrón de disolución.

En la segunda parte, el objetivo fue estudiar la disolución de cristales de sal con diferentes morfologías en saliva artificial y correlacionar los resultados con la percepción de salinidad sobre el tiempo. La morfología de cinco sales comerciales fue analizada a través de microscopía electrónica de barrido y microtomografía computarizada. Los parámetros de forma de los cristales fueron determinados utilizando imágenes de microscopía óptica. La disolución de los cristales en saliva artificial fue evaluada a través de video-microscopía y la percepción de la salinidad fue evaluada a través de la prueba sensorial de tiempo-intensidad a un contenido de sodio estandarizado. La morfología de la sal fue correlacionada con el índice de disolución y ciertos parámetros de tiempo-intensidad (tiempo a intensidad máxima, intensidad máxima y, ángulo de aumento). Cristales no cúbicos y aglomerados, tales como los de las sales Kosher y Maldon, fueron disueltos más rápido (índice de disolución hasta 3,8 veces mayor) y tuvieron la salinidad máxima (hasta 17% más) a menores tiempos (hasta un 40% menos). La morfología de los cristales puede ser una variable a considerar en la reducción de sodio manteniendo la intensidad de salado.

En la parte final se desarrolló una nueva metodología para obtener sal como microcristales. La cristalización de la sal por evaporación rápida del agua de gotas de solución salina dentro de una fase de aceite caliente fue evaluada. Los efectos de la temperatura del aceite (150; 165 y 180°C), del volumen de la gota (17 y 42 μL) y de la concentración de la salmuera (15 y 26% w/v) fueron estudiados. Partículas altamente cristalinas con tamaños medios entre 9 y 23 μm y con alrededor del 2% de aceite remanente fueron obtenidas. El tamaño del cristal disminuyó con el aumento de la temperatura, de la concentración de la solución y del volumen de las gotas. La tasa de disolución de los microcristales fue más del doble que la de los cristales originales.

En conclusión, estructuras aglomeradas, planas o piramidales y microcristales tienen una alta área superficial permitiendo una rápida disolución en la saliva y así una alta percepción de salinidad. Este tipo de cristales de sal pueden ser preferencialmente aplicados en alimentos que utilizan sal en su superficie, tales como snacks, ensaladas, etc.

Miembros de la Comisión de Tesis Doctoral

José Miguel Aguilera R.

Franco Pedreschi P.

César Sáez N.

Valerio Bifani C.

Lisa Duizer

Cristián Vial E.

Santiago, Agosto, 2016

LIST OF PAPERS

This thesis is based on the following papers:

- **Chapter 2:** Quilaqueo, M. & Aguilera, J.M. Dissolution of NaCl crystals in artificial saliva and water by video-microscopy. *Food Research International*, 69, 373–380, 2015.
- **Chapter 3:** Quilaqueo, M., Duizer, L. & Aguilera, J.M. The morphology of salt crystals affects the perception of saltiness. *Food Research International*, 76, 675-681, 2015.
- **Chapter 4:** Quilaqueo, M. & Aguilera, J.M. Crystallization of NaCl by fast evaporation of water in droplets of NaCl solutions. *Food Research International*, 84, 143- 149, 2016.

1. INTRODUCTION: ADVANCES IN REDUCTION OF SODIUM ADDED TO FOODS

1.1. Introduction

Sodium chloride (NaCl), commonly named salt, has played an important role in foods through the ages. One of the first written references to salt, is founded in the Bible where Job wonders: can something tasteless be eaten without salt? (Aguilera, 2012; Morton Salt, 1995). As far as 5000 years ago, the Chinese already used salt to preserve foods and the product gained economic significance mainly because of its scarcity (He & MacGregor, 2010).

Common table salt is obtained from underground rock salt deposits, sea water or natural brines (Codex Alimentarius, 1985). Underground deposits are drilled to mine the rock salt, which is later purified as required (Abu-Khader, 2006; Morton Salt, 1995). Salt crystals from sea water or natural brines are obtained by evaporating the water. The size and shape of salt crystals depend on evaporation conditions, i.e. evaporation rate and substrate characteristics (Busch, Yong & Goh, 2012; Vázquez et al., 2015). Trace elements may remain in the crystals depending on their origin and probably also on their differences in the drying conditions. Minerals such as calcium, magnesium and potassium have been found in rock salts, while magnesium, calcium, sulfur, potassium, iron, copper, fluorine, molybdenum, phosphorous, iodine, manganese, zinc and cobalt are usually present in sea salts (Drake & Drake, 2011).

The purity of food grade salt should be at least 97 % on a dry matter basis, exclusive of additives (Codex Alimentarius, 1985). Commercial salts may contain iodine added to

prevent iodine deficiency leading to brain damage, and anticaking agents such as sodium ferrocyanide or silicon dioxide to pick up free moisture which leads to agglomeration or caking (Drake & Drake, 2011).

Human salt intake has varied widely through ages. Due to the importance of salt in food preservation, salt became one of the most traded commodities in the world, reaching a peak around the 1870s. Later, salt intake decreased with the development of new food preservation technologies. However, with the recent significant increase in the consumption of highly salted processed foods (e.g., snacks), salt intake has augmented again (He & MacGregor, 2010). Today, per capita salt consumption in the world is between 5 and 17 g of salt per day (Brown, Tzoulaki, Candeias & Elliot, 2009). The global mean salt intake in 2010 was estimated in 10 g per day, equivalent to 3.9 g of sodium per day (Powles et al., 2013; WHO, 2014). However, the recommendation of salt intake is less than 5 g per day for adults (≥ 16 years old) and for children the maximum level should be adjusted downwards based on the energy requirements relative to those of adults (WHO, 2012). Sodium content of salt is approximately 40% by weight, hence 1 g of salt = 0.4 g of sodium.

The sodium occurs naturally in foods, but also comes from processed or restaurant-prepared foods with added salt, and from discretionary use of salt at home or at the table. The sodium naturally present in foods is between 10 and 12% of the total dietary sodium and less than 1% comes from water. In the diets of high-income European and Northern American populations over 75% of the sodium intake comes in the form of added salt from processed, pre-prepared and ready-made foods. Discretionary salt added at home when cooking or at the table represents between 10-20% of the total dietary sodium in European countries and in the U.S, where around 5 % is added when

cooking and 6% at the table in the U.S. (Brown et al., 2009; Sebastian, Enns, Steinfeldt, Goldman & Moshfegh, 2012). However, in developing countries the sodium intake comes mainly from salt added when cooking. For example, in China a 72% of sodium comes from salt added during cooking and 8% from soy sauce (Brown et al., 2009). It is worth noting that many developing countries are currently exhibiting a transition in terms of diets, with an increase in consumption of highly-salted prepared foods (Legowski & Legetic, 2011).

It is during processing or preparation of foods that most of the salt or sodium is added. Table 1.1 exhibits the differences in the sodium content of some natural foods and their processed counterparts. For example, canned chick peas contain up to 44 times the sodium content of the raw legume. Another example are pickles that contain 604 times the sodium amount of the fresh cucumber (Table 1.1). Also, differences have been reported between home-made and ready-to-eat foods, for instance, takeaway cheeseburgers and chips contain up to 13.5 times the sodium content of home-made steaks and chips (Brown et al., 2009). Bread, some cheeses, snacks, pickled vegetables, processed meats and sauces are foods with high sodium content, and obvious targets for salt reduction (Tables 1.1 and 1.2).

The purpose of this chapter is to review the importance of salt intake reduction and advances achieved so far with special emphasis on microstructural aspects of foods. First, the importance of salt reduction for human health and the motivation of the food industry to reduce the salt added to foods are presented. Then, the purpose of incorporating salt in foods, strategies developed for its reduction, and applications of these approaches to some specific foods are reviewed. Finally, the scope and objectives of this thesis are exposed.

Table 1.1. Differences of sodium content between some natural foods and their processed counterparts.

Food	Sodium content (mg/100 g)
Almonds	
Raw	1 ^c
Dry roasted, salted	498 ^c
Bakery products	
Wheat flour	2 ^c
White bread	478 ^c
Soda cookies	660 ^b
Crackers, standard snack-type, regular	726 ^c
Pretzels, salted	1240 ^c
Beef	
Topside, roast, lean and fat	48 ^a
Gravy, canned, ready-to-serve	560 ^c
Corned beef, canned	950 ^a
Bran	
Bran, wheat	28 ^a
Bran flakes	1001 ^a
Chick peas	
Dried, boiled in unsalted water	5 ^a
Canned, re-heated, drained	221 ^a
Chicken	
Raw	60 ^c
Chicken fingers, from kid's menu	809 ^c
Frankfurter, chicken	1027 ^c
Soup, chicken broth, ready-to-serve	371 ^c
Soup, ramen noodle, chicken flavor, dry	1923 ^c
Chicken broth bouillon dry	23875 ^d
Corn	
Raw	15 ^c
Tortilla chips	328 ^c
Corn flakes crumb	638 ^c
Extruded snacks	1022 ^c
Cucumber	
Raw	2 ^c
Pickles, sour	1208 ^c
Dairy products	
Milk	59 ^b
Butter, salted	642 ^c
Fresh cheese	265 ^b
Camembert cheese	842 ^c
Parmesan cheese	1376 ^c
Roquefort cheese	1809 ^c

Food	Sodium content (mg/100 g)
Onion	
Raw	4 ^c
Crunchy onion rings	833 ^c
Peas	
Raw	4 ^b
Canned, seasoned	254 ^c
Peanuts	
Plain	2 ^a
Dry toasted	789 ^a
Potatoes	
Raw	7 ^b
Chips (risps)	595 ^b
Salmon	
Raw, steamed	110 ^a
Canned	570 ^a
Smoked	1879 ^a
Tomato	
Raw	3 ^b
Tomato sauce	740 ^b
Ketchup	907 ^c

^aBrown et al. (2009)

^bSchmidt-Hebbel, Pennacchiotti, Masson & Mella (1990)

^cUSDA (2015)

Table 1.2. Sodium content of some of processed foods and target values.

Food	Sodium content ^a		
	Range	Mean	Target
Bread			
White	250-600	461	400
Whole-meal	243-535	449	400
Marraqueta ^b	-	831	400
Meat products			
Bacon	950-1,950	1243	1150
Sausages and hot dog	229-2157	825	450
Sliced meat	120-1720	1042	500
Salami	480-3300	1273	700
Burgers	55-1046	480	300
Canned meat	310-1179	686	500
Soups	13 – 640	304	290
Cheeses			
Hard	24-1740	738	750
Soft	32-1900	549	300
Processed	520-1875	1402	900
Snack foods			
Potato crisps	30-1404	641	650
Extruded snacks	364-1880	1085	1000

^aValues corresponding to Australian foods assigned by The United Kingdom Food Standards Agency (UK FSA) (Webster, Dunford & Neal, 2010)

^bValue corresponding to Chilean bread assigned by The Ministry of Health (Valenzuela et al., 2013)

1.2. Why is it necessary to reduce the dietary sodium?

Sodium is the main cation of the extracellular fluid in the human body and its intake is essential. Sodium contributes to the mechanism of blood pressure regulation, transport of intracellular water, regulation of osmotic pressure and transmission of nerve impulses (Cruz et al., 2011; Kaplan, 2000). The physiological need of sodium in adults is around 184–230 mg per day which could be supplied by a normal intake of vegetables and water. Excess ingested sodium is excreted via the kidneys, with only a small amount lost by other routes such as perspiration. The human organism is, however, incapable of excreting via the kidneys-pathway large quantities (excess) of sodium (Dahl, 1972; Elliott & Brown, 2006).

Numerous studies show that a high salt intake is related to several diseases such as hypertension, cardiovascular diseases, renal dysfunction, nephrolithiasis, osteoporosis, stroke, proteinuria, cataracts, diabetes, and gastric cancer (Dahl, 1972; D'Elia, Rossi, Ippolito, Cappuccio & Strazzullo, 2012; He, Marrero & MacGregor, 2008; Zacarías et al., 2011). It has also been suggested that a high salt intake may be indirectly linked with obesity (He, Marrero & MacGregor, 2008).

1.3. Salt in foods

Salt is added to foods to aid in preservation, impart saltiness, and as a functional ingredient to improve texture and increase the release of volatile compounds. The effects of salt in foods are presented in the following sections.

1.3.1 Effect of salt in food preservation

Salt has been used in foods as a preservative to inhibit the multiplication of pathogenic microorganisms. Due to its ability to decrease water activity, salt exerts a drying effect on foods and microorganisms. The cell membrane of microorganisms allows the passage of water in and out of the cell. Salt solutions with concentrations of 0.85 – 0.90 % produce an isotonic condition for non-marine microorganisms, which enables water fluxes across cell membranes in both directions. However, as the salt concentration of the outer solution increases, the water concentration becomes greater inside the cell than outside and in this case, water flows out from the cell by osmosis. This water loss causes contraction of the cell's cytoplasm, which results in growth inhibition and eventually the death of the microorganism. Different microorganisms have various degrees of tolerance to osmosis in foods. Most bacteria can be inhibited by a salt concentration of 20 % or less, however, some molds can tolerate higher levels of salt. These inhibitory effects of salt are not dependent on the pH of food, as are those of some other chemical preservatives (Jay, 2000; Potter & Hotchkiss, 1998; Tortora, Funke & Case, 2007).

New and better processing technologies and improved packaging, transport, and storage of foods have contributed to the reduction of the salt content in foods. Moreover, other types of salts, such as potassium chloride, may replace sodium chloride as an antimicrobial (Bidlas & Lambert, 2008).

1.3.2 Effect of salt in saltiness

Flavor is “the sensation produced by food taken in the mouth perceived principally by the senses of taste and smell, and also by the general pain, tactile and temperature receptors in the mouth” (deMan, 1999). Salt is added to foods primarily to give a salty taste and to enhance their palatability. Besides, salt decreases bitterness and increases sweetness, contributing to product quality and consumer acceptance (Desmond, 2006; Dötsch et al., 2009; Keast & Breslin, 2002; Saint-Eve, Lauerjat, Magnan, Déléris & Souchon, 2009).

Salty taste is a chemical stimulus that can be perceived when ions dissolved in saliva exceed the taste threshold, which for sodium chloride is between 0.016 and 0.234 g/100 g (Adams & Taylor, 2012). The time necessary for taste response is in the order of 25 milliseconds (deMan, 1999). Sodium is perceived by receptor cells located on the tongue after passing through specific ion channels in the taste buds. This leads to cell depolarization, neural transduction via nerve pathways to neurons at the base of the brain and from there to the frontal cortex via the thalamus (Rama et al., 2013). Although specific transduction mechanisms for salty compounds have not yet been determined for humans, rats express epithelial sodium channels that selectively allow the passage of sodium ions into taste tissue (McCaughey, 2007). Thus, the replacement of sodium chloride by other elements is not so simple due to the high specificity of the salt receptors for sodium (Beauchamp & Stein, 2008).

Sodium and lithium are the only elements that taste primarily salty to humans, although potassium and calcium have also a salty component in their taste (McCaughey, 2007). Salts with higher molecular weight cations and anions generally result in a bitter tasting

and a lower perceived saltiness (Murphy, Cardello & Brand, 1981). Among sodium-containing compounds, salts with larger anions produce less effective stimuli with NaCl being the saltiest (Delwiche, Halpern & Desimone, 1999; McCaughey, 2007).

1.3.3 Salt as functional ingredient

Salt imparts several functional properties to foods. Salt can modify the surface polarity of proteins, improving their binding properties. Salt itself has a water-holding capacity, defined as the ability of preventing water release from the food matrix (Chantrapornchai & McClements, 2002), which improves texture and can increase the viscosity of some foods (Desmond, 2006). Furthermore, salt helps control the microbiological flora, contributing to provide the adequate conditions for fermentation in the case of fermented foods (Hutton, 2002).

It has been pointed out that the physicochemical properties of aroma compounds and their interactions with the food components affect flavor release and perception. Salt can increase the concentration of selected volatile compounds in the vapor phase due to the salting-out effect (Flores, Gianelli, Pérez-Juan & Toldrá, 2007; Ventanas, Mustonen, Puolanne & Tuorila, 2010). In general, the release of alcohols, aldehydes and esters are affected by salt (Guichard, 2002). For example, some volatile compounds in meat products such as 2-methyl-butanal, 3-methyl-butanal, 2-pentanone, hexanal, methional, and octanal, are more readily released in the presence of salt (Flores et al., 2007).

1.4. Strategies for sodium reduction in foods

Many countries are developing guidelines and strategies to decrease salt intake. These guidelines include the following actions: implementation of campaigns through mass-media, cooperation with the food industry to reduce salt, and forcing labeling of high-salt products with warning messages. With these guidelines in practice since 1970, Finland was able to reduce the individual salt intake from 12 g per day in 1979 to less than 9 g per day in 2002, which coincided with a parallel decrease of the death rate from cardiovascular disease (He & MacGregor, 2010). In the United Kingdom, reduction targets were given to different food categories to lower their sodium content. The strategy started in 2003/2004 and the salt intake fell from 9.5 to 8.6 g salt per day in 2008 (Food Standards Agency, 2015; He & MacGregor, 2010; Wyness, Buttriss & Stanner, 2011). Other countries, such as Chile, Argentina, Spain and Brazil have developed voluntary campaigns involving particularly the bread and baked products, but there are still no reports on the results of these campaigns (Legowski & Legetic, 2011).

Several strategies have been developed by the food industry to produce foods with lower sodium contents while maintaining the quality. These strategies can mainly be grouped into the following categories: cognitive mechanisms, chemical mechanisms and product structure design (Busch, Yong & Goh, 2012).

1.4.1 Cognitive mechanisms

The first intervention to be considered is creating awareness in consumers regarding reduction of sodium consumption. As mentioned before key sources of sodium in the

diet are commercially prepared or processed foods and discretionary salt added by consumers during cooking and at the table. A change in consumer behavior is required to ensure that lower salt products are accepted and that no salt is added back before eating (Zandstra, Lion & Newson, 2016). The potential reduction of salt depends on many factors associated with the nature of the food product, which must be taken into account so as to avoid a decrease in the quality. If salt added to foods is decreased progressively between 10-25%, the change may not be detected by consumers (Belz, Ryan & Arendt, 2012; Cruz et al., 2011; Dötsch et al., 2009). However, reduction in small steps requires considerable time before the target sodium levels are reached (Dötsch et al., 2009).

The food industry is sometimes reluctant to reduce the salt added to foods for commercial reasons (He & MacGregor 2010). Due to its water-binding capacity, salt addition (through tumbling or injection) increases the yield of processed meat and poultry products with inexpensive water (Rongrong, Kerr, Toledo & Carpenter, 2000). Moreover, it has been argued that since salt promotes thirst, reducing salt content of certain foods (e.g. snacks) could cause a decrease in soft drink, beer and mineral water sales, that often are consumed together, bearing a “symbiotic relationship”(He, Marrero & MacGregor, 2008).

Little is known about whether preference for a single salt-reduced food can increase when it is not accompanied by a reduction in the salt levels of the total diet. However, some studies have shown that it may not be necessary to modify the general diet in order to alter preferences for lower salt content in single food items (Bolhuis et al., 2015; Zandstra, Lion & Newson, 2016).

To some extent, the success of gradual reduction of salt over time depends on the consumer's awareness and choice. One way of creating awareness in consumers so they choose lower salt products is via specific communication on the package. Nevertheless, it has been showed that sometimes messages can negatively influence taste perception and product acceptance. For example, the labels "Now with reduced salt" and "Now reduced in salt, great taste" had a negative effect in salt perception of soups. Labels or any information which accompanies the food will most likely affect consumers' expectation of the product. Even, when consumers are able to taste the sodium reduction, the perceived difference in terms of ideal saltiness is magnified, and consumers add more salt. Interestingly, many consumers might be more worried about taste than the potential health benefits of foods (Liem, Aydin & Zandstra, 2012; Liem, Miremedi, Zandstra & Keast, 2012).

1.4.2 Chemical mechanisms

The chemical mechanisms used to reduce salt in foods consists in adding some compounds in order to compensate for the loss of saltiness and to enhance or boost the salty taste. These compounds can be grouped in salt substitutes, flavor enhancing and masking agents. Salt substitute agents, which are applied as total salt replacement or in mixtures with sodium chloride, belong mainly to the following categories: minerals such as potassium and magnesium; amino acids and peptides; organic acids; and aroma compounds (Dötsch et al., 2009). Potassium chloride is probably the most common salt substitute used in low- or reduced salt/sodium foods with the added benefit of reducing blood pressure (Sorof, Forman, Cole, Jemerin & Morris, 1997). However,

replacement of salt by potassium chloride, as well as other salt substitutes, has the disadvantages of lowering the perception of salinity and increasing the bitterness and metallic taste. This negative effect is readily perceived in blends over 50:50 sodium chloride/potassium chloride in solution (Desmond, 2006; Dötsch et al., 2009; Murphy, Cardello & Brand, 1981; Ruusunen & Puolanne, 2005).

The flavor enhancers are compounds that are used to improve the acceptability of products and can compensate for salt reduction. There are different commercially available flavor enhancers that include yeast extracts, lactates, monosodium glutamate, and nucleotides, among others. Taste enhancers work by activating receptors in the mouth and throat and thus augmenting the perception of saltiness (Desmond, 2006).

The interaction taste-aroma has also been used to boost saltiness of foods. For example, the addition of beef flavor restored the lost saltiness of a 30% reduced sodium instant beef bouillon without a significant change in the flavor profile. However, there are relatively few studies about salt-aroma interactions (Dötsch et al., 2009).

The masking agents are added to foods to block the aftertaste of substitute agents (alkaline, metallic or bitter taste). Thus, masking agents can be used in combination with substitute agents. There are some commercially available masking agents (amino acids, yeast autolysates) that can be applied in processed meats (Desmond, 2006). Also, a formulation known as Beta™ containing KCl, adenosine 5'-monophosphate and other regulatory approved ingredients can improve the taste of low-sodium, KCl-containing foods (e.g. soups). This formulation reduce the bitterness and improves the saltiness (McGregor, 2007).

1.4.3 Product structure design

It is important to consider the interactions between sodium, the food matrix and saliva during the oral processing. The aim of the product structure design is to optimize the delivery of sodium ions toward the taste buds and cause maximum stimulation of the taste receptors (Busch, Yong & Goh, 2012). Kuo & Lee (2014) proposed that there are three stages in the process of saltiness perception. The first stage considers the sodium release from the food matrix via diffusive and/or convective transport. The second stage involves the delivery in the oral cavity where size reduction and lubrication of the matrix are the major processes in preparation of the food bolus to be swallowed. In the third stage the sodium enters to taste receptor cells where its diffusion depends on the concentration gradient of sodium across the ion channels and the resistance to sodium migration (Kuo & Lee, 2014). To achieve optimal product structures, these three stages should be boosted.

Sodium delivery is dependent on both effective mixing (oral processing) and effective delivery (dissolution and diffusion). If sodium reduction is required without modifying saltiness perception, the availability of sodium (molecular binding) and the delivery of sodium (dissolution, diffusion, mixing kinetics) must be taken into consideration (Rama et al., 2013) to be optimized. In the following sections the interaction of sodium with matrix, the influence of spatial distribution of sodium in the food matrix, and the dissolution of salt crystals are discussed.

1.4.3.1. Interaction of sodium with the food matrix

The interaction of sodium with the food matrix affects the initial availability of sodium as well as its diffusion in the oral cavity. The use of salt to accomplish desired textures is based on its capacity to interact with ionic polymers such as proteins and polysaccharides. These interactions usually lower the availability of sodium for ion perception (Kuo & Lee, 2014; Rosett, Shirley, Schmidt & Klein, 1994).

The diffusion of sodium in the oral cavity is affected by the microstructural properties and composition of the food. For example, the presence of fat globules or protein aggregates in the microstructure increases the tortuosity of the diffusion path. On the other hand, the presence of water in the matrix can enhance the release of sodium (Phan, Yven, Chabanet, Reparet & Salles, 2008).

Rheological and mechanical properties of foods can also influence sodium release and diffusion. Viscosity in the case of liquid foods or hardness/brittleness for solid foods determine the breakdown in the mouth and the subsequent movement of the food inside the oral cavity. A low viscosity liquid or a brittle matrix (which breaks down easily into small pieces) present a high contact area with an improvement in sodium release (de Loubens et al., 2011; Koliandris, Lee, Ferry, Hill & Mitchel, 2008; Kuo & Lee, 2014). Nevertheless, the extent of the effects of these texture-taste interactions tend to be to be relatively small meaning that significant reductions in salt are at the expense of drastic changes in texture (Busch, Yong & Goh, 2012).

When different textures are incorporated into a food matrix the sensory properties can be affected. The saltiness of a food matrix with a low viscosity component into a solid product would be improved. For example, an increase in the perception of flavor was

found when the release of a serum (low viscosity) incorporated into a gel matrix was favored (Sala, Stieger & van de Velde, 2010). However, this focus has not yet been studied in salty foods.

1.4.3.2. Distribution of salt across the food matrix

The spatial distribution of salt in the food matrix has shown to be an important factor to improve the saltiness perception in reduced sodium foods. When different layers with contrasting tastant concentration (non-homogeneous distribution) are created in a food (e.g. in breads and sausages), the saltiness perceived has been improved. This allows the sodium to be reduced without loss of saltiness perceived and without undesirable aftertastes (Noort, Bult, Stieger & Hamer, 2010; Mosca, Bult & Stieger, 2013).

Taste enhancement by non-homogeneous salt distribution across the food matrix is thought to be a result of discontinuous stimulation of taste receptors. For products with non-homogeneous salt distribution, some receptors are exposed to high tastant concentrations, while others are exposed to low concentrations, by fragments of the food moving in the mouth during oral processing. This leads to a desynchronized stimulation of taste receptors (Mosca, van de Velde, Bult, van Boekel & Stieger, 2010; Mosca, Bult & Stieger, 2013). It has been hypothesized that fast concentration changes in the tastant delivery to the receptor can reduce sensory adaptation, leading to an increase in the taste perception (Busch, Tournier, Knoop, Kooyman & Smit, 2009; Busch, Yong & Goh, 2012). In order to achieve a large concentration gradient of salt in the food matrix, additional processing steps may be required to prepare and combine

portions that contain different salt concentrations, and to avoid migration during storage (Busch, Yong & Goh, 2012; Noort, Bult & Stieger, 2012).

Heterogeneous distribution of salt in solid foods can be obtained by creating layers with different salt concentrations or adding encapsulated salt. 3D printing, a digitally-controlled, robotic construction process which builds up complex solid forms layer by layer, could be used to create structures with different layer compositions. However, the use of this technology is just emerging in the public domain, with most of its applications still being developed outside the food sector (Wegrzyn, Golding & Archer, 2012). Encapsulated salt can be obtained by coating granular salt with fat (Noort, Bult & Stieger, 2012). The encapsulated salt allows the creation of a large sensory contrast in the food matrix and could reduce up to 50% of salt maintaining saltiness in bread, for example. The advantage of using encapsulated salt is that it might be used in baking processes or at an industrial scale without major modifications in the process (Noort, Bult & Stieger, 2012). In liquid foods, such as soups, heterogeneous distribution of salt can be created by adding salty solid pieces in a liquid phase with lower salt content. Additionally, the particulate solids need to be chewed, thus remaining much longer in the mouth than the liquid phase. However, this approach is limited to instant foods as solids in which water is added only during preparation (Busch, Keulemans, van den Oever & Reckweg, 2008; Bush, Yong & Goh, 2012).

1.4.3.3. Dissolution of salt crystals

For solid foods that are consumed dry with salt applied on the surface such as salty snacks, the crystals should be dissolved in the mouth for the sodium ions to be detected

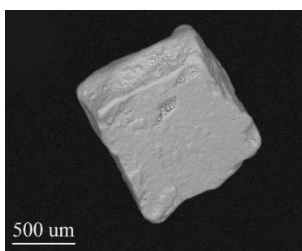
by the taste receptors (Busch, Yong & Goh, 2012). Maximum saltiness of these foods is achieved when salt crystals are dissolved completely and fast enough to reach the sodium receptors in the mouth before swallowing. It has been pointed out that a proportion of sodium of surface-salted foods (e.g. potato crisps) is consumed without being perceived, because the crystals are not dissolved completely in the mouth (Kilcast & den Ridder, 2007; Tian & Fisk, 2012). Optimizing the physical form and morphology of salt crystals so they dissolve faster and completely before swallowing may contribute to a decrease in salt content in surface-salted foods, while maintaining perception of saltiness. The dissolution rate of salt crystals in the mouth is partially determined by the surface area in contact with saliva. The contact surface area can be increased using smaller size and low bulk density crystals (Busch, Yong & Goh, 2012; Kilcast & den Ridder, 2007). However, research into understanding the dissolution kinetics of salt particles with different morphologies is almost inexistent.

As mentioned before, depending on the crystallization conditions, such as evaporation rate and substrate characteristics, different crystals sizes and shapes can be obtained (Figure 1.1). Sodium chloride can crystallize into a cubic or ring-like shape or into efflorescence-like crystals as dendritic, spherulitic or cauliflower shapes. If the evaporation rate is low, well-formed cubic crystals will grow (Vázquez et al., 2015). On the other hand, when some impurities are present in crystallization, non-cubic shapes will be obtained (Al-Jibbouri & Ulrich, 2001; Cheng, Blanchard & Cipriano, 1988; Glasner & Zidon, 1974; Gupta, Pel, Steiger & Kopinga, 2015). Research about application of these crystals with different morphologies in foods and their dissolution in saliva, is scarce.

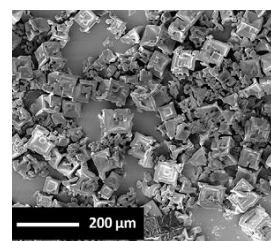
Several fast drying methods, such as spray-drying and antisolvent crystallization, can be used to obtain crystals with different physical properties (Figure 1.1). Spray-drying produces micro or nano sized particles from solutions that are dried within seconds or sometimes fractions of a second, without giving the molecules time to crystallize (Cho, Kim, Chun & Choi, 2015; Langrish, 2009). Thus, amorphous powders are obtained generally by spray-drying, but in the case of salt, crystalline powders are obtained that are only slightly amorphous. Langrish (2009) has pointed out that crystal formation in spray-dried salt occurs very fast because the nucleation and growth phase are fast, although the relative significance of nucleation and growth is less clear. For other spray-dried materials, e.g. sucrose, nucleation and growth rates are very slow (Dombrowsky, Litster, Wagner & He, 2007). In the case of spray-dried salt, the amorphous portions may undergo some recrystallization after spray drying (Langrish, 2009) which is undesirable because large agglomerates can be formed (Tang, Chan, Tam, de Gruyter & Chan, 2006). However, since amorphous particles can be dissolved faster than their crystallized counterparts (Hancock & Parks, 2000; Marabi et al., 2007), amorphous salt (or at least partly amorphous) could have higher dissolution rates than their crystalline counterparts. The spray-drying of a mixture salt-maltodextrin has been evaluated, using maltodextrin as a carrier (Goula & Adamopoulos, 2010), to obtain small-sized maltodextrin/salt complexes. These small-sized salt particles resulted in a salty taste that was released fast (Cho et al., 2015).

(a)

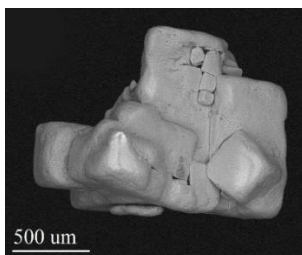
Well-formed cube
obtained from
rock deposits



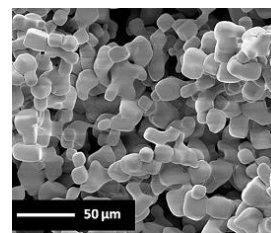
Cubic crystals
with a step like
depression on the
surfaces, obtained
by antisolvent
crystallization
under no stirring
(Lee et al., 2014)



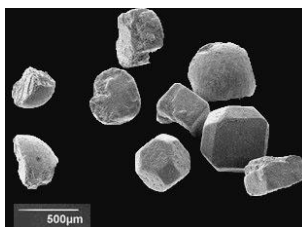
Agglomerated
shape from sea
(naturally dried)



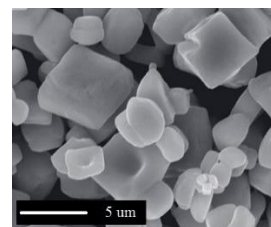
Irregular
geometries with
smooth surface
obtained by
antisolvent
crystallization
under stirring
(Lee et al., 2014)



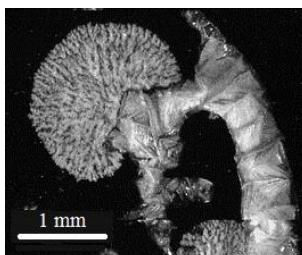
Milled Cubes
(Rama et al.,
2013)



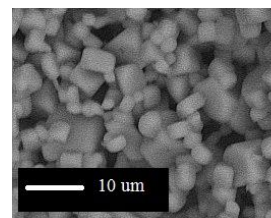
Irregular
geometries
obtained by nano
spray-dried at
95°C (Moncada et
al., 2015)



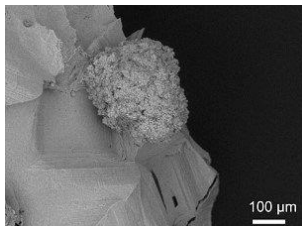
Fan-shaped
obtained by water
evaporation at
45°C from a
droplet (Optical
microscopy
image) (Vázquez
et al. 2015)



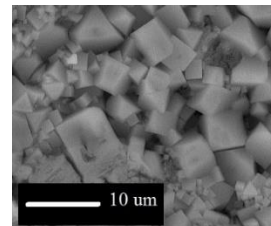
Irregular
geometries
obtained by
spray-drying at
134°C



Spherulitic-shape
that grew over
another crystal,
obtained by water
evaporation at
45°C from a
droplet (Vázquez
et al. 2015)



Irregular
geometries
obtained by
freeze-drying



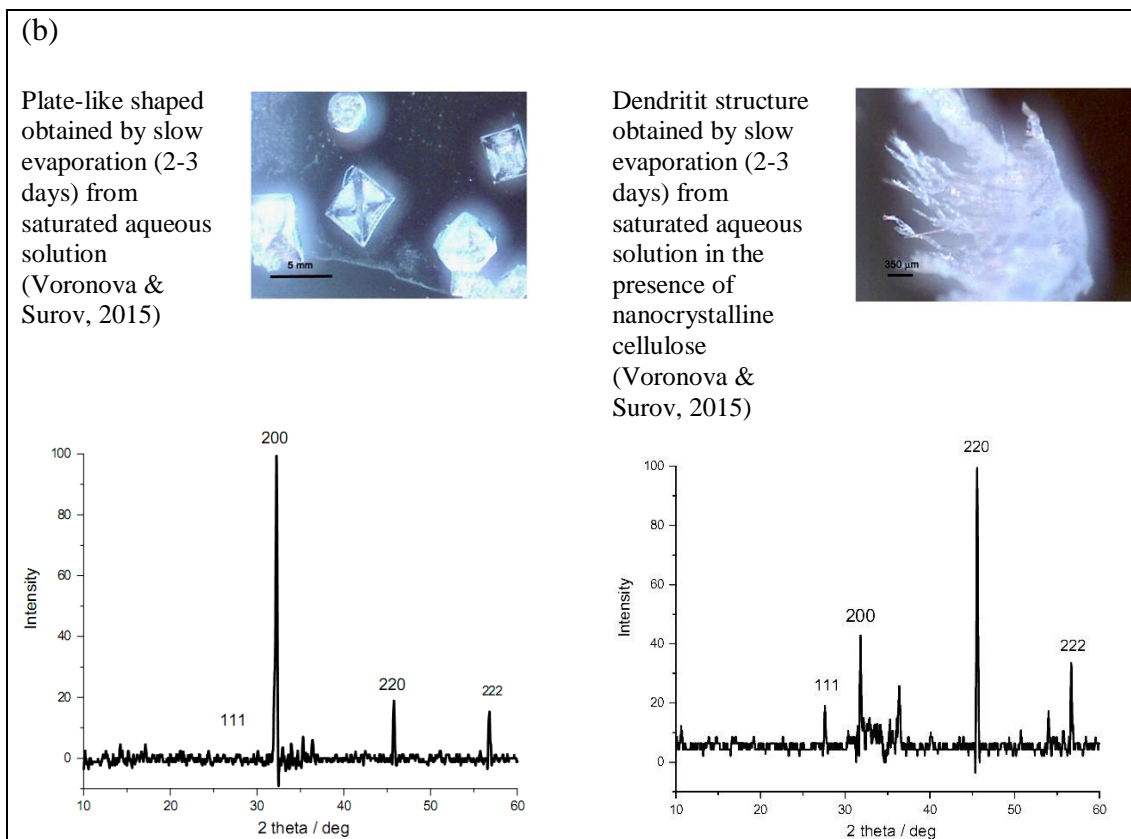


Figure 1.1. Morphologies of salt crystals obtained by different crystallization conditions: (a) SEM and optical microscopy images of crystals, and (b) photo images and their respective X-ray diffraction pattern.

Antisolvent crystallization allows reaching the supersaturation state of solution by adding another solvent in which the solute has a lower solubility. Irregular and asymmetric crystals of different sizes can be obtained (in the order of 200 μm or less) using this method applied to salt (Kadota, Shirakawa, Matsumoto, Shimosaka & Hidaka, 2007; Lee, Ashokkumar & Kentish, 2014). However, these crystals have not been applied in food products.

1.5. Advances in sodium reduction in different food products

Salt reduction in foods without impairing its quality requires that the effect of salt in specific foods be first identified. As mentioned before, over 75% of salt intake comes from processed foods as bread, processed meat and sauces, some cheeses, soups and snacks (Webster, Dunford & Neal, 2010). In the Table 1.2 there is a list of sodium data for some of these foods where the range, mean and reduction target are indicated. In the following sections, advances in salt reduction for some high-sodium products is revised.

1.5.1. Bread

Bread is basically elaborated by mixing flour, water, yeast, and salt. The functions of salt in bread are to impart flavor, improve texture, control yeast growth and fermentation rate, and reduce mould spoilage. During bread baking, salt promotes the development of the gluten structure (critical in trapping small bubbles in the dough), controls water activity, inhibits yeast activity, and permits formation of a fine elastic crumb (Belz, Ryan & Arendt, 2012). In Chile bread (marraqueta) has a great importance in the diet and provides almost 5 g of salt per day (Table 1.2) (Ministry of Health, 2015).

Due to the important technological effects of salt in bread, its replacement or reduction is not easy to implement. However, a one-quarter reduction in the salt content of bread can be put into effect without detection over time (Girgis et al., 2003). The use of salt substitutes (potassium, magnesium and calcium salts), layering dough with different salt concentrations, and the use of encapsulated salt have been proposed as alternatives

to achieve salt reduction without impairing the quality of bread (Cauvain & Tran, 2007; Charlton, MacGregor, Vordter, Levitt & Steyn, 2007; Noort, Bult & Stieger, 2012).

1.5.2. Meat products

In meat products, salt is added as a preservative and to enhance the sensory properties. Salt in meat products can reach 3300 mg of sodium/100 g (Table 1.2). Salt enhances the water binding capacity and hydration of meat proteins. It increases the solubility of the myofibrillar proteins myosin and actin so the viscosity of meat batters increases. This effect is partially because the proteins can interact to form networks (gels) and also because they can stabilize the water/fat interface, thus forming a stable emulsion (Desmond, 2006, 2007; Weiss, Gibis, Schuh & Salminen, 2010).

Osmotic treatments are performed by immersing meat in salt solutions, which leads to meat hydration or dehydration depending on the solution concentration. In the marinating process, the objective is to incorporate water and curing agents, by immersing the cuts of meat in a salt solution with a relatively low concentration. This treatment modifies the meat sensory characteristics and provides the final product with a characteristic flavor, softness and juiciness (Schmidt, Carciofi & Laurindo, 2008).

Several approaches have been suggested to reduce sodium in processed meats, besides gradually lowering the level of salt added to products. In most cases, salt contents of over 2% can be markedly lowered without substantial sensory deterioration or technological problems. For example, salt contents down to 1.4% NaCl in cooked sausages and 1.75% in lean meat products are enough to produce a heat stable gel with acceptable perceived saltiness as well as firmness, water-binding and fat retention

(Ruusunen & Puolanne, 2005). Additionally, the use of salt substitutes in combination with masking agents, and the use of flavors enhancers, such as mineral salt mixtures, yeast, lactates, monosodium glutamate and nucleotides among others, which improve the saltiness of products, are some strategies used to achieve salt reduction. The use of salt crystals with modified physical forms that allow a quick salt dissolution has been studied obtaining promising results (Desmond, 2006; 2007; Weiss et al., 2010).

1.5.3 Cheese

Salt content in some cheeses may reach high levels (1900 mg/100 g). Salt is added to cheese in order to control the activity of the starter culture, induce syneresis in the curd, inactivate or reduce spoilage bacteria, influence enzymatic activity during maturation, and impart typical texture and flavor characteristics (Cruz et al., 2011; Guinee & O’Kennedy, 2007; Lu & McMahon, 2015; Saint-Eve et al., 2009).

Lowering the amount of salt added should not significantly affect the quality of the product, to a certain extent. It has been suggested that a reduction in the amount of salt between 10 and 25% cannot be detected by consumers (Cruz et al., 2011). Cheeses with low sodium content have been developed using flavor enhancers and totally or partially substituting salt by KCl, MgCl₂, and CaCl₂, depending on the cheese type. However, a disadvantage of using of salt substitutes is their bitter or sour aftertaste (Cruz et al., 2011; Guinee & O’Kennedy, 2007). It has been pointed out that low-sodium cheese often exhibit an acidic flavor due to excessive acid production caused by ongoing starter culture activity facilitated by the low salt-in-moisture levels. The fortification of cheese milk with ultrafiltration retentates (to increase curd buffering),

and the application of high-hydrostatic pressure treatment to decreasing microbial activity helps to minimize these undesirable characteristics in low-sodium cheese (Ozturk, Govindasamy-Lucey, Jaeggi, Johnson & Lucey, 2015).

Some studies have indicated that the structural and textural properties of the cheese matrix could affect salt diffusion towards the taste receptors. The microstructure of model cheeses matrices with low protein concentration (coarser and fluffier) facilitates the diffusion of the solutes (Floury, Rouaud, Le Poullennec & Famelart, 2009). However, further research that integrates the diffusion phenomenon with the matrix microstructure of cheese is needed.

1.5.4 Soups

Salt is one of the most important components in soups, which may contain up to 640 mg of sodium per 100 g (Table 1.2). In instant soups and bouillons salt is used for preservation and to enhance sensorial quality (Gupta & Bongers, 2011; Krejčová, Černohorský & Meixner, 2007). Salt diminution in soups affects not only salty taste but also the liberation of volatile compounds (Mitchell, Brunton & Wilkinson, 2011). A 30% in the amount of salt in vegetable soup may be achieved without compromising its perceived saltiness (Gonçalves et al., 2014). It has been shown that a gradual 20% reduction in salt was achieved in canned soups without prompting a reaction from the consumers. However, a complete change in recipe is required for any further reduction of salt in canned soups. (Robinson, 2007). Non-homogeneous distribution of the salt in instant chicken soups allows a reduction of 15 % in salt without altering the intensity of saltiness (Dötsch et al., 2009).

1.5.5 Snacks

Snack foods are a wide range of products, including cereal bars, breakfast cereals, biscuits, chocolate bars and potato chips that can be sweet or savory. Savory snacks may contain up to 1880 mg of sodium per 100 g (Table 1.2) and it is added primarily to give saltiness, because the base material is bland. Moreover, salt offers a convenient vehicle for distributing micro-ingredients such as flavors, colors, vitamins and antioxidants (Ainsworth & Plunkett, 2007). Besides, salt influences the rheological and physical properties of snacks as it often interacts with other components. For example, in popcorn salt and oil can have a significant effect in the expansion volume (Ceylan & Karababa, 2004). In starchy snacks, when salt is added in the base recipe it can compete with starch for moisture, affecting starch gelatinization. In extruded snacks, salt increases the level of expansion obtained (Ainsworth & Plunkett, 2007).

Gradual reduction of salt in snacks can be applied, but changes in flowability, shelf life and texture may require additional changes to the formulation to be accepted. Also, salt substitutes and flavor enhancers can be used, although this must be limited as they can have a metallic/bitter flavor and low saltiness (Ainsworth & Plunkett, 2007).

In surface-salted snacks with salt as crystals, such as potato crisps, salted almonds, pretzels, tortilla chips, and crackers, whose sodium content can vary from 30 to 1880 mg/100g (see Tables 1 and 2), the level of sodium can be reduced by increasing the surface area of the crystals, leading to an increase in the dissolution rate of salt in the saliva. (Rama et al., 2013). For example, a reduction of between 25% and 50% in the level of salt would be suitable for cheese crackers if micro or nano-sized salt (550 nm

– 15 μm) is used instead regular salt with an average particle size of 1500 μm (Moncada et al., 2015). However, this approach has not yet been widely studied.

1.6. Perspectives

Salt is a very important ingredient in processed foods, but vast evidence associating high levels of sodium (contained in salt) with several diseases suggest that salt consumption should be reduced. Strategies to effectively reducing the salt contained in foods, aim at maintaining an acceptable salt perception and good quality. Salt particles, which are rapidly and completely dissolved in the mouth are especially suitable for surface-salted foods, and preclude addition of components which may elicit an undesirable aftertaste.

Salt particles with suitable sizes and morphologies may be designed or selected, either in crystalline or non-crystalline state, having a timely disengagement from the food matrix (e.g., microstructure), fast dissolution in saliva and rapid diffusion towards the taste buds in the mouth before being swallowed. Therefore, saltiness perception can be increased and salt content optimized and reduced.

1.7. Hypothesis and objectives of this thesis

The hypothesis of this thesis is that the dissolution of salt crystals in saliva depends on their microstructural characteristics, size and shape, as well as the viscosity of the saliva and exposure time. Changing the microstructure of the salt crystal will change its dissolution rate and, therefore, will also change the perception of saltiness.

The general objective of this thesis was to determine the influence of the microstructure of salt crystals on their dissolution rate in water and artificial saliva and its correlation with saltiness perception.

The specific objectives are the following:

- Characterize the crystals of several commercial salts according to microstructure and size.
- Develop a methodology of video-microscopy to assess the dissolution of salt particles in artificial saliva and in water, controlling the temperature.
- Evaluate the dissolution kinetics of the particles of several commercial salts in artificial saliva and in water.
- Assess the perception of saltiness for commercial salts with different microstructural characteristics using sensory evaluation. Correlate the perception of saltiness with the dissolution of salt in artificial saliva.
- Assess the salt crystallization by fast water evaporation from droplets of salt solutions as a method for obtaining microcrystals with high dissolution rates.

1.8. Outline

This thesis is divided into five chapters, with three chapters corresponding to experimental work as outlined below:

- In Chapter 2, a method to assess the dissolution kinetics of a single crystal was developed. The dissolution profile of five different commercial salts was determined by video-microscopy and image analysis. The effects of the

dissolution media and its temperature on the dissolution rate of salts were determined.

- In Chapter 3, five salt types of salt from the Canadian and Chilean market were selected based on their microstructure and their dissolution behavior in artificial saliva was studied. Saltiness perception was evaluated by sensory analysis and results were correlated with the dissolution rate and microstructure of crystals.
- In Chapter 4, a new method of crystallization of salt was assessed. Crystal formation was performed by fast water evaporation from droplets of salt solutions immersed in a hot oil phase. The effects of oil phase temperature, droplet volume and initial salt solution concentration on the size and morphology of crystals obtained were assessed.

Finally, in Chapter 5 the general conclusions are presented.

References

- Abu-Khader, M. M. (2006). Viable engineering options to enhance the NaCl quality from the Dead Sea in Jordan. *Journal of Cleaner Production*, 14, 80-86.
- Adams, S. & Taylor, A. (2012). Oral processing and flavour sensing mechanism. In Chen, J., & Engelen, L. (Eds.), *Food oral processing: Fundamentals of eating and sensory perception* (pp. 139-155). Singapore: Wiley-Blackwell.
- Aguilera, J.M. (2012). *Edible structures: The basic science of what we eat*. Boca Raton: Taylor & Francis Group.
- Ainsworth, P. & Plunkett, A. (2007). Reducing salt in snacks products. In Kilcast, D. & Angus, F. (Eds.), *Reducing Salt in Foods. Practical Strategies* (pp. 296-315). Cambridge: Woodhead Publishing Limited.
- Al-Jibbouri, S. & Ulrich, J. (2001). The influence of impurities on crystallization kinetics of sodium chloride. *Crystal Research and Technology*, 36, 1365-1375.
- Beauchamp, G.K. & Stein, L.J. (2008). Salt taste. In Basbaum A., Shepherd, G.M., Kaneko, A. & Westheimer, G. (Eds.). *The senses: A comprehensive reference*, Vol. 4 (pp. 401-408), New York: Elsevier.
- Belz, M.C.E., Ryan, L.A.M. & Arendt, E.K. (2012). The impact of salt reduction in bread: a review. *Critical Reviews in Food Science and Nutrition*, 52, 514-24.
- Bidlas, E. & Lambert, R.J.W. (2008). Comparing the antimicrobial effectiveness of NaCl and KCl with a view to salt/sodium replacement. *International Journal of Food Microbiology*, 124, 98-102.
- Bolhuis, D.P., Gijbbers, L., de Jager, I., Geleijnse, J.M. & de Graaf, K. (2015). Encapsulated sodium supplementation of 4 weeks does not alter salt taste preferences in a controlled low sodium and low potassium diet. *Food Quality and Preference*, 46, 58-65.
- Brown, I.J. Tzoulaki, I., Candeias, V. & Elliot, P. (2009). Salt intakes around the world: implications for public health. *International Journal of Epidemiology*, 38, 791-813.
- Busch, J.L.H.C., Keulemans, C., van den Oever, G.J. & Reckweg, F. (2008). Salty particulates. Unilever. <http://www.google.com/patents/WO2008074606A1?cl=en>
- Busch, J. L. H. C., Tournier, C., Knoop, J., Kooyman, G. & Smit, G. (2009). Temporal contrast of salt delivery in mouth increases salt perception. *Chemical Senses*, 34, 341-348.
- Busch, J.L.H.C., Yong, F.Y.S. & Goh, S.M. (2012). Sodium reduction: Optimizing product composition and structure towards increasing saltiness perception. *Trends in Food Science & Technology*, 29, 21-34.

- Cauvain, S.P. & Tran, B. (2007). Reduced salt in bread and other baked products. In Kilcast, D. & Angus, F. (Eds.), *Reducing Salt in Foods. Practical Strategies* (pp. 283-295). Cambridge: Woodhead Publishing Limited.
- Ceylan, M. & Karababa, E. (2004). The effects of ingredients on popcorn popping characteristics. *International Journal of Food Science and Technology*, *39*, 361-370.
- Chantrapornchai, W. & McClements, D.J. (2002). Influence of NaCl on optical properties, large-strain rheology and water holding capacity of heat-induced whey protein isolate gels. *Food Hydrocolloids*, *16*, 467-476.
- Charlton, K.E., MacGregor, E., Vordter, N.H., Levitt, N.S. & Steyn, K. (2007). Partial replacement of NaCl can be achieved with potassium, magnesium and calcium salts in brown bread. *International Journal of Food Sciences and Nutrition*, *58*, 508-521.
- Cheng, R.J., Blanchard, D.C. & Cipriano, R.J. (1988). The formation of hollow sea-salt particles from the evaporation of drops of seawater. *Atmospheric Research*, *22*, 15-25.
- Cho, H.y., Kim, B., Chun, J.Y. & Choi, M.J. (2015). Effect of spray-drying process on physical properties of sodium chloride/maltodextrin complexes. *Powder Technology*, *277*, 141-146.
- Codex Alimentarius. (1985). Codex standard for food grade salt. Codex stan 150-1985.
- Cruz, A.G., Faria, J.A.F., Pollonio, M.A.R., Bolini, H.M.A., Celeghini, R.M.S., Granato, D. & Shah, N.P. (2011). Cheeses with reduced sodium content: Effects on functionality, public health benefits and sensory properties. *Trends in Food Science & Technology*, *22*, 276-291.
- D'Elia, L., Rossi, G., Ippolito, R., Cappuccio, F. & Strazzullo, P. (2012). Habitual salt intake and risk of gastric cancer: a meta-analysis of prospective studies. *Clinical Nutrition*, *31*, 489-498.
- Dahl, L.K. (1972). Salt and hypertension. *The American Journal of Clinical Nutrition*, *25*, 231-244.
- de Loubens, C., Panouillé, M., Saint-Eve, A., Déléris, I., Tréléa, I. C., & Souchon, I. (2011). Mechanistic model of *in vitro* salt release from model dairy gels based on standardized breakdown test simulating mastication. *Journal of Food Engineering*, *105*, 161-168.
- Delwiche, J.F., Halpern, B.P. & Desimone, J.A. (1999). Anion size of sodium salts and simple taste reaction times. *Physiology & Behavior*, *66*, 27-32.
- deMan, J.M. (1999). *Principles of Food Chemistry* (3rd ed.). New York: Springer (Chapter 7).
- Desmond, E. (2006). Reducing salt: A challenge for the meat industry. *Meat Science*, *74*, 188-196.

Desmond, E. (2007). Reducing salt in meat and poultry products. In Kilcast, D. & Angus, F. (Eds.) *Reducing Salt in Foods. Practical Strategies* (pp. 233-255). Cambridge: Woodhead Publishing Limited.

Dombrowsky, R.D., Litster, J.D., Wagner, N.J. & He, Y. (2007). Crystallization of alpha-lactosemonohydrate in a drop-based microfluidic crystallizer. *Chemical Engineering Science*, 62, 4802-4810.

Dötsch, M., Busch, J., Batenburg, M., Liem, G., Tareilus, E., Mueller, R. & Meijer, G. (2009). Strategies to reduce sodium consumption: A food industry perspective. *Critical Reviews in Food Science and Nutrition*, 49, 841-851.

Drake, S.L. & Drake, M.A. (2011). Comparison of salty taste and time intensity of sea and land salts from around the world. *Journal of Sensory Studies*, 26, 25-34.

Elliott, P. & Brown, I. (2006). Sodium intakes around the world. *Forum and Technical meeting on Reducing Salt Intake in Populations*, 1-85.

Flores, M., Gianelli, M. P., Pérez-Juan, M. & Toldrá, F. (2007). Headspace concentration of selected dry-cured aroma compounds in model systems as affected by curing agents. *Food Chemistry*, 102, 488-493.

Floury, J. Rouaud, O., Le Poullennec, M. & Famelart, M. (2009). Reducing salt level in food: Part 2. Modelling salt diffusion in model cheese systems with regards to their composition. *LWT - Food Science and Technology*, 42, 1621-1628.

Food Standards Agency. (2015). Nutrition news. Salt. <http://collections.europarchive.org/tna/20100927130941/http://food.gov.uk/healthierating/salt/>

Girgis, S., Neal, B., Prescott, J., Prendergast, J., Dumbrell, S., Turner, C. & Woodward, M. (2003). A one-quarter reduction in the salt content of bread can be made without detection. *European Journal of Clinical Nutrition*, 57, 616-20.

Glasner, A. & Zidon, M. (1974). The crystallization of NaCl in the presence of $[\text{Fe}(\text{CN})_6]^{4-}$ ions. *Journal of Crystal Growth*, 21, 294-304.

Gonçalves, C., Monteiro, S., Padrao, P., Rocha, A., Abreu, S., Pinho, O. & Moreira, P. (2014). Salt reduction in vegetable soup does not affect saltiness intensity and liking in the elderly and children. *Food and Nutrition Research*, 58, 24825.

Goula, A.M. & Adamopoulos, K.G. (2010). A new technique for spray drying orange juice concentrate. *Innovative Food Science and Emerging Technologies*, 11, 342-351.

Guichard, E. (2002). Interactions between flavor compounds and food ingredients and their influence on flavor perception. *Foods Reviews International*, 18, 49-70.

Guinee, T.P. & O’Kennedy, T.O. (2007). Reducing salt in cheese and dairy gels. In Kilcast, D. & Angus, F. (Eds.), *Reducing Salt in Foods. Practical Strategies* (pp. 319-357). Cambridge: Woodhead Publishing Limited.

Gupta, S. & Bongers, P. (2011). Bouillon cube process design by applying product driven process synthesis. *Chemical Engineering and Processing*, 50, 9-15.

Gupta S., Pel, L., Steiger, M. & Kopinga, K. (2015). The effect of ferrocyanide ions on sodium chloride crystallization in salt mixtures. *Journal of Crystal Growth*, 410, 7-13.

Hancock, B.C. & Parks, M. (2000). What is the true solubility advantages for amorphous pharmaceuticals? *Pharmaceutical Research*, 17, 397-404.

He, F.J. & MacGregor, G.A. (2010). Reducing population salt intake worldwide: from evidence to implementation. *Progress in Cardiovascular Diseases*, 52, 363-382.

He, F.J., Marrero, N.M. & MacGregor, G.A. (2008). Salt intake is related to soft drink consumption in children and adolescents: a link to obesity? *Hypertension*, 51, 629-634.

Hutton, T. (2002). Sodium: technological functions of salt in the manufacturing of food and drink products. *British Food Journal*, 104, 126-152.

Jay, J.M. (2000). *Modern food microbiology* (6th ed.). Gaithersburg, Maryland: Aspen Publication (Chapter 13).

Kadota, K., Shirakawa, Y., Matsumoto, I., Shimosaka, A. & Hidaka, J. (2007). Formation and morphology of asymmetric NaCl particles precipitated at the liquid-liquid interface. *Advanced Powder Technology*, 18, 599-844.

Kaplan, N.M. (2000). The dietary guideline for sodium: should we shake it up? No. *The American Journal of Clinical Nutrition*, 71, 1020-1026.

Keast, R. & Breslin, P. (2002). An overview of binary taste–taste interactions. *Food Quality and Preference*, 14, 111-124.

Kilcast, D. & den Ridder, C. (2007). Sensory issues in reducing salt in food products. In Kilcast, D. & Angus, F. (Eds.), *Reducing Salt in Foods. Practical Strategies* (pp 201-220) Cambridge: Woodhead Publishing Limited.

Koliandris, A., Lee, A., Ferry, A.L., Hill, S. & Mitchel, J. (2008). Relationship between structure of hydrocolloid gels and solutions and flavour release. *Food Hydrocolloids*, 22, 623-630.

Krejčová, A., Černožský, T. & Meixner, D. (2007). Elemental analysis of instant soups and seasoning mixtures by ICP–OES. *Food Chemistry*, 105, 242-247.

- Kuo, W. & Lee, Y. (2014). Effect of food matrix on saltiness perception-implications for sodium reduction. *Comprehensive Reviews in Food Science and Food Safety*, 13, 906-923.
- Langrish, T.A.G. (2009). Assessing the relative tendency of different materials to crystallize in spray drying: a comparison between sodium chloride and lactose. *Journal of Food Engineering*, 91, 521-525.
- Lee, J., Ashokkumar, M. & Kentish, S.E. (2014). Influence of mixing and ultrasound frequency on antisolvent crystallisation of sodium chloride. *Ultrasonics Sonochemistry*, 21, 60-68.
- Legowski, B. & Legetic, B. (2011). How three countries in the Americas are fortifying dietary salt reduction: a north and south perspective. *Health Policy*, 102, 26-33.
- Liem, D.G., Aydin, N.T. & Zandstra, E.H. (2012). Effects of health labels on expected and actual taste perception of soup. *Food Quality and Preference*, 25, 192–197.
- Liem, D.G., Miremadi, F., Zandstra, E.H. & Keast, R.S.J. (2012). Health labelling can influence taste perception and use of table salt for reduced-sodium products. *Public Health Nutrition*, 15(12), 2340–2347.
- Lu, Y. & McMahon, D.J. (2015). Effects of sodium chloride salting and substitution with potassium chloride on whey expulsion of Cheddar cheese. *Journal of Dairy Science*, 89, 78-88.
- Marabi, A., Mayor, G., Raemy, A., Bauwens, I., Claude, J., Burbidge, A., Wallach, R. & Saguy, I.S. (2007). Solution calorimetry: A novel perspective into the dissolution process of food powders. *Food Research International*, 40, 1286-1298.
- McCaughey, S. (2007). Dietary salt and flavor: Mechanisms of taste perception and physiological controls. In Kiscast, D. & Angus, F. (Eds.), *Reducing Salt in Foods. Practical Strategies*, (pp.77-98).Cambridge: Woodhead Publishing Limited.
- McGregor, R. (2007). The use of bitter blockers to replace salt in the food products. In Kiscast, D. & Angus, F. (Eds.), *Reducing Salt in Foods. Practical Strategies*, (pp.221-230).Cambridge: Woodhead Publishing Limited.
- Ministry of Health. (2015). Salud suscribió acuerdo de producción limpia con Federación de Panaderos. <http://web2.minsal.cl/node/2312>
- Mitchell, M., Brunton, N.P. & Wilkinson, M.G., (2011). Impact of salt reduction on the instrumental and sensory flavor profile of vegetable soup. *Food Research International*, 44, 1036-1043.
- Moncada, M., Astete, C., Sabliov, C., Olson, D., Boeneke, C. & Aryana, K.J. (2015). Nano spray-dried sodium chloride and its effects on the microbiological and sensory characteristics of surface-salted cheese crackers. *Journal of Dairy Science*, 98, 5946-5954.

- Morton Salt. (1995). Available on: <http://www.mortonsalt.com/>.
- Mosca, A.C., Bult, J.H.F. & Stieger, M. (2013). Effect of spatial distribution of tastants on taste intensity, fluctuation of taste intensity and consumer preference of (semi-)solid food products. *Food Quality and Preference*, 28, 182-187.
- Mosca, A.C., van de Velde, F., Bult, J.H.F., van Boekel, M.A.J.S. & Stieger, M. (2010). Enhancement of sweetness intensity in gels by inhomogeneous distribution of sucrose. *Food Quality and Preference*, 21, 837-842.
- Murphy, C., Cardello, A.V. & Brand, J.G. (1981). Tastes of fifteen halide salts following water and NaCl: anion and cation effects. *Physiology & Behavior*, 26, 1083-1095.
- Noort, M.W.J., Bult, J.H.F. & Stieger, M. (2012). Saltiness enhancement by taste contrast in bread prepared with encapsulated salt. *Journal of Cereal Science*, 55, 218-225.
- Noort, M.W.J., Bult, J.H.F., Stieger, M. & Hamer, R. J. (2010). Saltiness enhancement in bread by inhomogeneous spatial distribution of sodium chloride. *Journal of Cereal Science*, 52, 378-386.
- Ozturk, M., Govindasamy-Lucey, S., Jaeggi, J.J., Johnson, M.E. & Lucey, J.A. (2015). Low-sodium Cheddar cheese: Effect of fortification of cheese milk with ultrafiltration retentate and high-hydrostatic pressure treatment of cheese. *Journal of dairy Science*, 98, 6713-6726.
- Phan, V.A., Yven, C., Chabanet, C., Reparet, J.M. & Salles, C. (2008). In vivo sodium release related to salty perception during eating model cheeses of different textures. *International Dairy Journal*, 18, 956-963.
- Potter, N.N. & Hotchkiss, J.H. (1998). *Food Science* (5th ed.). Gaithersburg, Maryland: Aspen Publication (Chapter 7).
- Powles, J., Fahimi, S., Micha, R., Khatibzadeh, S., Shi, P., Ezzati, M., Engell, R., Lim, S., Danaei, G. & Mozaffarian, D. (2013). Global, regional and national sodium intakes in 1990 and 2010: a systematic analysis of 24 h urinary sodium excretion and dietary surveys worldwide. *British Medical Journal Open*, 3, e003733.
- Rama, R., Chiu, N., Carvalho, M., Hewson, L., Hort, J. & Fisk, I. (2013). Impact of salt crystal size on in-mouth delivery of sodium and saltiness perception from snack foods. *Journal of Texture Studies*, 44, 338-345.
- Robinson, T. (2007). Reducing salt in canned foods. In Kilcast, D. & Angus, F. (Eds.), *Reducing Salt in Foods. Practical Strategies* (pp. 358-368). Cambridge: Woodhead Publishing Limited.
- Rongrong, L., Kerr, W.L., Toledo, R.T. & Carpenter, J.A. (2000). H NMR studies of water in chicken breast marinated with different phosphates. *Journal of Food Science*, 65, 575-580.

- Rosett, T.R., Shirley, L., Schmidt, S.J. & Klein, B. (1994). Na⁺ binding as measured by ²³Na nuclear magnetic resonance spectroscopy influences the perception of saltiness in gum solutions. *Journal of Food Science*, 59, 206-210.
- Ruusunen, M. & Puolanne, E. (2005). Reducing sodium intake from meat products. *Meat Science*, 70, 531-541.
- Saint-Eve, A. Lauverjat, C., Magnan, C., Déléris, I. & Souchon, I. (2009). Reducing salt and fat content: Impact of composition, texture and cognitive interactions on the perception of flavoured model cheeses. *Food Chemistry*, 116, 167-175.
- Sala, G., Stieger, M. & van de Velde, F. (2010). Serum release boosts sweetness intensity in gels. *Food Hydrocolloids*, 24, 494-501.
- Schmidt, F.C., Carciofi, B.M.A. & Laurindo, J.B. (2008). Salting operational diagrams for chicken breast cuts: Hydration–dehydration. *Journal of Food Engineering*, 88, 36-44.
- Schmidt-Hebbel, H., Pennacchiotti, I., Masson, L. & Mella, M.A. (1990). Table of chemical composition of Chilean foods. <http://www.libros.uchile.cl/files/presses/1/monographs/426/submission/proof/files/assets/common/downloads/publication.pdf>
- Sebastian, R.S., Enns, C. W., Steinfeldt, L.C., Goldman, J.D. & Moshfegh, A.J. (2012). Discontinuation of data processing step: Salt adjustment on designated foods likely to be home prepared. *United States Department of Agriculture: National Agricultural Library*, <http://handle.nal.usda.gov/10113/55318>
- Sorof, J.M. Forman, A., Cole, N., Jemerin, J. & Morris, C. (1997). Potassium intake and cardiovascular reactivity in children with risk factors for essential hypertension. *The Journal of Pediatrics*, 131, 87-94.
- Tang, P. Chan, H., Tam, E., de Gruyter, N. & Chan, J. (2006). Preparation of NaCl powder suitable for inhalation. *Industrial & Engineering Chemistry Research*, 45, 4188-4192.
- Tian, X. & Fisk, I.D. (2012). Salt release from potato crisps. *Food & Function*, 3, 376-380.
- Tortora, G.J., Funke, B.R. & Case, C.L. (2007). *Microbiology: An introduction* (9th ed.) (pp. 161-163). Pearson Education, Inc. Benjamin Cummings: San Francisco.
- USDA (2015). USDA National Nutrient Database for Standard Reference. Release 28. <http://www.ars.usda.gov/Services/docs.htm?docid=8964>
- Valenzuela, K., Quitral, V., Villanueva, B., Zavala, F. & Atalah, E. (2013). Evaluation of the pilot program to reduce salt/sodium in bread in Santiago of Chile. *Revista Chilena de Nutrición*, 40, 119-122.

Vázquez, P., Thomachot-Schneider, C., Mouhoubi, K., Fronteau, G., Gommeaux, M., Benavente, D., Barbin, V. & Bodnar, J. (2015). Infrared thermography monitoring of the NaCl crystallisation process. *Infrared Physics & Technology*, 71, 198-207.

Ventanas, S., Mustonen, S., Puolanne, E. & Tuorila, H. (2010). Odour and flavour perception in flavoured model systems: Influence of sodium chloride, umami compounds and serving temperature. *Food Quality and Preference*, 21, 453-462.

Voronova, M.I. & Surov, O.V. (2015). Dendritic crystallization of inorganic salts in the presence of nanocrystalline cellulose. *Materials Letters*, 145, 336-339.

Webster, J.L., Dunford, E.K. & Neal, B.C. (2010). A systematic survey of the sodium contents of processed foods. *The American Journal of Clinical Nutrition*, 91, 413-420.

Wegrzyn, T.F., Golding, M. & Archer, R.H. (2012). Food layered manufacture: A new process for constructing solid foods. *Trends in Food Science & Technology*, 27, 66-72.

Weiss, J. Gibis, M., Schuh, V. & Salminen, H. (2010). Advances in ingredient and processing systems for meat and meat products. *Meat Science*, 86, 196-213.

WHO (2012). Guideline: Sodium intake for adults and children. Geneva, World Health Organization (WHO).

WHO (2014). Salt reduction. Fact sheet N°393. (<http://www.who.int/mediacentre/factsheets/fs393/en/>)

Wyness, L.A., Butriss, J.L. & Stanner, S.A. (2011). Reducing the population's sodium intake: the UK Food Standards Agency's salt reduction programme. *Public Health Nutrition*, 15, 254-261.

Zacarías, I., Vera, G., Olivares, S., de Pablo, S., Reyes, M., Rpdriíguez, L., Uauy, R. & Araya, M. (2011). Estudio "propuesta de criterios y recomendación de límites máximos de nutrientes críticos para la implementación de la ley de composición de alimentos y su publicidad". Ministerio de Salud. Available on: <http://www.minsal.gob.cl/portal/url/item/bf99bade8a76768ee0400101640118ce.pdf>

Zandstra, E.H., Lion, R. & Newson, R.S. (2016). Salt reduction: Moving from consumer awareness to action. *Food Quality and Preference*, 48, 376-381.

2. DISSOLUTION OF NaCl CRYSTALS IN ARTIFICIAL SALIVA AND WATER BY VIDEO-MICROSCOPY

2.1. Introduction

Sodium is essential to maintain diverse functions in our bodies and a primary solute of extracellular fluids. Sodium contributes to various processes including blood and osmotic pressure regulation, transportation of water and nutrients across cells, and transmission of nerve impulses (Cruz et al., 2011; Haring, Deal, & Kuo, 2014). However, a high consumption of sodium has been associated with non-communicable diseases (including hypertension, cardiovascular disease and stroke), besides kidney disease and gastric cancer, among others (D'Elia, Rossi, Ippolito, Cappuccio, & Strazzullo, 2012; Kaplan, 2000). Thus, the recommended consumption dose of sodium for adults (≥ 16 years old) is not to exceed 2 g/day, equivalent to 5 g/day of salt (NaCl), while for children (2-15 years old) is lower than for adults and should be adjusted based on the energy requirements (WHO, 2012). Currently, the range of salt intake around the world is between 5 and 17 g/day. The main sources of added salt are processed, pre-prepared and ready-made foods, accounting for up to 75% of salt intake in European and Northern American adults (Brown, Tzoulaki, Candeias, & Elliott, 2009). Several strategies for salt reduction have been developed by the food industry mostly based on cognitive mechanisms, chemical approaches, and product structure design. Cognitive mechanisms aim at increasing awareness of the problem and shifting consumer preferences towards low-salt foods. Chemical mechanisms involve the use

of certain ingredients as salt substitutes and masking agents to increase the perception of true saltiness (Jensen *et al.*, 2011; Murphy, Cardello, & Brand, 1981). Finally, product structure design is targeted at modifying the product structure to optimize the delivery of salt or sodium ions from the food to the taste buds in order to cause maximum stimulation (Busch, Yong, & Goh, 2013). To accomplish this last strategy it is fundamental to understand the dissolution behavior of salt crystals in the mouth, the properties of salt particles in their kinetics of dissolution in saliva, as well as the delivery of salt ions from the food matrix. For salt and many other tastants, saliva is the solvent that conveys ions to the taste buds. The perception of saltiness is affected by the way salt ions are released from the food and this in turn depends on the way food breaks down during the oral process (Chen & Engelen, 2012).

Commercial salt can be obtained from underground rock salt deposits (as halide mineral) and from sea water or natural brines (Codex Alimentarius Commission, 1997). The salt that comes from sea water or natural brines is usually obtained by evaporation of water. Salt crystals are typically cubic, sometimes octahedral, colorless or white, and soluble in water. But salt can also contain various amounts of minerals, organic substances, clay, liquids and gases (Drake & Drake, 2011; Kraus & Hunt, 1920). Different particle sizes and shapes can be obtained depending on the conditions in which the evaporation process is carried out (Buck & Barringer, 2007). Salt particles with different sizes and shapes added to food have shown diverse time-intensity salt perception profiles (Jensen *et al.*, 2011). Thus, in order to design food structures that maximize the salty taste potential all the factors that influence the rate of salt dissolution in saliva must be understood. Although there is great interest in reducing

the salt content in food, there has not been much research on the properties of different salt types (i.e. by origin, shape of crystals, composition) in regard to their dissolution rate in saliva and their role in contributing to the salty taste (Vella, Marcone, & Duizer, 2012).

Several *in vivo* methods have been developed to study in-mouth salt release. For example, ion electrodes installed in dental plates can monitor the salt content in saliva. This technique has its drawbacks, however, as recorded levels may not adequately reflect the signal received by the taste buds. Moreover, having a wire inside the mouth can make chewing difficult (Chen & Engelen, 2012). For this reason *in vitro* methods have been developed that are less difficult to implement while providing data to screen among alternatives (Vella, Marcone, & Duizer, 2012). These methods include developing systems simulating conditions in the mouth and the use of natural or artificial saliva in experiments, wherein the salt dissolution is measured using conductivity probes, ion chromatographic techniques or multisensory systems (De Loubens *et al.*, 2011; Lauverjat, De Loubens, Déléris, Tréléa, & Souchon, 2009; Lvova *et al.*, 2012).

The main objective of this study is to understand the kinetics of dissolution of crystals of five different types of commercial salt in artificial saliva and in water (as may occur in aqueous salty formulations) by an *in vitro* method. The rate of crystal dissolution under different temperatures and saliva composition is quantified by image analysis of video-microscopy images taken at real time conditions.

2.2. Materials and methods

2.2.1. Samples

Five commercial salts were evaluated according to their kinetics of dissolution. The salt types analyzed came from different sources and had diverse compositions (Table 2.1): three were rock salts (RSA, RSB and RSC) and two were sea salts (SSA and SSB). The products were purchased and stored at room temperature in a low humidity setting.

Each salt type (500 g) was sieved using a sieve shaker for 20 min and the fraction that was retained between sieves N° 18 (1.00 mm) and sieve N° 14 (1.40 mm) was used to analyze the kinetics of dissolution. This cut in size dimension was present in all samples thus avoiding grinding of material. It was also adequate for microscopy observations.

Table 2.1. Description and nomenclature of commercial salts.

Salt type	Description	Supplier
Rock Salt A (RSA)	Iodized salt from rock deposits	SLP salt, Chile
Rock Salt B (RSB)	Iodized salt from rock deposits with anti-caking agent	SLP salt, Chile
Rock Salt C (RSC)	Salt from rock deposits	Terre Exotique, Iran
Sea Salt A (SSA)	Iodized sea salt	SLP salt, Chile
Sea Salt B (SSB)	Sea salt free of artificial additives	Maldon Salt, UK

2.2.2. Elaboration of artificial saliva

Artificial saliva was used instead of natural human saliva due to the complexity of accessing and manipulating the latter. Whole saliva is a complex mixture of electrolytes, proteins and other nitrogenous compounds in water (more than 99%). Saliva composition varies greatly both intra- and inter-individuals, thus, standardization and exact duplication of a “human saliva” is impossible (Gal, Fovet, & Myriam, 2001; Humphrey & Williamson, 2001; Schipper, Silletti, & Vingerhoeds, 2007).

Deionized water (W) and two formulations of artificial saliva (AS and AS-Mu), based on inorganic compounds were used to dissolve salt crystals. The solution of artificial saliva AS contained 5.208 g of NaHCO₃, 1.045 g of K₂HPO₄, 0.877 g of NaCl, 0.477 g of KCl and 0.441 g CaCl₂•2H₂O dissolved in 1 L of deionized water. The composition of AS-Mu was the same as AS, with the addition of 2.160 g of mucin (porcine pancreasmucin, Sigma-Aldrich, St. Louis, MO, USA) (Van Ruth, Grossmann, Geary, & Delahunty, 2001).

2.2.3. Viscosity of artificial saliva

Viscosity measurements of AS and AS-Mu were conducted at 25 °C, using a DV-II Brookfield viscometer with a UL adapter spindle (Brookfield Engineering Laboratories, Inc., MA). All measurements were carried at the same speed of 50 rpm, using a volume of 15 mL of sample in each test. The viscosity of each sample was measured after three minutes of starting the procedure.

2.2.4. Determination of moisture content

The moisture content of the salts was determined with an infrared moisture analyzer model MA 30 (Sartorius, Göttingen, Germany) at 130 °C until constant weight. The results are expressed on wet basis.

2.2.5 Determination of insoluble material

Insoluble material was quantified dissolving completely 4.00 g of salt in 200 mL of water by stirring during 20 min at 25 °C. Insoluble material was collected over a hydrophilic filter (0.22 µm pore size, GVWP filter, Millipore Corp., MA, USA) by vacuum filtration and dried at 105 °C in a static oven (Binder WTC, Tuttlingen, Germany) during 48 h until constant weight. The insoluble material was determined by mass difference and expressed as percentage on dry mass basis.

2.2.6. Scanning electron microscopy (SEM) and energy dispersive spectroscopy (EDS)

Samples were examined with a scanning electron microscope (LEO 1420VP, Carl Zeiss, Oberkochen, Germany) equipped with an energy dispersive spectroscopy (EDS) system (Oxford Instruments Ltd., Oxford, United Kingdom). Crystals were fixed on the sample holders using double-side sticky tape. Morphology and surface of crystals was analyzed from images obtained by SEM at an accelerating voltage of 25 kV. EDS gave information about the presence of elemental chemical components.

2.2.7. Porosity

The porosity of salt crystals was determined according to the following relation:

$$\varepsilon = 1 - (\rho_{app} / \rho_t) \quad (2.1)$$

where ε is the porosity (dimensionless), ρ_{app} is the apparent density (kg/m^3), and ρ_t is the true density (kg/m^3) of the solid material (Matějček et al., 2006; Moreno & Bouchon, 2013; Oikonomopoulou, Krokida, & Karathanos, 2013).

The apparent density was determined by the following expression:

$$\rho_{app} = m_s / V_{app} \quad (2.2)$$

where m_s is the mass of dry solids (kg) and V_{app} corresponds to the apparent volume (m^3). The mass of the samples was measured in a UX620H analytical scale (Shimadzu, Philippines) with an accuracy of 10^{-3} g. The apparent volume was determined by the liquid displacement method in a glass pycnometer (accuracy of 0.05 mL) by immersing the samples in n-heptane at ambient temperature (about 25 °C). Results were based on four replicates (Oikonomopoulou, Krokida, & Karathanos, 2013).

The true density of the corresponding solid crystals was obtained from the following relation:

$$\rho_t = m_s / V_t \quad (2.3)$$

where m_s is the mass of dry solids (kg), and V_t corresponds to the true volume (m^3). The true volume was measured with a gas pycnometer ULTRAPYC 1200e (Quantachrome Instruments, Boynton Beach, USA) which operates with nitrogen at 19 psi. Measurements were performed in duplicate.

2.2.8. Kinetics of dissolution of single crystals

A special methodology was developed in order to study the kinetics of dissolution of a single crystal. It consisted of image analysis of video-microscopy images obtained

with a digital videocamera ToupCam Ucmos08000 KPA (Touptek Photonics, China) coupled to a stereo microscope (model SMZ 2B-2T, Nikon Corp., Japan). Image sequences were acquired with ToupView 3.5 software (ToupTek, Zhejiang, China) and recording began when a single particle of salt was placed into the glass capsule in the hot-stage system maintained at a constant temperature (Figure 2.1). Immediately afterwards 500 μL of W or solution (AS or AS-Mu) previously warmed at the temperature of the experiment (20; 25; 30 or 36 ± 1.0 $^{\circ}\text{C}$) were added. Temperatures were selected in the range of ambient temperature (20 $^{\circ}\text{C}$) and close to human body temperature (36 $^{\circ}\text{C}$) because a wide range of salty foods are consumed within this interval. Each salt type was tested in quintuplicate. The recorded images were analyzed with ImageJ 1.45s software (National Institutes of Health, USA) and converted into an 8-bit image, processed (sharpened), and thresholded.

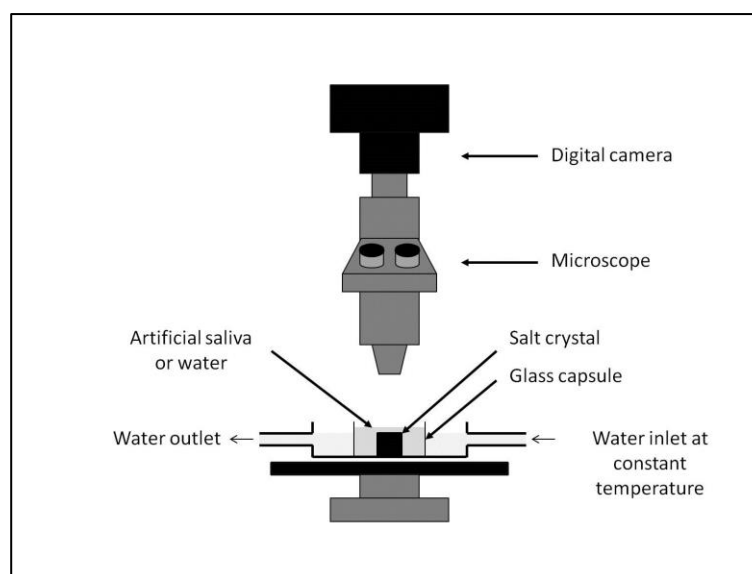


Figure 2.1. System for the *in situ* observation of dissolution of each salt crystal.

The projected area of crystals as a function of time of dissolution was calculated from video-microscopy images by counting pixels, thus, time profiles of dissolution and dissolution rates of salts were estimated. In order to compare the dissolution profiles of different salts, mathematical models (zero order and first order kinetic models) were fitted to data of remaining undissolved crystal area as a function of time.

Images acquired of each crystal before adding the solvent were analyzed to obtain shape parameters. Circularity (C) was calculated by the following expression (Ferreira and Rasband, 2012):

$$C = 4\pi Area/Perimeter^2 \quad (2.4)$$

Aspect ratio (AR) of the ellipse fitting the particle shape was calculated by (Ferreira and Rasband, 2012):

$$AR = Major\ axis/Minor\ axis \quad (2.5)$$

2.2.9. Statistical analysis

Data were subjected to an analysis of variance (ANOVA) and Tukey's test to determine difference between the samples at significance level of $p < 0.05$.

2.3. Results

2.3.1 Viscosity of artificial saliva

Viscosity of solutions of artificial saliva were 2.61 ± 0.01 and 2.89 ± 0.09 mPa·s for AS and AS-Mu respectively. The increase in viscosity in AS-Mu was attributed to the presence of mucin. Human saliva is classified as non-Newtonian fluid, decreasing its viscosity as the shear rate increases, ascribed to the presence of mucin (Schipper, Silletti, & Vingerhoeds, 2007). Thus, viscosity values reported in the literature differ

depending on the measuring conditions, but values of artificial saliva indicated above are within the range reported for human saliva i.e., between 1-10 mPa·s (De Loubens et al., 2011; Rantonen & Meurman, 1998; Schipper, Silletti, & Vingerhoeds, 2007).

2.3.2. Chemical and physical characterization of crystals

Besides being largely Na and Cl, salt has traces of other chemical elements which can be detected by EDS analysis (Table 2.2). The K mineral was found in almost all salts, with exception of SSB and RSB. Sea salts had a different mineral profile than rock salts, e.g., Mg and S were found in both sea salts while Ca was found only in one type of sea salt (SSB). This has also been noted by Drake and Drake (2011) who found higher mineral content in sea salt than in rock salt. In that study the different mineral profiles resulted in distinct salty taste intensity and time-intensity profile. As they have suggested, this fact would possibly allow a reduction in the sodium content of foods by adjusting the mineral profile.

Table 2.2. Characteristics of salt particles studied.

Salt type	Main elements detected by EDS	Insoluble material (%)	Moisture (%)	ρ_{app}	ρ_t	ε
RSA	O, Na, S, Cl, K	1.212 ± 0.268 ^{bc}	2.30 ± 0.02 ^b	1974 ± 0.031 ^a	2148 ± 0.011 ^{ab}	0.081
RSB	O, Na, Cl	1.251 ± 0.179 ^{bc}	0.18 ± 0.01 ^a	2097 ± 0.034 ^b	2145 ± 0.002 ^{ab}	0.022
RSC	O, Na, Cl, K	1.783 ± 0.132 ^c	0.27 ± 0.07 ^a	2109 ± 0.055 ^b	2128 ± 0.009 ^a	0.009
SSA	O, Na, Mg, S, Cl, K	0.943 ± 0.001 ^{ab}	0.69 ± 0.08 ^a	1949 ± 0.038 ^a	2171 ± 0.004 ^b	0.101
SSB	O, Na, Mg, S, Cl, Ca	0.422 ± 0.138 ^a	4.07 ± 0.30 ^c	1961 ± 0.048 ^a	2176 ± 0.019 ^b	0.099

Means followed by different letters in each column indicate significant differences according to ANOVA and Tukey's test ($p < 0.05$).

ρ_{app} : Apparent density (kg/m³), mean of four replicates

ρ_t : True density (kg/m³), mean of two replicates

ε : Porosity (dimensionless)

NaCl crystals are commonly translucent or white, however, since mineral impurities are absorbed from surroundings, salts can display an assortment of colors (Weselucha-Birczyńska, Tobała, & Natkaniec-Nowak, 2008). For example, different sea salts have varieties of color such as grey, black, pink, peach and brownish-red (Drake & Drake, 2011). Of the salts studied in this work, RSA, RSB, SSA and SSB were white, but crystals of RSC were white with blue inclusions. According to the supplier their blue color comes from potassium (<http://www.terreexotique.fr/en/eboutique/produit/553/persian-blue-salt-for-grinder>) and EDS analysis confirmed that potassium was present in blue section of RSC crystals.

The insoluble material varied among the salts studied. Rock salts had the highest content of insoluble material (Table 2.2) while SSB had the lowest amount of insoluble material, the salt free of additives. On the other hand, the moisture content of the salts used in the experiments varied significantly; RSB, RSC and SSA crystals had the lowest water content (0.18 ± 0.01 ; 0.27 ± 0.07 ; and 0.69 ± 0.08 %), while SSB had the highest (4.07 ± 0.30 %) (Table 2.2).

The difference in the morphology of salt types could be observed from the SEM images (Figure 2.2). In general, the crystals did not exhibit simple cubical shapes and some of them showed agglomeration of units of different sizes. The rock salts were similar in morphology being simple crystals and crystals with primary agglomeration, which according to a Mersmann's definition correspond to the result of malgrowth during crystallization (Mersmann, 2001). Salt crystals formed from pure aqueous solutions

have a cubic form but their shape changes when impurities, such as mineral components as well as of other insoluble materials, are added to the solution (Aquilano, Pastero, Bruno, & Rubbo, 2009; Ferreira, Faria, Rocha, Feyer de Azevedo & Lopes, 2005; Glusker, Lewis, & Rossi, 1994).

The SSA crystals had morphologies with primary and secondary agglomerates according to Mersmann's classification (Mersmann, 2001). Secondary agglomeration is the result of crystal-crystal collision in a solution. In SSA crystals small crystals were observed adhered to the surface of large crystals or incrustated into the structure (Figure 2.2d). SSB were pyramidal flaked crystals (Figure 2.2e) with the presence of voids in the crystals.

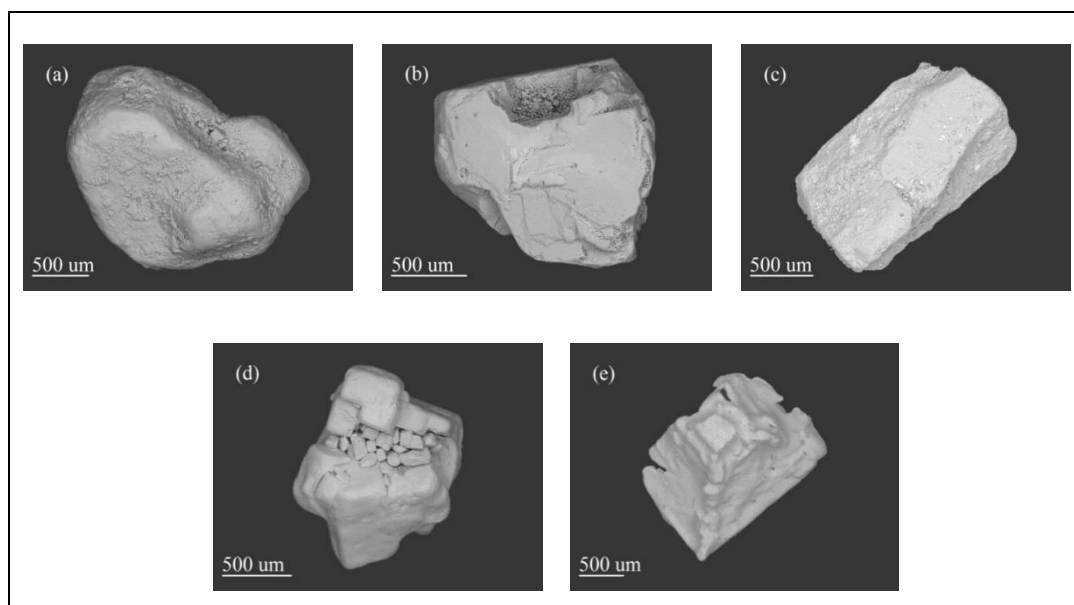


Figure 2.2. Scanning electron photomicrographs of representative crystals: (a) RSA, (b) RSB, (c) RSC, (d) SSA, and (e) SSB.

The true density of rock and sea salts were (Table 2.2) similar to values reported in the literature (e.g., 2165 kg/m³) (Lide, 2005), except for RSC (2128 kg/m³) that showed the lowest density. This can be attributed to the presence of a higher amount of potassium which has a lower density (1988 kg/m³) (Lide, 2005). Apparent density of rock salt was higher than sea salt, except for RSA that was similar to sea salts. These differences of densities are due to the irregularity in the shape of salt particles (Kelly & McMurry, 2014). Differences in density also explain differences in the porosity of salt particles (Table 2.2): a low porosity for rock salts (between 0.009 and 0.081), and a high porosity for sea salt. SSA with small crystals incrusting in the surface had the highest porosity (0.101), followed by SSB pyramidal salt (0.099). These values seem to agree with SEM images that show a compact structure for rock salts and a more open surface structure of SSA (Figure 2.2).

Significant differences on projected area were found between salts, despite the sieving classification (Table 2.3). Size determination based on projected area is biased by the equilibrium position adopted by the crystal, and this in turn is influenced by crystal morphology that was different between salt types. SSB (pyramidal shape) had the highest value of projected area followed by samples RSA, RSC, RSB, and SSA.

The shape parameters based on the projected area of crystals before dissolution also showed significant differences between salt types (Table 2.3). The circularity (1 for a perfect circle and a value tending to 0 indicating an increasingly elongated shape), was highest in RSA and RSB, followed by RSC and SSA, whereas the lowest circularity was for SSB. Lastly, aspect ratio and area/perimeter relationship were similar between salt types, except for RSC that was different from the other salt types. Shape parameters

of salt crystals largely depend on growth rate, i.e., impurity presence and concentration, and supersaturation (Ferreira *et al.*, 2005).

Table 2.3. Area and shape parameters for single crystals before dissolution.

Salt type	Area (mm ²)	Circularity*	Aspect ratio**
RSA	2.26 ± 0.42 ^c	0.71 ± 0.07 ^c	1.41 ± 0.26 ^a
RSB	1.86 ± 0.37 ^{ab}	0.71 ± 0.06 ^c	1.41 ± 0.29 ^a
RSC	2.03 ± 0.42 ^b	0.66 ± 0.07 ^b	1.61 ± 0.38 ^b
SSA	1.79 ± 0.50 ^a	0.67 ± 0.06 ^b	1.46 ± 0.32 ^{ab}
SSB	2.62 ± 0.46 ^d	0.60 ± 0.08 ^a	1.44 ± 0.33 ^a

Means of 60 replicates for each salt type followed by different letters in a column are significantly different according to ANOVA and Tukey's test ($p < 0.05$).

* Circularity is defined as $4 \cdot \pi \cdot \text{area}/\text{perimeter}^2$.

** Aspect ratio is the relation between the major and the minor axis of an equivalent ellipse

2.3.3. Dissolution kinetics of single crystals

The dissolution profile and a sequence of images taken every 20 s during the dissolution of a single crystal are presented in Figure 2.3. In order to analyze the dissolution profile models were adjusted to the relation between crystal area (%) and time (s). After an initial lag period RSA, RSB, RSC and SSA showed a linear behavior (R^2 between 0.8325 and 0.9996), corresponding to a zero order kinetic model given by the following equation:

$$A_t = -K_0 t + A_0 \quad (2.6)$$

where A_t is the crystal area (as percentage of the initial area) at time t (s), K_0 is a proportionality constant related to the dissolution velocity and A_0 is the initial crystal

area. Generally, this model represents adequately the dissolution of solutes that do not disaggregate and are slowly dissolved (Costa & Sousa, 2001).

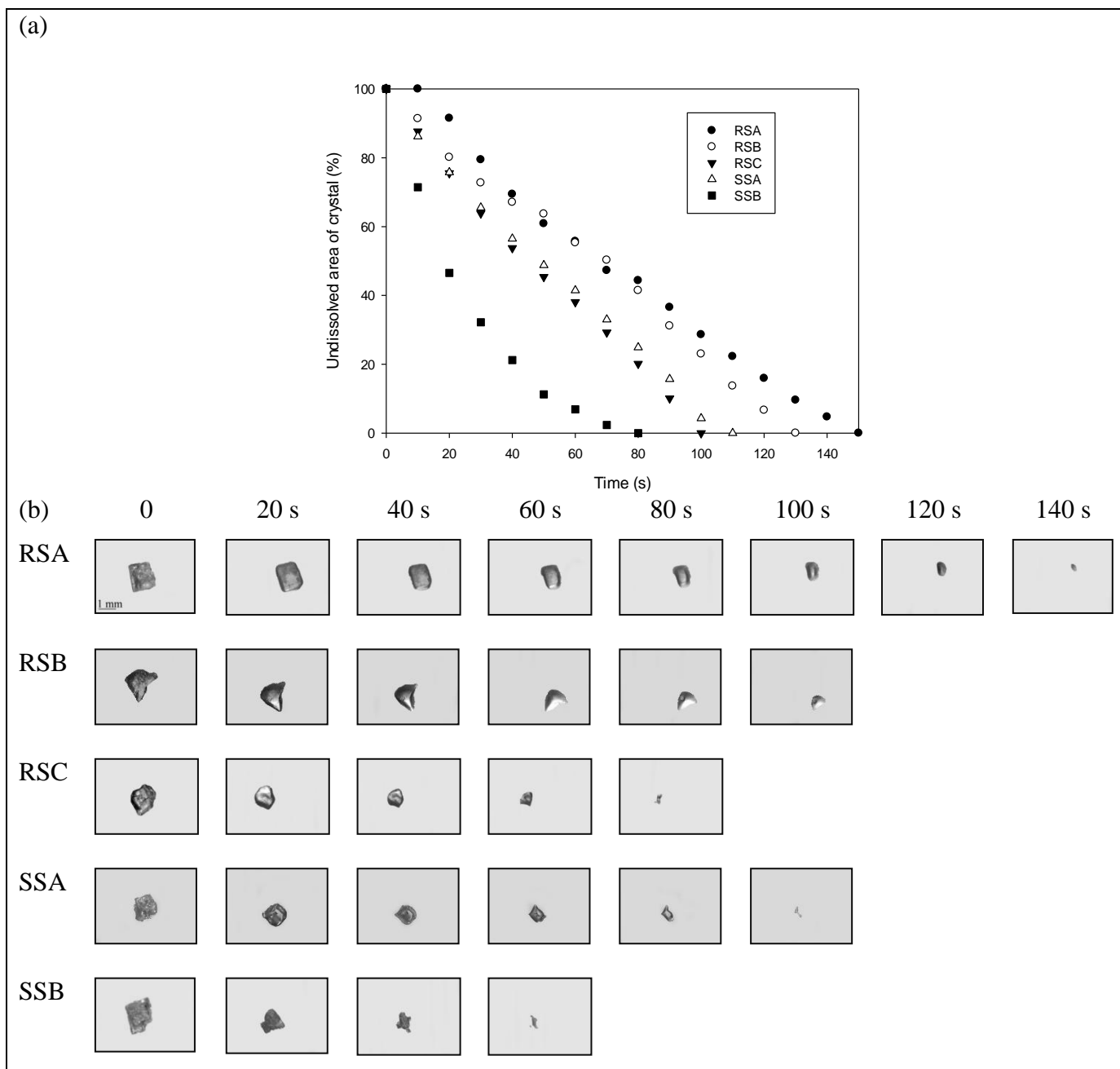


Figure 2.3. (a) Representative dissolution curves of single salt crystals of different samples dissolved at 36 °C in AS-Mu, and; (b) microscopy images for the sequence of the dissolution.

The differences in K_0 values of these commercial salts are shown in Table 2.4. Significant differences were found in K_0 values by multifactor ANOVA having as independent variables salt type, dissolution media and temperature (analysis not shown). RSA had the lowest K_0 , indicating a slow dissolution, followed by RSB and SSA with similar K_0 values and finally, RSC which had the highest K_0 . In order to see more clearly the effect of dissolution media and temperature on K_0 two-way ANOVA was carried out and results are in Table 2.4.

Table 2.4. Rate constants of dissolution kinetics ($K \cdot 10^{-4}$ values in s^{-1}) of the different commercial salts. K_0 were calculated for samples RSA, RSB, RSC and SSA, while K_1 was calculated for samples of SSB salt after fitting data to a zero and first order kinetic models, respectively.

Solution/ Temperature (°C)	Salt type				
	RSA	RSB	RSC	SSA	SSB
Water					
20	73 ± 13 ^{aAB}	76 ± 12 ^{aA}	99 ± 15 ^{aA}	62 ± 12 ^{aA}	536 ± 115 ^{aA}
25	72 ± 21 ^{aA}	110 ± 12 ^{aB}	90 ± 7 ^{aA}	77 ± 12 ^{aA}	472 ± 111 ^{aA}
30	75 ± 8 ^{aAB}	80 ± 15 ^{aAB}	93 ± 8 ^{aB}	86 ± 17 ^{aAB}	597 ± 143 ^{aA}
36	75 ± 8 ^{aB}	102 ± 7 ^{aB}	140 ± 40 ^{aB}	101 ± 13 ^{aB}	944 ± 215 ^{aB}
AS					
20	62 ± 10 ^{bAB}	84 ± 10 ^{bA}	76 ± 11 ^{abA}	79 ± 25 ^{aA}	388 ± 66 ^{aA}
25	60 ± 7 ^{bA}	78 ± 14 ^{bB}	91 ± 10 ^{abA}	75 ± 13 ^{aA}	638 ± 72 ^{aA}
30	63 ± 5 ^{bAB}	84 ± 7 ^{bAB}	116 ± 12 ^{abB}	65 ± 11 ^{aAB}	456 ± 60 ^{aA}
36	74 ± 19 ^{bB}	92 ± 20 ^{bB}	102 ± 11 ^{abB}	86 ± 18 ^{aB}	672 ± 161 ^{aB}
AS-Mu					
20	59 ± 7 ^{bAB}	56 ± 11 ^{cA}	70 ± 12 ^{bA}	79 ± 10 ^{aA}	472 ± 174 ^{aA}
25	58 ± 6 ^{bA}	74 ± 10 ^{cB}	66 ± 12 ^{bA}	71 ± 8 ^{aA}	462 ± 87 ^{aA}
30	70 ± 6 ^{bAB}	73 ± 16 ^{cAB}	103 ± 12 ^{bB}	83 ± 5 ^{aAB}	559 ± 68 ^{aA}
36	74 ± 3 ^{bB}	92 ± 20 ^{cB}	91 ± 13 ^{bB}	92 ± 19 ^{aB}	603 ± 132 ^{aB}

Means of 5 replicates with different superscript letters in columns are significantly different ($p < 0.05$) for two-way ANOVA and Tuckey test with solution type (small letters) and temperature (capital letters).

Dissolution media had a significant effect on salt solubilization for samples RSA, RSB and RSC, with W having higher K_0 than artificial salivas. The increment in viscosity due to the presence of electrolytes and the weak gelling effect of mucin (Schipper, Silletti, & Vingerhoeds, 2007), may explain this reduction in K_0 . Temperature of the solution had a positive effect on dissolution rate, although it has been reported that salt dissolution depends slightly of temperature (Zijlema, Holman, Witkamp, & Van Rosmalen, 1999).

The dissolution of SSB crystals was adjusted to a first order kinetics (R^2 between 0.8405 and 0.9964) (Table 2.4). The following equation expresses this model:

$$\ln (A_t/A_0) = K_1 t \quad (2.7)$$

where A_t is the crystal area (as percentage of initial area) at time t (s), K_1 is the first order dissolution constant and A_0 is the initial crystal area. This model has been applied when the dissolution of solutes is proportional to the amount of solute remaining undissolved (Costa & Sousa, 2001). The different kinetic observed for SSB was attributed to the fractionation of most of the crystals as observed directly in video-microscopy images. Figure 2.4 shows the percentage of crystals that were fragmented for each salt type (Figure 2.4a) and image sequences of crystals that were dissolved as a block or fragmented (Figure 2.4b). While fractionation in SSB salt was observed in close to 90 % of crystals, this percentage did not exceed 28 % for other salt types.

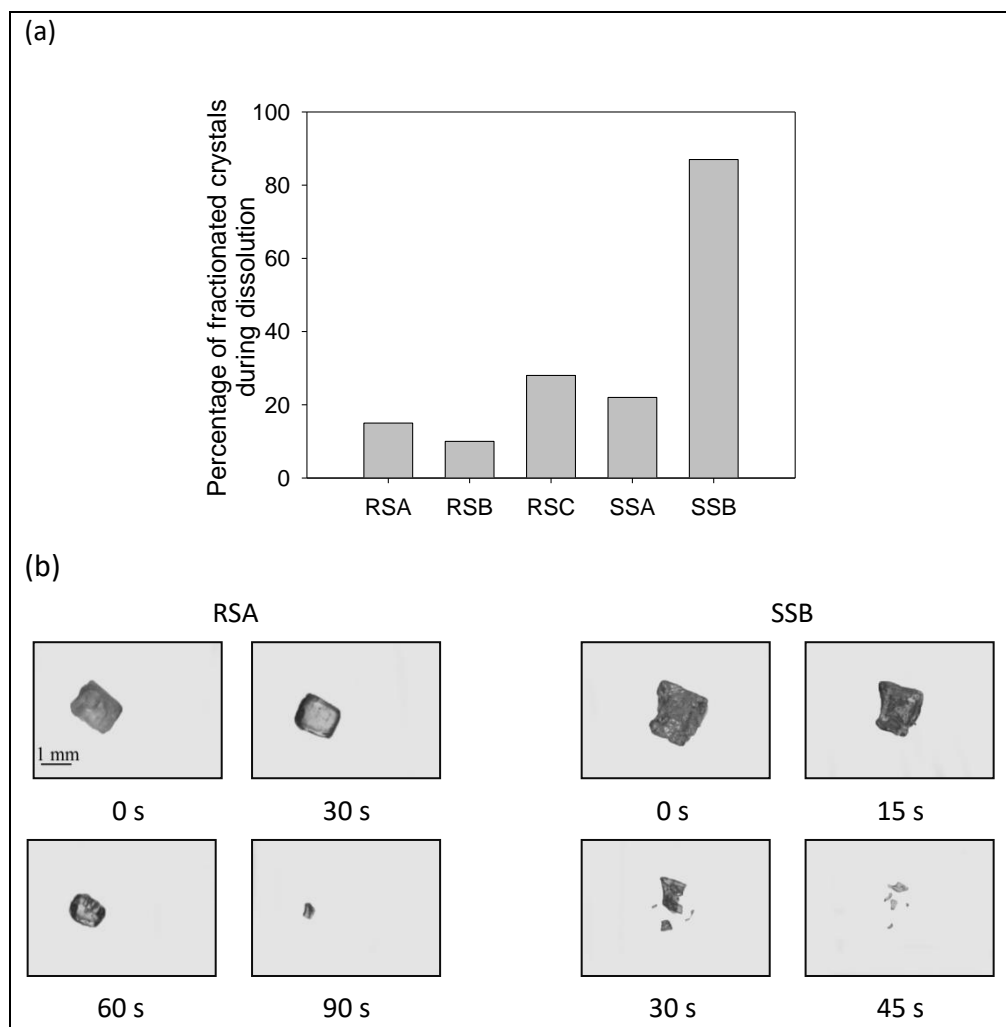


Figure 2.4. Behavior of crystals during dissolution. (a) Percentage of fractionated crystals of different salts ($n = 60$ per salt type). (b) Representative image sequences of dissolution of a salt crystal in water at $25\text{ }^{\circ}\text{C}$, that is not fragmented (RSA) and another that is fragmented (SSB).

Samples were compared in their total dissolution time after grouping by salt type, media of dissolution and temperature. Figure 2.5 shows that the SSB salt exhibited the shortest dissolution time followed by RSC, RSB, and SSA while RSA showed the longer dissolution time. Results correlated with circularity ($R^2 = 0.812$): a lower

circularity yielding a faster dissolution. Less circular and pyramidal crystals with a large surface area (and fractionated during dissolution, increasing the total surface area) had the fastest dissolution, indicating that morphology differences among salts are influential in their dissolution rate. Sensorial studies of salty foods (such as meat pate, popcorn and potato chips) have shown that size and shape of salt crystals influence in salt intensity (Jensen *et al.*, 2011; Kilcast & Den Ridder, 2007; Shepher, Wharf, & Farleigh, 1989). Small particles and hollow pyramids exhibited higher salty intensity than cubic and dense morphologies. Rapid rise in perceived salty taste intensity is related with rapid dissolution rates of crystals (Vella, Marcone, & Duizer, 2012). RSC, the salt type that had the second faster total dissolution time and highest K_0 , had blue inclusions attributed to KCl, known to have a different solubility than NaCl, depending on temperature (Pinho & Macedo, 2005). Above 30 °C KCl solubility in water is slightly higher than that of NaCl, but this difference increases with temperature (Hamlin, Northam, & Wagner, 1965; Pinho & Macedo, 2005; Remington, 2006). Thus, the presence of inclusions of KCl in the salt crystal may modify its dissolution rate at temperatures above 30 °C.

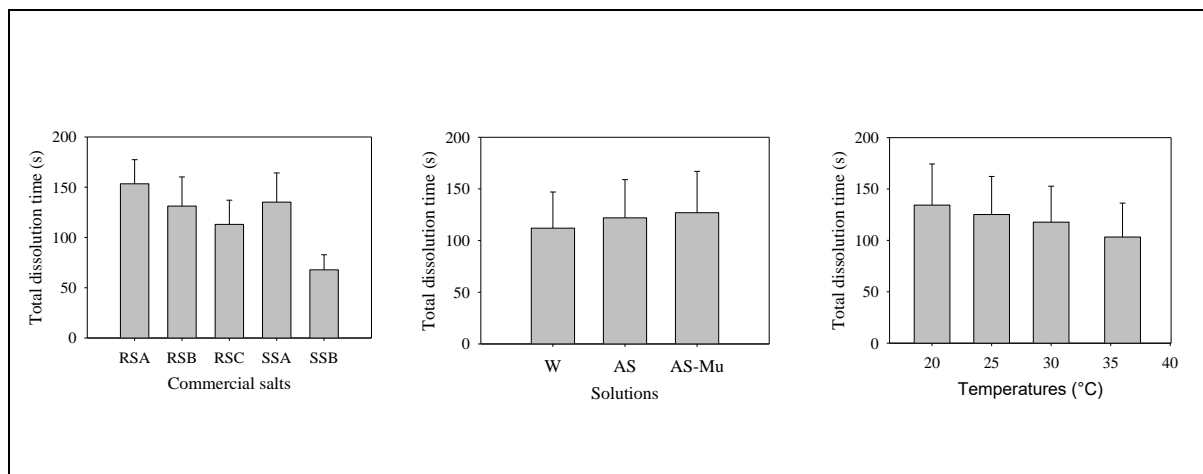


Figure 2.5. Average dissolution time (pooled values of all data) of salt crystals from different commercial salts and effect of solution type and temperature.

To use all the salt potential as tastant in foods complete dissolution of crystals in the mouth should be achieved. In only 20-30 s of mastication time (residence time in the mouth), crystals should be solubilized, release the ions that must diffuse and be detected by the receptors of saltiness. Undissolved crystals remaining after this time are swallowed and do not contribute to taste (Kilcast & Den Ridder, 2007; Tian & Fisk, 2012). Under the conditions of this study (average size 1.20 mm and system without agitation) SSB crystals were dissolved on average in 68 s, although according to average residence times of foods in the mouth the target for total dissolution is less than 20 - 30 s. Agitation due to mastication as well as smaller sizes could have an important effect in diminishing the time of total dissolution. Size reduction of salt crystals (increasing surface area per unit volume) allows increases the dissolution rate in saliva (De Loubens *et al.*, 2011; Rama *et al.*, 2013).

The morphology of salt crystals not only influences solubilization but also adhesion onto solid foods. Hollow pyramids and crushed flake morphologies have more surface area than cubic shapes and therefore have better adherence onto popcorn (Miller & Barringer, 2002). For potato chips, cubic crystals demonstrated the best adhesion followed by flake and dendritic crystals, but the oily surface may have a great influence on adhesion (Buck & Barringer, 2007).

To accomplish an optimum food design and minimize salt content, spatial distribution of salt in the matrix should be considered. A heterogeneous salt distribution allows that salt delivery be at different levels or in the form of pulses, thus, allowing a lower salt content without reducing the salt taste perception (Emorine, Septier, Thomas-Danguin & Salles, 2013; Noort, Bult, Stieger & Hamer, 2010). Thus, controlling salt distribution within the food and increasing salt dissolution in saliva (using crystals with morphologies exhibiting high surface area and that are fragmented into smaller crystals during dissolution), may be an alternative to diminish the salt content.

2.4. Conclusions

Analysis of video-microscopy images taken during the immersion of single salt crystals (sieved to particle size of 1.00 - 1.40 mm) in water and artificial saliva has been demonstrated to generate quantitative data to assess the kinetics of dissolution. Type and morphology of salt crystals were important factors affecting the rate of dissolution in both media. Moreover, video-microscopy was instrumental in providing direct information on the effect of particle fragmentation and its positive effect (due to a larger surface area in contact with the solution) on the rate of dissolution. Contact

area has been demonstrated to be the major factor in the rate of release of salt from food matrices. It appears that salt crystals that effectively release Na in the mouth may be tailored-made into porous structures by lightly sticking together microcrystals that are easily released after dissolution of the bridges between them.

Further work should be accomplished by studying the effect of other particle sizes, different crystal morphologies and the presence of agitation under stress rates similar to those existing in the mouth.

Acknowledgments

Author Quilaqueo acknowledges the financial support of CONICYT.

References

- Aquilano, D., Pastero, L., Bruno, M., & Rubbo, M. (2009). {100} and {111} forms of the NaCl crystals coexisting in growth from pure aqueous solution. *Journal of Crystal Growth*, 311, 399-403.
- Brown, I. J., Tzoulaki, I., Candeias, V., & Elliott, P. (2009). Salt intakes around the world: implications for public health. *International Journal of Epidemiology*, 38, 791-813.
- Buck, V. E., & Barringer, S. A. (2007). Factors dominating adhesion of NaCl onto potato chips. *Journal of Food Science*, 72, E435-E441.
- Busch, J. L. H. C., Yong, F. Y. S., & Goh, S. M. (2013). Sodium reduction: Optimizing product composition and structure towards increasing saltiness perception. *Trends in Food Science & Technology*, 29, 21-34.
- Chen, J., & Engelen, L. (2012). Role of saliva in the oral processing of food. In G. Carpenter (Ed.), *Food Oral Processing: Fundamentals of Eating and Sensory Perception* (pp. 45-60). Singapore: Wiley-Blackwell.
- Codex Alimentarius Commission. (1997). *Codex Standard for Food Grade Salt*. Codex Stan 150-1985 Rev. 1-1997.
- Costa, P., & Sousa, J. M. (2001). Modeling and comparison of dissolution profiles. *European Journal of Pharmaceutical Sciences*, 13, 123-133.
- Cruz, A. G., Faria, J. A. F., Pollonio, M. A. R., Bolini, H. M. A., Celeghini, R. M. S., Granato, D., & Shah, N. P. (2011). Cheeses with reduced sodium content: Effects on functionality, public health benefits and sensory properties. *Trends in Food Science & Technology*, 22, 276-291.
- D'Elia, L., Rossi, G., Ippolito, R., Cappuccio, F. P., & Strazzullo, P. (2012). Habitual salt intake and risk of gastric cancer: A meta-analysis of prospective studies. *Clinical Nutrition*, 31, 489-498.
- De Loubens, C., Panouillé, M., Saint-Eve, A., Déléris, I., Tréléa, I. C., & Souchon, I. (2011). Mechanistic model of *in vitro* salt release from model dairy gels based on standardized breakdown test simulating mastication. *Journal of Food Engineering*, 105, 161-168.
- Drake, S. L., & Drake, M. A. (2011). Comparison of salty taste and time intensity of sea and land salts from around the world. *Journal of Sensory Studies*, 26, 25-34.
- Emorine, M., Septier, C., Thomas-Danguin, T., & Salles, C. (2013). Heterogeneous salt distribution in hot snacks enhances saltiness without loss of acceptability. *Food Research International*, 51, 641-647.

- Ferreira, A., Faria, N., Rocha, F., Feyo de Azevedo, S., & Lopes, A. (2005). Using image analysis to look into the effect of impurity concentration in NaCl crystallization. *Chemical Engineering Research & Design*, 83, 331-338.
- Ferreira, T., & Rasband, W. (2012). *ImageJ User Guide*. IJ 1.46r. <http://imagej.nih.gov/ij/docs/guide/>
- Gal, J., Fovet, Y., & Myriam, A. (2001). About a synthetic saliva for *in vitro* studies. *Talanta*, 53, 1103-1115.
- Glusker, J. P., Lewis, M., & Rossi, M. (1994). *Crystal Structure Analysis for Chemists and Biologists*. New York: Wiley-VCH, (Chapter 2).
- Hamlin, W.E., Northam, J.I., & Wagner, J.G. (1965). Relationship between *in vitro* dissolution rates and solubilities of numerous compounds representative of various chemical species. *Journal of Pharmaceutical Sciences*, 54, 1651-1653.
- Harring, T. R., Deal, N. S., & Kuo, D. C. (2014). Disorders of sodium and water balance. *Emergency Medicine Clinics of North America*, 32, 379-401.
- Humphrey, S. P., & Williamson, R. T. (2001). A review of saliva: Normal composition, flow, and function. *The Journal of Prosthetic Dentistry*, 85, 162-169.
- Jensen, M., Smith, G., Fear, S., Schimoeller, L., & Johnson, C. (2011). Seasoning and method for seasoning a food product while reducing dietary sodium intake. United States Patent. US 7,923,047 B2.
- Kaplan, N. (2000). The dietary guideline for sodium: should we shake it up? No. *The American Journal of Clinical Nutrition*, 71, 1020-1026.
- Kelly, W. P., & McMurry, P. H. (2014). Measurement of particle density by inertial classification of differential mobility analyzer-generated monodisperse aerosols. *Aerosol Science & Technology*, 17, 199-212.
- Kilcast, D., & Den Ridder, C. (2007). Sensory issues in reducing salt in food products. In Kilcast, D. & Angus, F. (Eds.), *Reducing Salt in Foods: Practical Strategies* (pp. 201-220). Cambridge: Woodhead Publishing Limited.
- Kraus, E. & Hunt, W. (1920). *Mineralogy: An Introduction to the Study of Minerals and Crystals*. (1th edition). New York: McGraw-Hill, (Chapter XVI).
- Lauverjat, C., De Loubens, C., Déléris, I., Tréléa, I. C., & Souchon, I. (2009). Rapid determination of partition and diffusion properties for salt and aroma compounds in complex food matrices. *Journal of Food Engineering*, 93, 407-415.
- Lide, D. R. (2005). *CRC Handbook of Chemistry and Physics*. (86th edition). Boca Raton: CRC Press. Boca Raton, (Section 4).

- Lvova, L., Denis, S., Barra, A., Mielle, P., Salles, C., Vergoignan, C., Di Natale, C., Paolesse, R., Temple-Boyer, P., & Feron, G. (2012). Salt release monitoring with specific sensors in “*in vitro*” oral and digestive environments from soft cheeses. *Talanta*, 97, 171-180.
- Matějčíček, J., Kolman, B., Dubský, J., Neufuss, K., Hopkins, N., & Zwick, J. (2006). Alternative methods for determination of composition and porosity in abrasible materials. *Materials Characterization*, 57, 17-29.
- Mersmann, A. (2001). *Crystallization Technology Handbook*, (2nd edition). New York: Marcel Dekker, (Chapter 6).
- Miller, M. J., & Barringer, S. A. (2002). Effect of NaCl particle size and shape on nonelectrostatic and electrostatic coating of popcorn. *Food Engineering and Physical Properties*, 67, 198-201.
- Moreno, M. C., & Bouchon, P. (2013). Microstructural characterization of deep-fat fried formulated products using confocal scanning laser microscopy and a non-invasive double staining procedure. *Journal of Food Engineering*, 118, 238-246.
- Murphy, C., Cardello, A., & Brand, J. (1981). Tastes of fifteen halide salts following water and NaCl: Anion and cation effects. *Physiology & Behavior*, 26, 1083-1095.
- Noort, M. W. J., Bult, J. H. F., Stieger, M., & Hamer, R. J. (2010). Saltiness enhancement in bread by inhomogeneous spatial distribution of sodium chloride. *Journal of Cereal Science*, 52, 378-386.
- Oikonomopoulou, V., Krokida, M., & Karathanos, V. (2013). Influence of structure on saltiness and sweetness of dehydrated food products. *Drying Technology*, 31, 837-847.
- Pinho, S., & Macedo, E. (2005). Solubility of NaCl, NaBr, and KCl in water, methanol, ethanol, and their mixed solvents. *Journal of Chemical and Engineering Data*, 50, 29-32.
- Rama, R., Chiu, N., Carvalho, M., Hewson, L., Hort, J. & Fisk, I. (2013). Impact of salt crystal size on in-mouth delivery of sodium and saltiness perception from snack foods. *Journal of Texture Studies*, 44, 338-345.
- Rantonen, P., & Meurman, J. (1998). Viscosity of whole saliva. *Acta Odontologica Scandinavica*, 56, 210-214.
- Remington, J. P. (2006). *Remington: The science and practice of pharmacy*. (21st edition). Philadelphia: Lippincott Williams & Wilkins, (Part 2).
- Schipper, R. G., Silletti, E., & Vingerhoeds, M. H. (2007). Saliva as research material: Biochemical, physicochemical and practical aspects. *Archives of Oral Biology*, 52, 1114-1135.

Shepher, R., Wharf, S. G., & Farleigh, C. A. (1989). The effect of a surface coating of table salt of varying grain size on perceived saltiness and liking for paté. *International Journal of Food Science and Technology*, 24, 333-340.

Tian, X., & Fisk, I. D. (2012). Salt release from potato crisps. *Food & Function*, 3, 376.

Van Ruth, S. M., Grossmann, I., Geary, M., & Delahunty, C. M. (2001). Interactions between artificial saliva and 20 aroma compounds in water and oil model systems. *Journal of Agricultural and Food Chemistry*, 49, 2409-2413.

Vella, D., Marcone, M., & Duizer, L. M. (2012). Physical and sensory properties of regional sea salts. *Food Research International*, 45, 415-421.

Wesełucha-Birczyńska, A., Tobała, T., & Natkaniec-Nowak, L. (2008). Raman microscopy of inclusions in blue halites. *Vibrational Spectroscopy*, 48, 302-307.

WHO. (2012). *Guideline: Sodium intake for adults and children*. Geneva, World Health Organization (WHO).

Zijlema, T. G., Holman, R. J. A. J., Witkamp, G. J., & Van Rosmalen, G. M. (1999). The production of pure NaCl by the antisolvent crystallisation of NaCl 2H₂O and a consecutive recrystallization step. *Journal of Crystal Growth*, 198/199, 789-795.

3. THE MORPHOLOGY OF SALT CRYSTALS AFFECTS THE PERCEPTION OF SALTINESS

3.1. Introduction

High sodium intake has been associated with a high risk of non-communicable diseases (NCDs), including hypertension, cardiovascular disease and stroke. NCDs are the main contributor to mortality and morbidity in the world. Reducing salt intake, the main source of sodium in the diet, could therefore be an important target for improving public health (WHO, 2003; 2012; Bibbins-Domingo et al., 2010). The maximum level of sodium intake recommended by the World Health Organization is 2 g per day for adults (≥ 16 years old) equivalent to 5 g of salt (NaCl) per day (WHO, 2003; 2012). However, most people consume too much salt, on average between 9 and 12 g per day, or around twice the recommended maximum level of intake (WHO, 2014).

The main source of sodium in the diet comes from salt that is added to foods. In the USA and Europe, between 75-80% of salt intake comes from processed foods (Brown, Tzoulaki, Candeias, & Elliott, 2009; Mattes & Donnelly, 1991). Therefore, it is necessary for the food industry to implement strategies to reduce the content of salt.

Several strategies have been developed by the industry to reduce the level of sodium in foods while maintaining the overall quality and acceptability. Most of these are strategies focused on cognitive mechanisms (increasing consumer awareness of preferring low sodium foods) and chemical approaches (using ingredients to increase the perception of true saltiness). The option of designing structures to optimize the

perception of saltiness has received lesser attention (Busch, Yong, & Goh, 2013). It emphasizes the control of the release of salt from food matrices, its delivery in the oral cavity, and the generation of saltiness perception (Kuo & Lee, 2014). Thus, this strategy involves the improvement of the dissolution rate of crystals from dry foods, the spatial distribution of salt in food matrices, and the textural effects on the food matrix (Busch, Yong, & Goh, 2013).

Phan et al. (2008) showed that between 70-95% of sodium (or salt) may remain in the food matrix after swallowing. With regard to salt crystals applied topically to dry foods (i.e. potato chips), Tian and Fisk (2012) suggest that a significant proportion of sodium can be swallowed without being perceived, because saltiness is not perceived when the sodium is delivered after swallowing. Ideally most sodium in the matrix should become solubilized and contribute to the perception of saltiness.

There is a relationship between the dissolution rate of salt crystals and perception of saltiness. Salt crystals that have a greater surface area are dissolved faster. Increasing the surface area of a crystal can be achieved with a smaller crystal size, a hollow shape, or a crystal structure that can be fractionated during dissolution (Jensen, Smith, Fear, Schimoeller, & Johnson, 2011; Rama et al., 2013; Quilaqueo & Aguilera, 2015). However, the influence of characteristics of different salt types, specifically different morphologies, origin, composition, on dissolution rate and perception of saltiness, remains relatively unstudied (Quilaqueo & Aguilera, 2015; Vella, Marcone, & Duizer, 2012). The aim of this paper is to study the dissolution of salt crystals with different morphologies using artificial saliva, and to correlate the results with the perception of salt intensity over time.

3.2. Materials and methods

3.2.1 Materials

Five varieties of commercial salts were used in this work (Table 3.1), selected by their morphology. A uniform size fraction of crystals was isolated between sieves number 20 and 14 (0.850 and 1.41 mm of aperture respectively) by manually sieving 200 g of each salt variety for 2 min.

Table 3.1. Description of commercial salts analyzed and amount of salt containing 20 mg of sodium (used for sensory testing).

Salt type	Description	Supplier	Salt amount (g)
Brittany Grey	Grey sea salt free of artificial additives	Drogheria e alimentari SpA, France	0.056
Extra Coarse	Iodized salt from rock deposits	SLP salt, Chile	0.053
Kosher	Diamond crystals free of artificial additives	Cargill Inc., USA	0.052
Maison Orphée	Grey sea salt free of artificial additives	La Maison Orphée Inc., France	0.055
Maldon	Sea salt free of artificial additives	Maldon Salt, UK	0.049

3.2.2 Salt characterization

3.2.2.1 Mineral analysis

Minerals, sodium, calcium, magnesium, phosphorous, potassium, sulfur, and iron in salt crystals were determined by inductively coupled plasma optical emission

spectrometry (VISTA-pro, Varian Canada, Mississauga, ON, Canada). Samples were evaluated in duplicate.

3.2.2.2 Moisture content

The moisture content of the salt crystals was obtained through an infrared moisture analyzer (MA 30, Sartorius, Göttingen, Germany) working at 130 °C until constant weight of sample. The results are expressed on wet basis of triplicates.

3.2.2.3 Apparent density

The apparent density (ρ_{app}) was determined by the equation $\rho_{app} = m_s/V_{app}$ where m_s is the mass of dry solids (kg) and V_{app} corresponds to the apparent volume (m³). The mass of the samples was determined in a UX620H analytical scale (Shimadzu, Philippines). The apparent volume was obtained by liquid displacement in a glass pycnometer (accuracy of 0.05 mL) after immersing the samples in n-heptane at ambient temperature (about 25 °C). Results were based on four replicates (Oikonomopoulou, Krokida, & Karathanos, 2013).

3.2.2.4 Scanning electron microscopy and micro computed tomography

Samples of salt were assessed by scanning electron microscopy (SEM) (Hitachi S 570, Hitachi High Technologies, Tokyo, Japan) at an accelerating potential of 10 kV. Salt crystals were placed on a specimen stub and coated with gold/palladium. At least triplicate specimens were viewed at several magnifications.

In order to examine qualitatively the external and internal structure of crystals qualitatively, micro computed tomography (micro-CT) was done. Micro-CT scanning was carried out in single crystal (at least one of each sample) using Skyscan 1272 (Bruker MicroCT, Kontich, Belgium). The 3D reconstruction was done with the software programs called NRecon and CTvox (Bruker microCT, Kontich, Belgium).

3.2.2.5 Optical microscopy

The morphology of salt crystals was assessed by image analysis of images obtained by optical microscopy. Crystals deposited on a glass slide were observed under stereo microscope (SMZ 2B-2T, Nikon Corp., Japan) and images were acquired with a digital camera ToupCam (Ucmos08000 KPA, Touptek Photonics, China) coupled to the microscope and using ToupView 3.5 software (ToupTek, Zhejiang, China). The images obtained were processed and analyzed using ImageJ 1.45s software (National Institutes of Health, USA).

2D shape and size descriptors were determined, based on image analysis. The descriptors were: projected area (A); equivalent diameter ($D_{eq} = 2\sqrt{A/\pi}$); circularity ($C = 4\pi(A/P^2)$) where P corresponds to perimeter; Feret diameter (F) distribution, from which the maximal (F_{max}) and minimal (F_{min}) were determined; elongation ($E = F_{max}/F_{min}$); and aspect ratio ($AR = \text{Major axis}/\text{Minor axis of fitted ellipse}$) (Ferreira, Faria, Rocha, Fayo de Azevedo & Lopes, 2005; Ferreira & Rasband, 2012).

3.2.3 Crystal dissolution in artificial saliva by video-microscopy

The dissolution of single crystals in artificial saliva at 37 °C was assessed by image analysis of video-microscopy images as described in Quilaqueo and Aguilera (2015).

The artificial saliva was composed by 5.208 g of NaHCO₃, 1.045 g of K₂HPO₄, 0.877 g of NaCl, 0.477 g of KCl, 0.441 g CaCl₂·2H₂O and 2.160 g of mucin (porcine pancreasmucin, Sigma-Aldrich, St. Louis, MO, USA) dissolved in 1 L of deionized water. NaN₃ was added at a concentration of 0.5 g/L to prevent microbial growth (Van Ruth, Grossmann, Geary, & Delahunty, 2001).

The acquisition of images during crystal dissolution was performed as described before for single crystals. Recording began when a single particle of salt was placed into a glass capsule. Immediately after artificial saliva (500 µL) at 37 °C was added and temperature was maintained through a hot-stage system (Quilaqueo & Aguilera, 2015). Recorded images were processed and analyzed with ImageJ 1.45s software (National Institutes of Health, USA) and each salt type was tested at least in quintuplicate.

The dissolution rate was calculated based on the reduction of the projected area of crystals over time and the dissolution kinetics were fitted to a model. Zero order (linear) and first order (non-linear) models were used (Quilaqueo & Aguilera, 2015), according to the following equations: $A_t = -K_0 \cdot t + A_0$ for zero order, where A_t is the crystal area (as percentage of the initial area) at time t (s), K_0 (s⁻¹) is a constant related to the dissolution velocity and A_0 is the initial crystal area and; $\ln(A_t/A_0) = K_1 \cdot t$ for the first order model, where K_1 (s⁻¹) is a constant related to the dissolution velocity (Costa & Sousa, 2001).

3.2.4 Sensory evaluation

Time-intensity (TI) analysis was performed to evaluate salt intensity of commercial salts perceived in mouth over time. The procedures of the sensory TI test were first

approved by the University of Guelph Ethics Review Board (REB number 14AU014). Eleven panelists, not allergic or sensitive to salt, food preservatives, iodine and anticaking agents present in commercial salts, with experience in sensory evaluation were selected for the sensory panel. The panelists were trained (6 sessions) about evaluation of salt taste intensity over time using a TI scale (scale of 15 cm). Testing was conducted in sensory booths (Sensory Testing Laboratory, Food Science Building, University of Guelph, Canada) under standard sensory laboratory conditions and white light.

The samples of salts were presented in their unaltered crystal form at constant sodium amount (20 mg) detailed in Table 3.1. Disposable syringes of 3 cm³ of capacity (Leur-lock 309582, Becton-Dickinson and Company) were cut in order to provide an orifice large enough to release crystals at moment of depressing the plunger, as proposed by Vella et al. (2012). The contents of each syringe were obscured by an adhesive white label on which was printed a three digit code, according to the sensory testing protocol. Samples were served monadically, on a tray via a hatch in the sensory booth. Filtered water, crackers and apples were provided to panelists to cleanse their palate between trials. Panelists were instructed to fully depress the plunger to release the salt crystals onto their tongue. At this point they began the time intensity test. During the test they were instructed to move their tongue slowly and constantly and, swallow a little bit of saliva when indicated (40; 80; and 120 s) in order to maintain an adequate level of saliva in the mouth. A spit cup was provided to panelists to use at the end of the test (180 seconds or when the salt taste was no longer perceived). A recovery period of five minutes elapsed before evaluation of the following sample.

TI results were collected using Compusense five release 5.0 software (Compusense Inc, Guelph, Canada). Through a horizontal line scale, with left meaning no saltiness and right meaning very salty, each panelist indicated salt intensity over time. The following parameters were determined from TI curve: Time to maximum intensity (T_{max}), maximum intensity (I_{max}), duration of salt taste perceived (Dur), area under the curve (AUC), increase angle ($IncAng$), increase area under the curve ($IncArea$), angle of decrease ($DecAng$) and decrease area under the curve ($DecArea$) (Figure 3.1). The samples were presented in a randomized order during each session and four replicates of testing of each sample were completed.

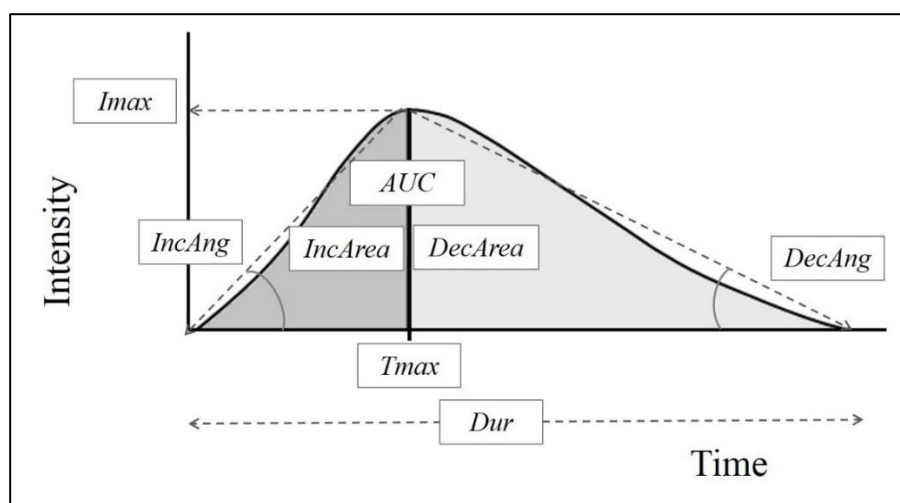


Figure 3.1. Time-intensity parameters extracted for curve.

3.2.5 Statistical analysis

Differences among samples were determined using ANOVA and Tukey's test with the software Statgraphic Centurion XV 15.1.02 version (StatPoint Inc., VA, USA). Correlations between TI parameters and morphological parameters or values of *in vitro*

dissolution were calculated using Microsoft Excel (Microsoft Office Professional Plus 2013), and their significance were determined by the Pearson product-moment correlation coefficient.

3.3. Results and discussion

3.3.1 Salt characterization

Table 3.2 shows the mineral profiles of the salts. Depending on its origin, elements other than Na^+ and Cl^- were also found in the salt crystals. To have a salty taste, both Na^+ and Cl^- are required. However, it has been suggested that the cation rather than anion impart saltiness (Man, 2007; Schiffman, Mcleroy & Erickson, 1980). The sodium content was slightly different between the samples. The Maldon salt had the highest level of sodium (405 mg/g), while the Brittany Grey salt had the lowest (355 mg/g). The Kosher salt contained fewer minerals other than sodium, while the Brittany Grey and Maison Orphée salts had the highest levels of mineral content. Given that the mineral profile was different and ions other than sodium could modify the quality of the salty taste, the amount of sodium was standardized for sensory analysis (Murphy, Cardello, & Brand, 1981; Schiffman et al., 1980; Van der Klaauw & Smith, 1995).

Table 3.2. Mean values of minerals present in salts studied.

Salt type	Minerals present in 1 g of salt						
	Na (mg)	Ca (μ g)	Mg (μ g)	P (μ g)	K (μ g)	S (μ g)	Fe (μ g)
Brittany Grey	355	1750	4150	< 18	1400	3300	120
Extra Coarse	375	270	86	< 20	640	530	4
Kosher	385	18.5	< 15	< 21	375	180	< 2
Maison Orphée	365	2850	2400	< 19	1100	3350	125
Maldon	405	1350	525	< 17	375	1300	< 2

The moisture content revealed significant differences between the salt types (Table 3.3). The Brittany Grey salt had the highest moisture content (3.75 ± 0.44 %) significantly different from the other salts (between 1.24 and 1.93 %). In general, commercial salts have low water content, with levels between 0.91 % and 7.36 %. However, it is not known whether moisture affects the perception of saltiness (Vella et al., 2012; Quilaqueo & Aguilera, 2015).

The apparent density of different salts did not reveal any significant differences, and was between 1862 and 2015 kg m^{-3} (Table 3.3). These values were lower than the true density of pure NaCl (2165 kg m^{-3}) (Lide, 2005). It is attributed to the fact that the crystals contained materials other than Na^+ and Cl^- and also to differences in the crystal structure.

Table 3.3. Characteristics of salt particles studied.

Salt type	Moisture (%)	ρ_{app} (kg m⁻³)
Brittany Grey	3.75 ± 0.44 ^a	1862 ± 96 ^a
Extra Coarse	1.24 ± 0.14 ^b	2015 ± 73 ^a
Kosher	1.26 ± 0.42 ^b	1873 ± 110 ^a
Maison Orphée	1.93 ± 0.46 ^b	1918 ± 53 ^a
Maldon	1.33 ± 0.16 ^b	1876 ± 76 ^a

Means followed by different letters in each column indicate significant differences according to ANOVA and Tukey's test ($p < 0.05$).

Differences in the morphology and internal structure of salts can be seen in Figure 3.2. Based on crystallization conditions (e.g., evaporation rate and substrate characteristics), several morphologies of crystal salt can be obtained (Vázquez et al., 2015). The Brittany Grey crystals revealed an imperfect cubic shape with large secondary agglomeration, which can be the result of crystal – crystal collision (Ferreira et al., 2005; Mersmann, 2001). Moreover, the surface of these crystals was rough and the internal structure exhibited some cavities and cracks. The Extra Coarse salt crystals were simpler, more cubic, and its surface was smoother than the other crystals. Through micro-CT images it can be seen that there were very small internal cavities and no cracks in these crystals. The Kosher salt had an uneven surface and revealed two main morphologies in their crystals: a non-cubic flat structure and an assembly of small agglomerated crystals. The internal structure of flat crystals revealed some cracks but not cavities. However, the internal structure of agglomerated crystals showed

cavities, due to small crystals that conform the structure were assembled in irregular shape. The crystals of the Maison Orphée salt were less cubic and exhibited small crystals attached to the surface of large crystal. The surface of these crystals was rough and some internal cavities could be observed. Finally, the Maldon salt crystals were highly complex, with a hollow pyramid structure and a relatively rough surface.

The projected area and shape parameters of the salt crystals were significantly different (Table 3.4). The coefficient of variation ($n = 150$) was 28% in Extra Coarse samples, followed by 33% for Brittany Grey, 48% for Maldon, 60% for Maison Orphée, and 67% for Kosher salt. The projected area depends on the equilibrium position of the crystals under the microscope lens. The position adopted by the crystal is influenced by the crystal morphology, which is not always a perfect cube due to the presence of impurities (minerals other than Na^+ and Cl^-) and different crystallization conditions. Therefore, differences in morphology can explain the high variability and differences in the projected area. Moreover, the differences in shape parameters between salt types reflect the differences in morphology (see Figure 3.2). Simple and cubic crystals had high circularity, while more agglomerated, flat or pyramidal crystals had low circularity. Similarly, aspect ratio and elongation were lower in symmetrical, cubic crystals than in agglomerated and pyramidal crystals.

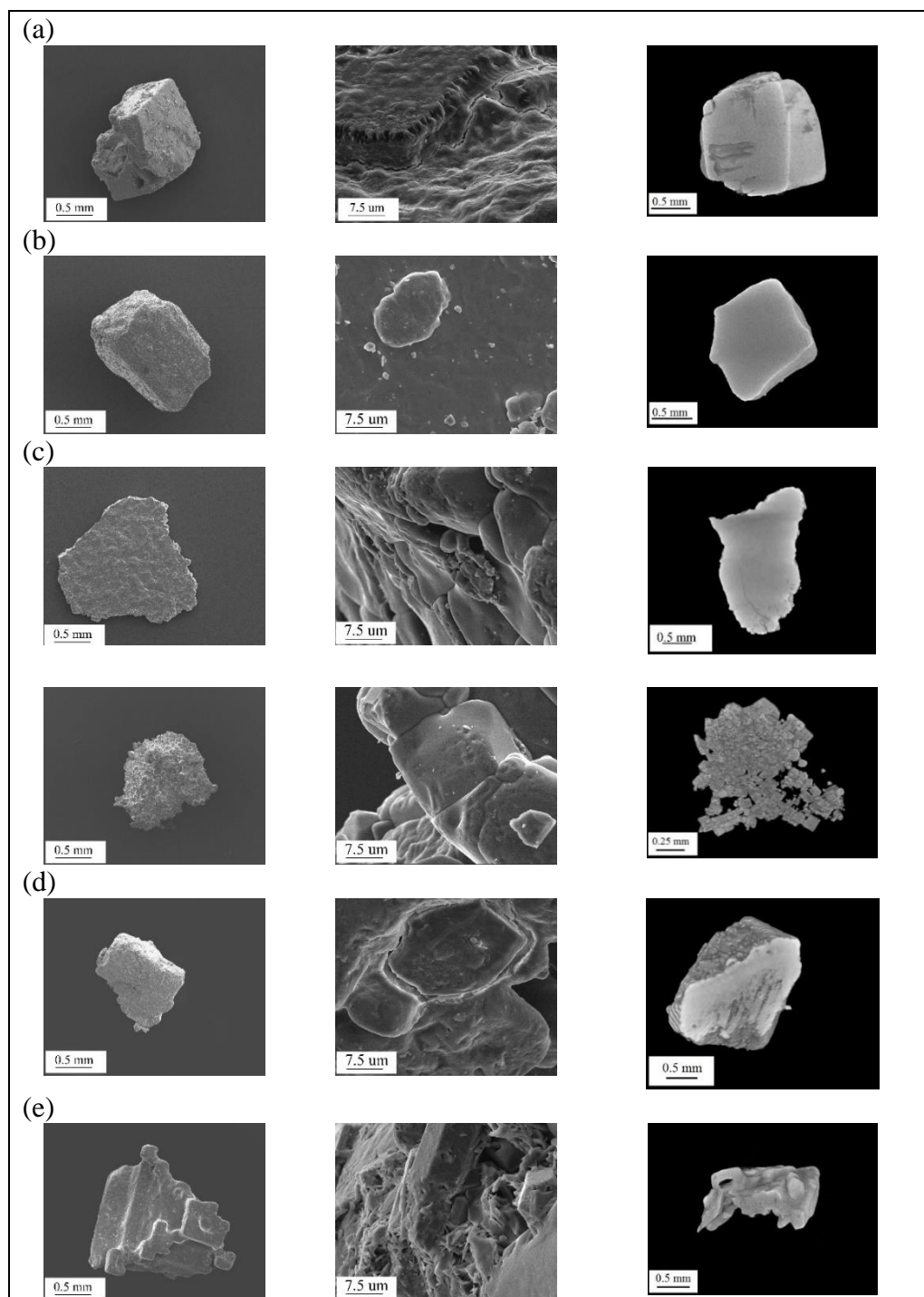


Figure 3.2. SEM images and micro-CT images of cross-section (last column) of crystals.

Table 3.4. Projected area and shape parameters for salt crystals.

Salt type	Projected area (mm ²)	Circularity ¹	Aspect ratio ²	Equivalent diameter ³ (mm)	Elongation ⁴
Brittany Grey	1.70 ± 0.56 ^c	0.64 ± 0.07 ^c	1.37 ± 0.25 ^a	1.45 ± 0.27 ^c	1.42 ± 0.20 ^a
Extra Coarse	2.10 ± 0.59 ^d	0.70 ± 0.06 ^d	1.53 ± 0.34 ^b	1.61 ± 0.27 ^d	1.55 ± 0.29 ^c
Kosher	1.16 ± 0.77 ^b	0.55 ± 0.09 ^a	1.49 ± 0.38 ^b	1.14 ± 0.43 ^b	1.48 ± 0.29 ^b
Maison Orphée	0.84 ± 0.51 ^a	0.59 ± 0.11 ^b	1.55 ± 0.41 ^b	0.96 ± 0.40 ^a	1.52 ± 0.30 ^{bc}
Maldon	1.53 ± 0.74 ^c	0.58 ± 0.09 ^{ab}	1.57 ± 0.40 ^b	1.35 ± 0.34 ^c	1.58 ± 0.33 ^c

Means of 150 replicates for each salt type followed by different letters in a column are significantly different according to ANOVA and Tukey's test ($p < 0.05$).

¹ Circularity is defined as $4 \pi \text{ area}/\text{perimeter}^2$.

² Aspect ratio is the relation between the major and the minor axis of an equivalent ellipse

³ Equivalent diameter is calculated as $2\sqrt{\text{area}/\pi}$

⁴ Elongation is defined as maximum Feret's diameter/minimum Feret's diameter

3.3.2 Crystal dissolution in artificial saliva through video-microscopy

The kinetic of dissolution of single crystal in artificial saliva revealed differences between different salt types. Figure 3.3 shows the reduction in projected area over time for each salt type. Four salt types (Brittany Grey, Extra Coarse, Kosher and Maison Orphée) followed a linear trend after a short lag time that was fitted to the zero-order model. This behavior was similar to that observed by Quilaqueo and Aguilera (2015) for commercial salts with simple and agglomerated cubic shapes. The mean of K_0 values indicate that the Kosher salt presented the highest rate of dissolution, followed by Maison Orphée that was (55% lower than Kosher) and followed by Brittany Grey and Extra Coarse salts (Table 3.5). For example, the dissolution rate of Kosher salt was 3.8 times faster than that of Extra Coarse salt. On the other hand, the Maldon salt had a non-linear tendency and was adjusted to a first-order kinetic model.

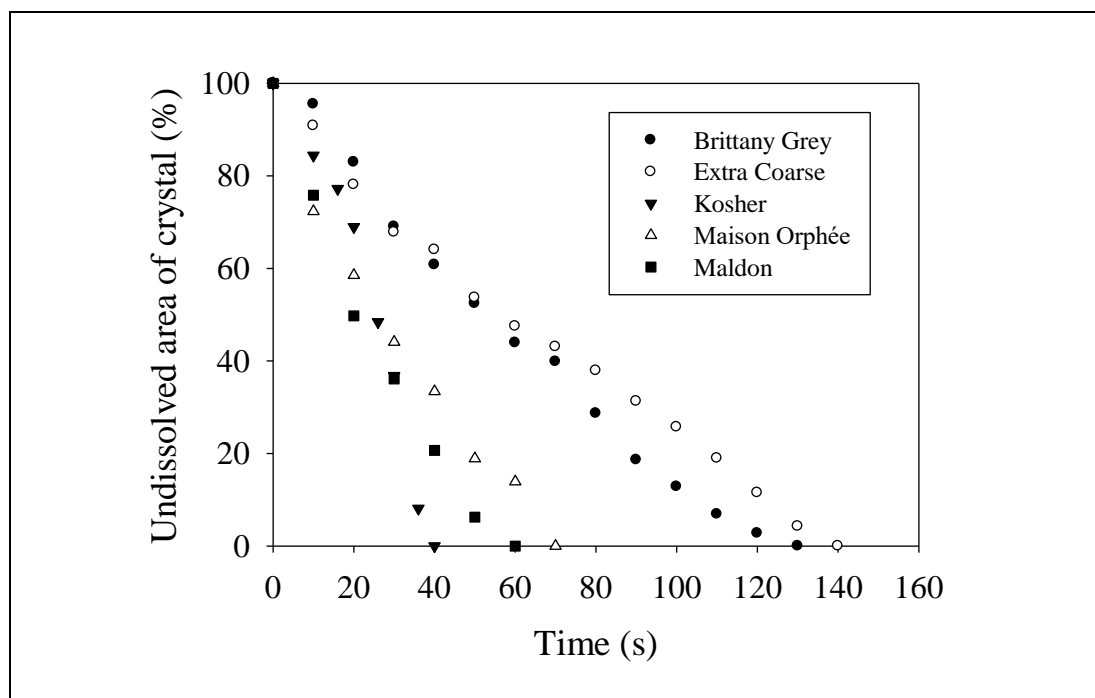


Figure 3.3. Area reduction (%) of one representative crystal of each salt type.

Table 3.5. Model adjusted to area reduction, rate constants (K values in s^{-1}), coefficient of determination ranges (R^2), and total dissolution time (s) of crystals analyzed.

Salt type	Adjusted model	K_0 (s^{-1})	K_1 (s^{-1})	R^2 range	Dissolution time (s)
Brittany Grey	Linear	0.953 ± 0.203^{ab}	-	0.9415 - 0.9880	105 ± 21^b
Extra Coarse	Linear	0.750 ± 0.047^a	-	0.9624 - 0.9958	132 ± 7^a
Kosher	Linear	2.851 ± 0.375^c	-	0.9236 - 0.9894	37 ± 5^d
Maison Orphée	Linear	1.297 ± 0.183^b	-	0.8580 - 0.9726	72 ± 11^c
Maldon	Non-linear	-	0.060 ± 0.024	0.8031 - 0.9322	54 ± 12^{cd}

Means of 5 replicates for each salt type followed by different letters in a column are significantly different according to ANOVA and Tukey's test ($p < 0.05$).

From the five crystals analyzed for each salt type, fragmentation during dissolution occurred in one crystal of Maison Orphée, two crystals of Brittany Grey, and four crystals of Kosher, and Maldon salts. After disintegration the surface area in contact with the saliva increased dramatically. The Extra Coarse salt that did not undergo fragmentation had the best fitting to a lineal model (highest R^2 values). This implies that fragmentation during dissolution may modify the solubilization rate of crystal thus deviating from the linear model. Disintegration may be related to the internal structure of a crystal. Extra Coarse salt exhibiting no fragmentation during dissolution revealed a compact structure. In contrast, Maison Orphée and Brittany Grey salts had cavities and cracks in the structure as revealed by micro-CT analysis (Figure 3.2) and fragmentation was observed during dissolution. Kosher and Maldon salts revealed extensive fragmentation during dissolution in saliva showed external morphologies (i.e., less monolithic and regular) quite different from the other three types.

A comparison can be made based on the total dissolution time (Table 3.5). The lowest dissolution time was for Kosher salt (37 ± 5 s) followed by Maldon (54 ± 12 s), and Maison Orphée (72 ± 11 s). Brittany Grey and Extra Coarse (105 ± 21 and 132 ± 7 s respectively) were the slowest in being dissolved with Extra Coarse approximately 3.6 times slower than Kosher salt.

3.3.3 Sensory evaluation

The TI curves of different salt types were similar in shape. An initial fast increase in intensity was followed by a short period of maximum intensity to end with a prolonged tail of decreasing intensity (Figure 3.4). Eight parameters extracted from TI curves

(Figure 3.1) are reported in Table 3.6. Significant differences were found in some of the TI parameters: T_{max} , I_{max} , $IncAng$ and $IncArea$. Moreover, good correlations were found between some of these TI parameters and shape parameters, dissolution time and K_0 values.

The shortest time at maximum intensity (T_{max}) was for Kosher salt, followed by Maldon and Maison Orphée salts, and finally by Extra Coarse and Brittany Grey salts. The maximum intensity for Kosher salt was detected in 40% less time than Extra Coarse salt. T_{max} was positively correlated with circularity ($r = 0.8465$) and dissolution time ($r = 0.9054$), and negatively with K_0 values ($r = -0.9946$). This means that crystals with low circularity (probably with a large surface area) have fast dissolution rates, reaching their maximum value of salt intensity at short times.

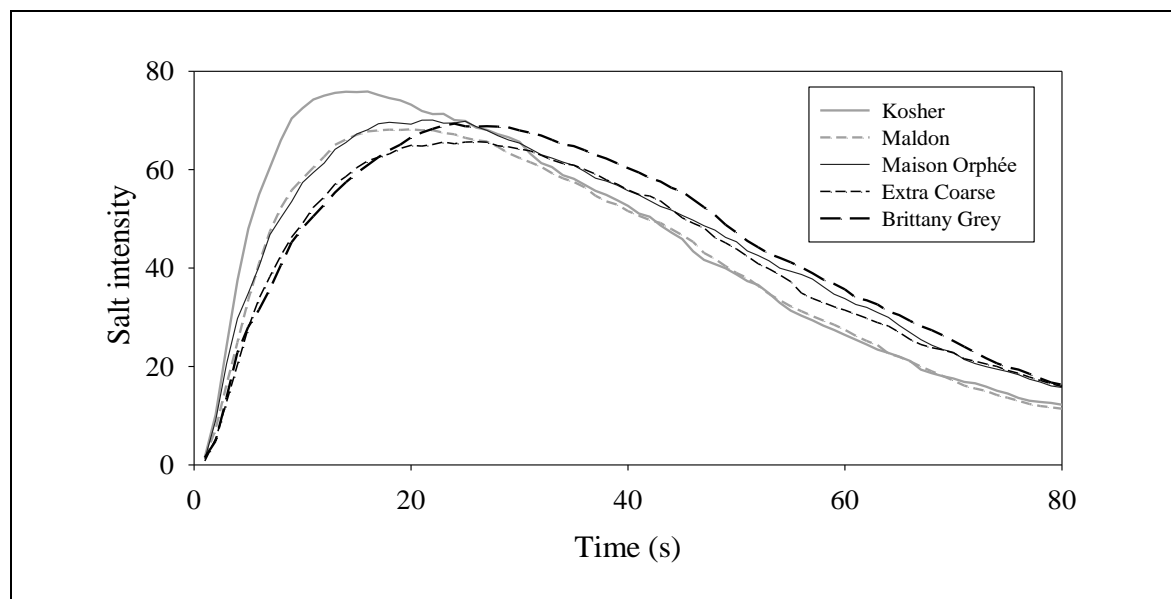


Figure 3.4. Average time-intensity curves of different salts.

Table 3.6. Mean values of time intensity curve parameters of salts studied.

Salt	Tmax	Imax	Dur	AUC	IncAng	IncArea	DecAngle	DecArea
Kosher	14.1 ± 1.1 ^a	83.4 ± 4.0 ^b	89.9 ± 1.2 ^a	3990.0 ± 271.6 ^a	78.9 ± 1.8 ^c	655.4 ± 96.1 ^a	49.6 ± 0.8 ^a	3334.6 ± 178.1 ^a
Maldon	18.7 ± 2.2 ^b	77.5 ± 2.2 ^{ab}	87.8 ± 3.3 ^a	3662.0 ± 205.5 ^a	75.5 ± 2.9 ^{bc}	811.2 ± 146.2 ^{ab}	49.3 ± 1.5 ^a	2850.8 ± 164.0 ^a
Maison Orphée	20.9 ± 3.7 ^{bc}	79.4 ± 1.7 ^b	92.8 ± 4.1 ^a	4066.6 ± 374.3 ^a	74.3 ± 2.0 ^{abc}	979.2 ± 298.1 ^b	49.3 ± 2.0 ^a	3087.4 ± 123.8 ^a
Extra Coarse	23.3 ± 2.4 ^c	71.5 ± 7.5 ^a	92.4 ± 4.1 ^a	3811.6 ± 522.6 ^a	70.4 ± 3.7 ^a	1003.3 ± 200.8 ^b	48.0 ± 4.5 ^a	2808.3 ± 435.6 ^a
Brittany Grey	23.8 ± 3.1 ^c	76.2 ± 2.5 ^{ab}	94.4 ± 5.2 ^a	4020.1 ± 176.6 ^a	71.4 ± 2.9 ^{ab}	1063.9 ± 264.1 ^b	48.6 ± 2.7 ^a	2956.2 ± 433.4 ^a

Means followed by different letters in same column are significantly different according to ANOVA and Tukey's test ($p < 0.05$).

The maximum intensity of saltiness (I_{max}) was found in Kosher salt, followed by Maison Orphée, Maldon, Brittany Grey and finally Extra Coarse salt. Extra Coarse was significantly different from Kosher and Maison Orphée salts. The I_{max} of Kosher salt was 17% higher than Extra Coarse salt. The I_{max} values were correlated with projected area ($r = -0.8421$), equivalent diameter ($r = -0.8210$) and circularity ($r = -0.9281$). As projected area and equivalent diameter (size parameters) decreased the I_{max} value increased. Furthermore, crystals with low circularity had high I_{max} . On the other hand, I_{max} was negatively correlated with dissolution time ($r = -0.9118$), meaning that salt taste perception was higher when salt crystals were dissolved faster. Moreover, salt crystals that had high I_{max} had low T_{max} .

The angle of increase ($IncAng$) was higher in Kosher, Maldon and Maison Orphée, followed by Brittany Grey and Extra Coarse salt. This TI parameter was negatively related with circularity ($r = -0.9343$). Similarly, $IncAng$ was related negatively with dissolution time ($r = -0.9683$) and positively with K_0 values ($r = 0.9713$). Moreover, salt crystals with high I_{max} and low T_{max} had high $IncAng$.

Finally, $IncArea$ was lowest in Kosher and Maldon salts, followed by Maison Orphée, Extra Coarse and Brittany Grey salts. There was no significant correlation between $IncArea$ and the size or shape of the crystals. However, $IncArea$ was correlated positively with dissolution time ($r = 0.8476$) and negatively with K_0 values ($r = -0.9829$), with $IncArea$ being low when the crystal was dissolved quickly. Salt crystals with high I_{max} , low T_{max} and high $IncAng$ had low $IncArea$.

Other TI parameters, Dur and AUC were similar among the salts, probably because the sodium content was equal for all samples. Also, the TI parameters that occurred after

reaching maximum intensity, DecAngle and DecArea were similar between samples. This means that significant changes can occur before T_{max} with changing the morphology of the crystals.

These results are in accordance with those found in other studies. Rama et al. (2013) who investigated salt applied in potato crisps, and Vella et al. (2012) who studied salt in unaltered crystal form, showed TI curves with an initial rapid increase in intensity, a peak of maximum intensity followed by a fall over time. In these researches it was found that smaller crystal sizes had a shorter time to maximum intensity and highest maximum intensity. As shown in our work not only crystal size can be altered to modify the TI curve but also crystal morphology (for a given crystal size). Pyramidal, flat or highly agglomerated crystals produce higher salt intensity and faster release than simple cubic crystals.

The total dissolution time in the dissolution experiments was shorter than the duration of the perception of saltiness (D_{ur}), despite that there was no agitation during the solubilization experiment while sensorial evaluation crystal suspensions were subjected to the action of the tongue. However, the concentration of sodium for the *in vitro* dissolution was lower than for the sensorial evaluation (one crystal *in vitro* versus several crystals contained in 20 mg of sodium). This may have increased the dissolution rate and decreased the total time of dissolution of *in vitro* measurements. A more plausible explanation is that although total dissolution of the crystals may have been completed before D_{ur} the judges continued to perceive the saltiness while the some ions remained on the taste buds.

In order to achieve sodium reduction in foods without diminishing saltiness perception, salt should be released from the food matrix and rapidly transported to the taste receptors. Thus, the T_{max} should be short and I_{max} must not diminish. The fast dissolution of non-cubic and agglomerated crystals of Kosher salt accomplished this effect, compared with the other more cubic crystals. In solid foods with topical application of salt, the use of salt crystals like Kosher salt, would allow to reduce sodium levels without to lose saltiness. Exact T_{max} and I_{max} should be estimated to know the optimum sodium amount applied to different food matrices.

3.4. Conclusions

The morphology of salt crystals influences its dissolution in saliva, as well as the perception of saltiness. Highly agglomerated, flat or pyramidal crystals, with low circularity, experienced faster dissolution rates and lower dissolution times. This was evidenced when evaluating dissolution in artificial saliva using video-microscopy. Similarly, TI measurements of salts revealed that some TI parameters (T_{max} , I_{max} , $IncAng$ and $IncArea$) are correlated with crystal morphology and with dissolution rate. Kosher salt, which was composed of two main morphologies, flat and highly agglomerated crystals, revealed the highest dissolution rate. The dissolution rate of Kosher was 3.8 times higher than Extra Coarse salt, which was composed of simple, cubic crystals. Moreover, Kosher salt had 17% more salt intensity than Extra Coarse salt, detected in 40% less time. Therefore, in salty food with surface crystals of salt, a reduction in sodium could be achieved by using flat or highly agglomerated crystals, without lowering the salt intensity levels.

Future research should look at designing specific morphologies of salt crystals (e.g., through crystallization kinetics), analyzing the effect of other crystal sizes and microstructures, and evaluating the effect of food matrices on salt dissolution.

Acknowledgments

Author Quilaqueo acknowledges the financial support of CONICYT (21110317). Special thanks to Patricia Aguilar and Richelle Yacon for technical support in sensory evaluation, and to María Paz Quilaqueo for technical support in images analysis.

References

- Bibbins-Domingo, K., Chertow, G. M., Coxson, P. G., Moran, A., Lightwood, J. M., Pletcher, M. J., & Goldman, L. (2010). Projected effect of dietary salt reductions on future cardiovascular disease. *New England Journal of Medicine*, *362*, 590–599.
- Brown, I. J., Tzoulaki, I., Candeias, V., & Elliott, P. (2009). Salt intakes around the world: implications for public health. *International Journal of Epidemiology*, *38*, 791-813.
- Busch, J. L. H. C., Yong, F. Y. S., & Goh, S. M. (2013). Sodium reduction: Optimizing product composition and structure towards increasing saltiness perception. *Trends in Food Science & Technology*, *29*, 21-34.
- Costa, P., & Sousa, J.M. (2001). Modeling and comparison of dissolution profiles. *European Journal of Pharmaceutical Sciences*, *13*, 123–133.
- Ferreira, A., Faria, N., Rocha, F., Feyer de Azevedo, S., & Lopes, A. (2005). Using image analysis to look into the effect of impurity concentration in NaCl crystallization. *Chemical Engineering Research and Design*, *83*(A4), 331–338.
- Ferreira, T., & Rasband, W. (2012). ImageJ User Guide. IJ 1.46r. <http://imagej.nih.gov/ij/docs/guide/>
- Jensen, M., Smith, G., Fear, S., Schimoeller, L., & Johnson, C. (2011). Seasoning and method for seasoning a food product while reducing dietary sodium intake. United States Patent. US 7,923,047 B2.
- Kuo, W. Y., & Lee, Y. (2014). Effect of food matrix on saltiness perception. Implications for sodium reduction. *Comprehensive Reviews in Food Science and Food Safety*, *13*, 906-923.
- Lide, D. R. (2005). *CRC Handbook of Chemistry and Physics* (86th ed.). Boca Raton: CRC Press (Section 4).
- Man, C.M.D. (2007). Technological functions of salt in food products. In D., Kilcast, & F., Angus (Eds.), *Reducing Salt in Foods. Practical Strategies* (pp. 157-173). Cambridge: Woodhead Publishing Limited.
- Mattes, R.D., & Donnelly, D. (1991). Relative contributions of dietary sodium sources. *Journal of the American College of Nutrition*, *10*, 383-93.
- Mersmann, A. (2001). *Crystallization Technology Handbook* (2nd ed.). New York: Marcel Dekker (Chapter 6).
- Murphy, C., Cardello, A., & Brand, J. (1981). Tastes of fifteen halide salts following water and NaCl: anion and cation effects. *Physiology and Behavior*, *26*, 1083-1095.

- Oikonomopoulou, V., Krokida, M., & Karathanos, V. (2013). Influence of structure on saltiness and sweetness of dehydrated food products. *Drying Technology*, 31, 837-847.
- Phan, V.A., Yven, C., Lawrence, G., Chabanet, C., Reparet, J.M., & Salles, C. (2008). In vivo sodium release related to salty perception during eating model cheeses of different textures. *International Dairy Journal*, 18, 956-963.
- Quilaqueo, M., & Aguilera, J.M. (2015). Dissolution of NaCl crystals in artificial saliva and water by video-microscopy. *Food Research International*, 69, 373-380.
- Rama, R., Chiu, N., Carvalho, M., Hewson, L., Hort, J., & Fisk, I. (2013). Impact of salt crystal size on in-mouth delivery of sodium and saltiness perception from snack foods. *Journal of Texture Studies*, 44,338–345.
- Schiffman, S. S., Mcleroy, A. E., & Erickson, R.P. (1980). The range of taste quality of sodium salts. *Physiology and Behavior*, 24, 217-224.
- Tian, X., & Fisk, I. (2012) Salt release from potato crisps. *Food & Function*, 3, 376-380.
- Van der Klaauw, N. J., & Smith, D. V. (1995). Taste quality profiles for fifteen organic and inorganic salts. *Physiology and Behavior*, 58, 295-306.
- Van Ruth, S. M., Grossmann, I., Geary, M., & Delahunty, C. M. (2001). Interactions between artificial saliva and 20 aroma compounds in water and oil model systems. *Journal of Agricultural and Food Chemistry*, 49, 2409-2413.
- Vázquez, P., Thomachot-Schneider, C., Mouhoubi, K., Fronteau, G., Gommeaux, M., Benavente, D., Barbin, V., & Bodnar, J. (2015). Infrared thermography monitoring of the NaCl crystallisation process. *Infrared Physics & Technology*, 71, 198-207.
- Vella, D., Marcone, M., & Duizer, L. M. (2012). Physical and sensory properties of regional sea salts. *Food Research International*, 45, 415-421.
- WHO. (2003). Prevention of recurrent heart attacks and strokes in low and middle income populations: Evidence-based recommendations for policy makers and health professionals. Geneva, World Health Organization (WHO), (http://www.who.int/cardiovascular_diseases/resources/pub0402/en/).
- WHO. (2012). Guideline: Sodium intake for adults and children. Geneva, World Health Organization (WHO).
- WHO. (2014). Salt reduction. Fact sheet N°393. (<http://www.who.int/mediacentre/factsheets/fs393/en/>)

4. CRYSTALLIZATION OF NaCl BY FAST EVAPORATION OF WATER IN DROPLETS OF NaCl SOLUTIONS

4.1. Introduction

Sodium chloride, commonly named salt, provides about 90% of sodium in the human diet (He, 2012; Kloss, Meyer, Graeve & Vetter, 2015). Salt is added to foods to improve taste, as a preservative, and to improve rheological properties (e.g. contributing to structure and color in snacks) (Beck, Jekle & Becker, 2012; Kloss et al., 2015; Rama et al., 2013). In 2010 the global mean sodium consumption was estimated in 3.9 g/day (equivalent to approximately 10 g/day of salt) which exceeded the maximum recommended intake of 2 g/day of sodium, equivalent to 5 g/day of salt (Powles et al., 2013; WHO. 2014).

The food industry has developed different strategies to reduce the salt content without decreasing the perceived quality of foods. These strategies include a small stepwise reduction of salt, substitution or replacement of sodium chloride, the incorporation of agents to improve taste, and the design (or redesign) of the food matrix in order to improve the delivery of salt ions to the taste buds (Kloss et al., 2015; Kuo & Lee, 2014). Within the scope of this latter approach, optimizing the physical form of salt has not yet been broadly developed and applied.

The salt release from the food matrix, the diffusion of sodium ions in the oral cavity, and their detection by the taste receptors are complex processes that determine the perception of saltiness (Kuo & Lee, 2014). In surface-salted foods (such as salty

snacks, French fries and potato chips) the salt crystals are mixed with the food matrix during chewing to form the bolus, dissolved in the saliva and distributed across the mouth until they reach the taste buds. Finally, the hydrated bolus is swallowed after a residence time which may last a few seconds or longer depending on several factors, among them the microstructure of food (Chen, 2012; Tian & Fisk, 2012). Salt crystals that are partly dissolved are swallowed without giving saltiness.

Improving saltiness perception while avoiding that salt particles be swallowed before they are dissolved in the mouth, requires that the dissolution rate of salt crystals be increased. The dissolution rate of crystals may be increased by raising surface area to volume ratio in contact with saliva (solvent). This can be achieved by using smaller crystals or by using crystal structures with lower bulk density as hollow pyramidal or highly agglomerated cubes (Moncada et al., 2015; Quilaqueo & Aguilera, 2015; Quilaqueo, Duizer & Aguilera, 2015; Rama et al., 2013).

Salt crystals with small sizes can be obtained by mechanical grinding of large crystals or by methods of solvent removal such as spray-drying and anti-solvent crystallization (Cho, Kim, Chun & Choi, 2015; Langrish, 2009; Lee, Ashokkumar & Kentish, 2014). However, sometimes the particles obtained have a broad size distribution and an asymmetric crystal morphology (Lee, Ashokkumar & Kentish, 2014). Although sodium chloride has been widely studied in different applications, the crystallization mechanism is not completely understood yet. Further research on salt crystallization from solutions, single or multicomponent, is still needed (Vázquez et al., 2015). The aim of this research was to evaluate salt crystallization by fast water evaporation from droplets of salt solutions, using hot oil as bath phase. The crystallization was made by

adding droplets of salt solutions into the hot oil at a controlled temperature. Thus, the effects of the oil temperature, droplet volume, and salt solution concentration on characteristics of crystals obtained were determined.

4.2. Materials and methods

4.2.1. Materials

Sodium chloride (NaCl) 99.1 % of purity (Winkler, Santiago, Chile) was used to prepare the salt solutions (brine) in deionized water. Food grade extra-virgin olive oil (Chef, San Bernardo, Chile) acquired at a grocery store, was used as the immiscible hot medium into which brine droplets were dispersed.

4.2.2. Crystallization process

The crystallization of salt by fast water evaporation from droplets of brine was made by adding the brine droplets with a syringe to a beaker containing the olive oil (22.0 g). Two sizes of syringes were used: a small syringe with a needle of 0.8 mm of nominal diameter and a large syringe (without needle) with 3.7 mm of orifice diameter. The beaker was kept within a thermoregulated bath (One 7-45, Memmert, Schwabach, Germany) filled with silicone oil to control the temperature (Figure 4.1). Two different solution concentrations of salt in deionized water (15 and 26 % w/v) were used. Besides, two droplet volumes ($17 \pm 1 \mu\text{L}$ and $42 \pm 12 \mu\text{L}$, determined by weighing a series of water droplets and adjusting for density), and three oil phase temperatures (150, 165 and 180°C) were evaluated. In order to reach the desired temperature, the olive oil was maintained at the set temperature during 15 minutes before starting the

addition of the brine droplets. The brine droplets stayed in the olive oil until completely water evaporation and NaCl crystal formation.

After the crystallization process, the olive oil containing salt particles was left at ambient temperature (20 °C) during at least 12 h, so that salt particles could sediment. Then, the supernatant oil was discarded and acetone was added in relation 1:10 (slurry of salt and oil: acetone) in order to wash the salt particles. The mixture of salt, oil and acetone was stirred (using a magnetic stirrer) for 10 min and then transferred to a glass funnel to be vacuum filtered (0.22 μm pore size, GVWP filter, Millipore Corp., MA, USA). Finally, the salt particles or salt microcrystals, (as referred to later) were dried at ambient temperature (20 °C) until constant weight was achieved.

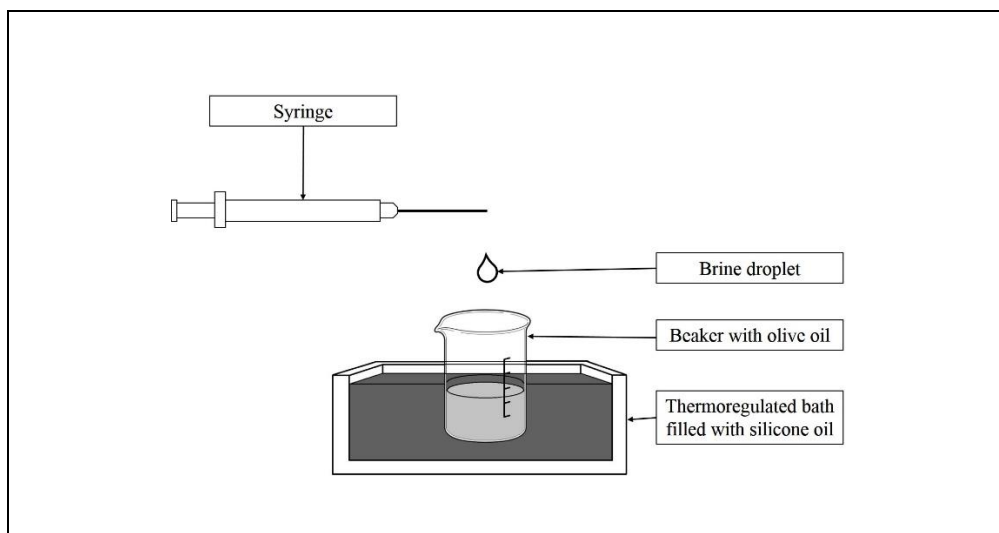


Figure 4.1. Scheme of the experimental set-up used to form salt microcrystals. The brine droplets were added to the beaker with olive oil using a syringe. The beaker was maintained inside the thermoregulated bath filled with silicone oil to control the temperature.

4.2.3. Salt characterization

Salt particles obtained under different conditions were analyzed by microscopy and colorimetry. Based on these results, two crystallization conditions (that allowed obtaining small S and large L microcrystal sizes) were selected to carry out the following analyses: thermogravimetry, X-ray diffraction, moisture determination, and dissolution in artificial saliva.

4.2.3.1. Size and shape measurements

Size distribution of salt crystals was determined by image analysis from images captured with a light microscope (BX50, Olympus Co., Tokyo, Japan) coupled to a camera (ToupCam Ucmos08000 KPA, Touptek Photonics, Zhejiang China). Samples of microcrystals were directly removed from the oil phase. The slurry of salt and oil was stirred in a magnetic stirrer to disperse the microcrystals in the oil and 250 μ L of sample were taken using a micropipette, placed in a glass slide and, examined under the microscope lens. Images of at least 100 particles per sample were processed and analyzed with ImageJ 1.45s software (National Institutes of Health, MD, USA). Equivalent diameter (D_{eq}) equal to that of a circle with similar area and circularity (C) were calculated from the following equations (Ferreira, Faria, Rocha, Feyer de Azevedo & Lopes, 2005; Ferreira & Rasband, 2012):

$$D_{eq} = 2 (Area/\pi)^{1/2} \quad (4.1)$$

$$C = 4\pi(Area/Perimeter^2) \quad (4.2)$$

The frequency distribution of D_{eq} of salt particles was determined using Microsoft Excel (Microsoft Office Professional Plus 2013, Redmond, WA, USA).

4.2.3.2. Scanning electron microscopy (SEM)

Salt crystals were examined by scanning electron microscopy (LEO 1420VP, Carl Zeiss, Oberkochen, Germany) to assess their morphology and surface characteristics. Crystals were fixed on the sample holders using double-side sticky tape. Images were obtained at an accelerating voltage of 25 kV.

4.2.3.3. Color determination

Color of salt crystals was measured using a computer vision system (DVS-Lab, Digital Vision Solutions, Santiago, Chile). Total color difference (ΔE) between original pure salt (L_0^* , a_0^* , b_0^*) and salts crystallized by sudden evaporation of water (L^* , a^* , b^*) was calculated by the following relation (Luna & Aguilera, 2014):

$$\Delta E = ((L_0^* - L^*) + (a_0^* - a^*) + (b_0^* - b^*))^{1/2} \quad (4.3)$$

where L^* (black 0 to white 100), a^* (green -120 to red 120) and b^* (blue -120 to yellow 120) are values corresponding to lightness, redness and yellowness of the CIELAB color scale, respectively (Luna & Aguilera, 2014). Measurements were done in triplicate.

4.2.3.4. Thermogravimetric analysis

The thermogravimetric analysis (TGA) of salt crystals was performed with a TGA/SDTA 851E calorimetric system (Mettler Toledo Intl. Inc., Greifensee, Switzerland). Thermograms were obtained between 26 and 890 °C at a scanning rate of 20 °C/min under nitrogen atmosphere and a flow rate of 60 mL/min. Results were processed using STAR[®] software (Mettler Toledo Intl. Inc., Schwerzenbach, Switzerland). Runs were performed in duplicate.

4.2.3.5. X-ray diffraction (XRD)

Salt microcrystals were analyzed in a X-ray diffractometer (D8 Advance, Bruker, Karlsruhe Germany) equipped with a $\text{CuK}_{\alpha 1,2}$; K_{β} X-ray tube set to 40 kV and 40 mA, without Gobel mirror. The samples were mounted on a Lucita sample plate and gently compressed. Scans were collected from $2\theta = 10^{\circ}$ to 80° with step sizes of 0.02° at 2 s per step. EVA software (Bruker Corp., MA, USA) was used for identification and analysis of peaks.

4.2.3.6. Moisture content

The moisture content of the salt crystals was determined using an infrared moisture analyzer (model MA 30, Sartorius, Göttingen, Germany) at 130°C until constant weight. Results were expressed on wet basis as the average of duplicates.

4.2.3.7. Salt dissolution in artificial saliva

Dissolution rates of salt microcrystals in artificial saliva were compared with the dissolution rate of the original crystals. Artificial saliva was prepared as indicated by Quilaqueo, Duizer & Aguilera (2015).

The dissolution rate was determined by conductivity using a pH/conductivity meter (Orion 4-Star, Thermo Scientific, MA, USA) with a conductivity electrode (4 cell conductivity electrode graphite, Thermo Scientific, MA, USA). 1.6 g of salt (d.w.) were dissolved in 80 mL of artificial saliva at room temperature (20°C) and under gentle agitation (magnetic stirrer at minimum intensity). Recording of the solution conductivity began before salt was added into the artificial saliva and finished when

the maximum conductivity was reached, assuming that total salt dissolution was achieved (Vella, Marcone & Duizer, 2012). Runs were done in duplicate.

4.2.4. Statistical analysis

Differences among samples were determined using analysis of variance (ANOVA) and Tukey's test at a significance level of $p < 0.05$, using the software Statgraphics Centurion XV (Statpoint Technologies, Inc., VA, USA).

4.3. Results and discussion

Crystallization is a process where solid particles are precipitated from supersaturated liquid solutions. The fundamental driving force for crystallization from solutions is the difference in the chemical potential between the solution and the solid phase. It is convenient to represent this in terms of the supersaturation, which is the difference between the actual solution concentration and the saturation concentration. Supersaturation can be achieved by evaporation of the solvent, cooling of a solution or by adding an antisolvent (drowning-out precipitation) (Braatz, 2002; Lee, Ashokkumar & Kentish, 2014). The degree of supersaturation is controlled by several factors such as the initial solution concentration and temperature, reported in this study, as well as others such as relative humidity, surface area and roughness of the substrate (Rodriguez-Navarro & Doejhne, 1999). In antisolvent crystallization an aqueous salt solution is poured into another solvent (e.g., ethanol) in which the solute has a lower solubility, thus, the interfacial area becomes supersaturated allowing the crystal formation (Kadota et al., 2007; Lee, Ashokkumar & Kentish, 2014). In our case, the

supersaturation was achieved by evaporation of water from the solutions as they contacted the hot oil.

4.3.1. Size and shape of crystals

The equivalent diameter (D_{eq}) for all crystal samples ranged from 4 to 139 μm , and the mean D_{eq} varied between 9 and 23 μm (Table 4.1 and Figure 4.2). The large standard deviations shown in Table 4.1 means that the method gives a high polydispersity of sizes, which was later corroborated by the SEM study (see below). A wide range of particle sizes has also been reported for other cases of NaCl crystallization and other compounds (El-Yafi & El-Zein, 2015; Kadota et al., 2007; Lee, Ashokkumar & Kentish, 2014). At the lowest oil phase temperature (150°C) the solution concentration and the droplet size had a significant effect on D_{eq} ($p < 0.05$). Small microcrystals (e.g., small D_{eq}) were obtained from the high solution concentration (26% w/v) and the large droplet size ($42 \pm 12 \mu\text{L}$). At the intermediate temperature (165°C) the droplet size had a significant effect on D_{eq} , where small microcrystals were obtained from large droplet sizes. At the highest oil temperature (180°C) both the solution concentration and the droplet size had no significant effect on D_{eq} of microcrystals. Although the oil temperature had no statistical significant effect on D_{eq} , there was a clear tendency to decrease D_{eq} when temperature increases suggesting that a faster evaporation of water led to more nuclei formation. Also, in ice crystals formation a high rate of freezing results in numerous fine ice crystals (Kim, Liesse, Kemp & Balan, 2015). The size distribution of salt microcrystals (Figure 4.2) showed that the main variability in D_{eq}

occurred at the low temperature (150 °C), while at 180 °C the distributions of D_{eq} was more homogeneous.

Table 4.1. Equivalent diameter (μm) and circularity of microcrystals.

Parameter	Solution (%)	Solution droplet	Temperature (°C)		
			150	165	180
Equivalent diameter	15	Small	23 ± 25^{bB}	16 ± 9^{bB}	13 ± 7^{aA}
		Large	13 ± 7^{bA}	11 ± 5^{bA}	11 ± 9^{aA}
	26	Small	9 ± 5^{aB}	13 ± 10^{aB}	12 ± 10^{aA}
		Large	10 ± 16^{aA}	12 ± 10^{aA}	12 ± 11^{aA}
Circularity	15	Small	0.73 ± 0.19^{aA}	0.70 ± 0.16^{aA}	0.70 ± 0.12^{aA}
		Large	0.79 ± 0.13^{aB}	0.80 ± 0.09^{aB}	0.72 ± 0.12^{aA}
	26	Small	0.80 ± 0.14^{bA}	0.74 ± 0.10^{aA}	0.77 ± 0.11^{bA}
		Large	0.80 ± 0.13^{bB}	0.77 ± 0.11^{aB}	0.76 ± 0.14^{bA}

100 particles were measured to estimate equivalent diameter and circularity. Different letters in a column (for each parameter) are significantly different ($p < 0.05$) according to two-way ANOVA and Tuckey's test with solution concentration (small letters) and droplet size (capital letters) as independent variables.

The microcrystals obtained by fast water evaporation exhibited different shapes, from simple to agglomerated cubes. The shape of crystals was quantified by the circularity (C) (Table 4.1) which is equal to 1 for a circle, 0.79 for a square and elongated shapes take lower values (Ferreira & Rasband, 2012). The temperature of the oil phase, solution concentration and volume of the droplet had a significant effect on C (Table 4.1). The lowest circularity was found at high temperatures (165 and 180°C), low concentration of solution (15% w/v), and small droplet volume ($17 \pm 1 \mu\text{L}$). It has been reported that non isometric structures results from the non-equilibrium growth of the crystals in a supersaturated solution (Gupta et al., 2015; Vázquez et al., 2015).

However, when solutions requires more evaporation time to reach saturation levels suitable for salt precipitation, the crystal precipitation is slower and the resulting crystals are more cubic (Vázquez et al., 2015). This fact could explain that at lower temperature and at higher droplet size the crystals are more cubic and less agglomerated (higher C) (see Figure 4.3).

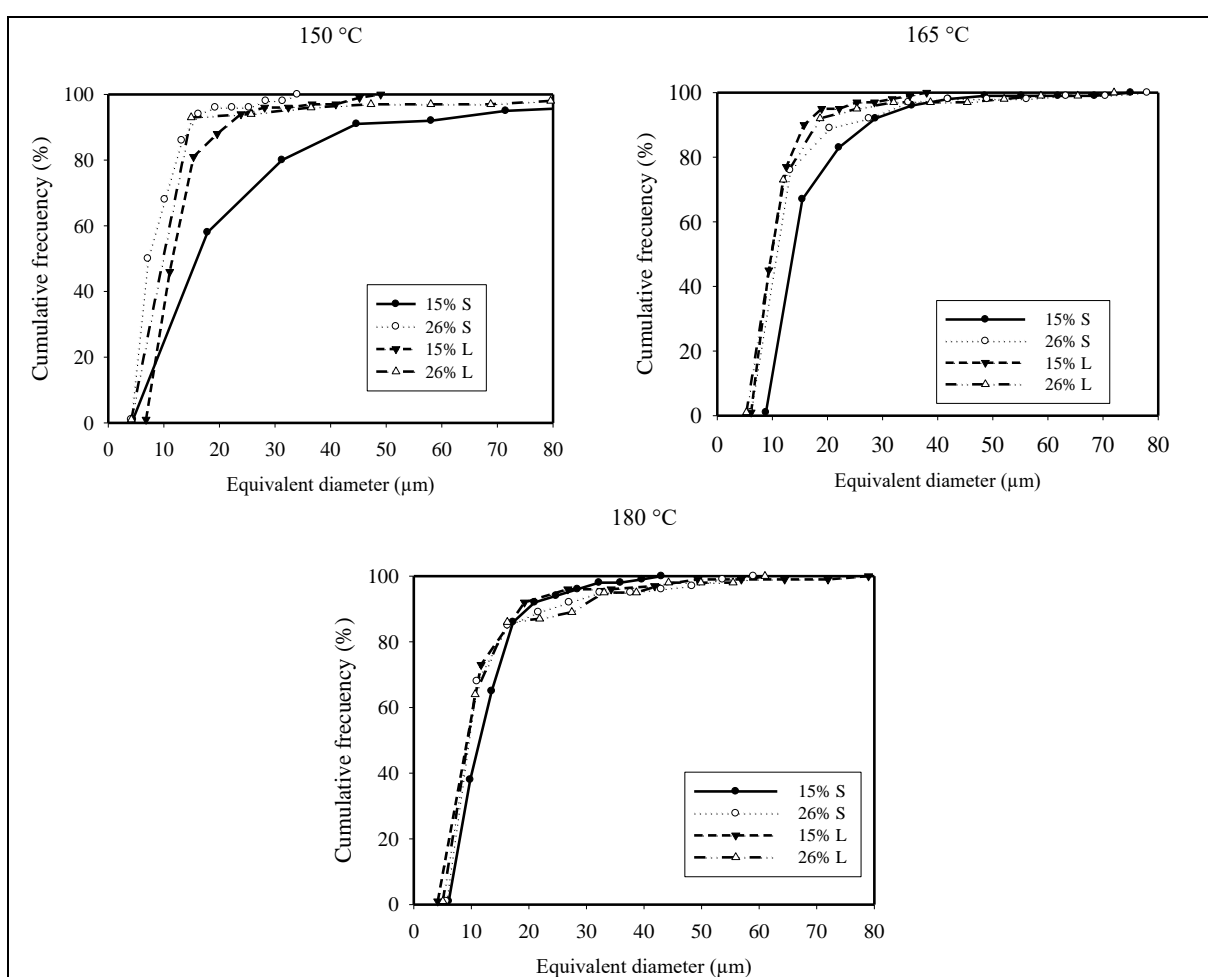


Figure 4.2. Size distribution of salt microcrystals at different oil temperatures.

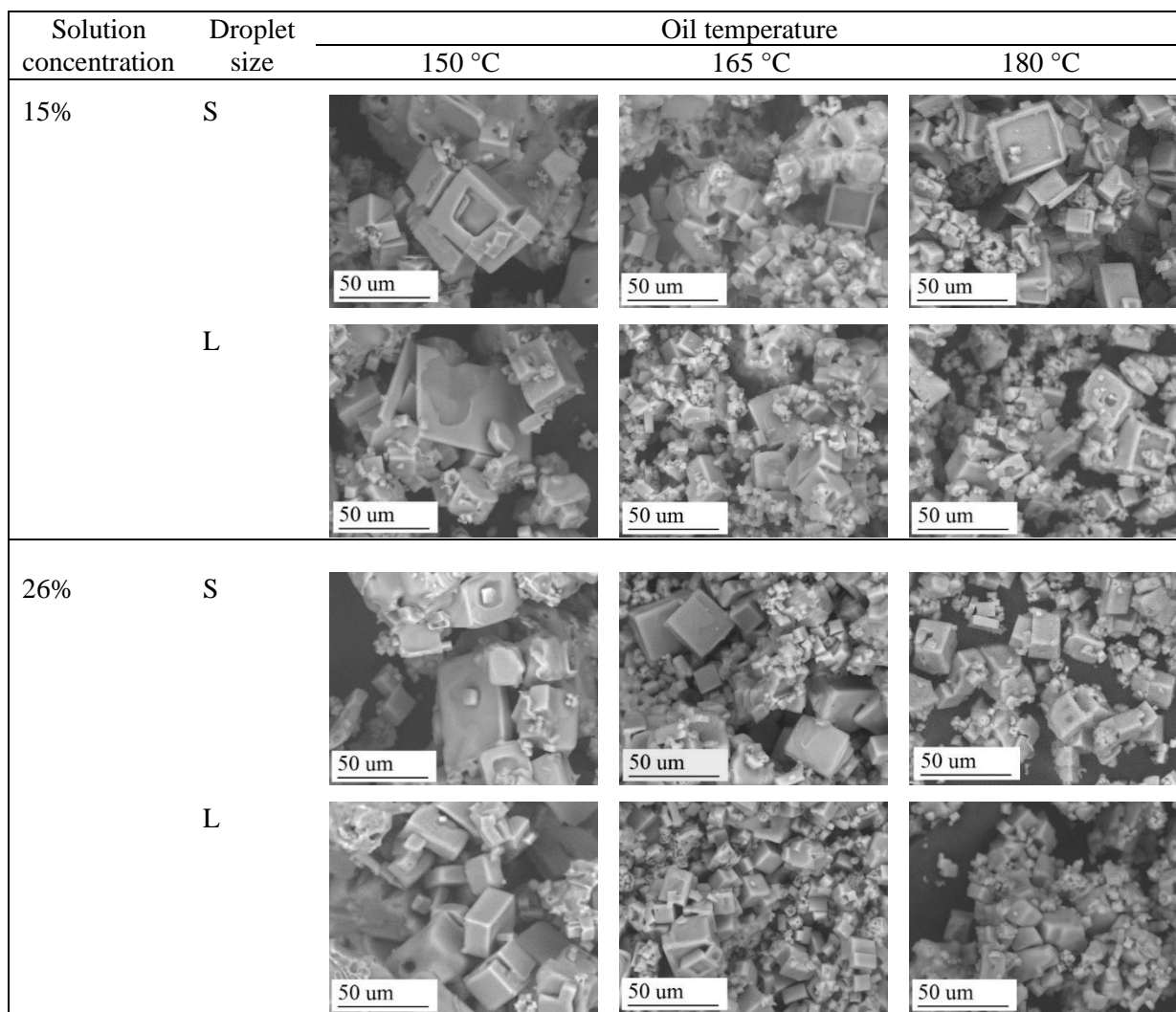


Figure 4.3. SEM images of microcrystals obtained by fast water evaporation from droplets of salt solutions as a function of oil temperature, salt concentration and droplet size (S, small; L, large).

A wide variation in size and shapes of microcrystals, from isometric cubes to cubes with imperfections like holes and surface rims is observed in Figure 4.3. This is not strange for fast crystallization as demonstrated by Kadota et al. (2007) and Lee, Ashokkumar & Kentish, (2014). Our results may suggest that concentrated solutions (26%) yield crystals with smoother surfaces than dilute solutions (15%).

Vázquez et al. (2015) obtained crystals with different morphologies and sizes from an evaporating single droplet. Droplets with volumes 5-20 μL , initial salt concentration 5-26%, and dried at a constant temperature of 45 °C, produced crystals that varied from cubic to agglomerated and dendritic shapes. At the center of the droplet, the crystals formed were cubic, but at the edges were dendritic, fan-shaped and spherulite-like. Since the evaporation rate was low, smaller cubic crystals were obtained from dilute solutions. In our case microcrystals were neither more cubic nor smaller when obtained from a dilute solution. Additionally, Vázquez et al. (2015) reported that crystallization in large droplets and at high salt concentrations gave agglomerated and bigger crystals. In our case small crystals and with high circularity (e.g, less agglomerated) were formed from large droplets.

In contrast to direct water evaporation into the surrounding air as occurs in salt crystallization from sea water, the use of hot oil implies migration of steam bubbles released from the droplets through the hot oil and into the atmosphere. In this sense, it is quite similar to what happens in deep-fat frying of foods (Bouchon & Aguilera, 2001). The temperature of the oil is a key factor which influences the rate of water evaporation (Mariscal & Bouchon, 2008). Moreover, a mixing effect may be produced

by the turbulence associated with the escaping bubbles, thus favoring heat transfer to the evaporating droplets.

Based on the size and shape of microcrystals, two conditions were selected to carry out the following analyses: thermogravimetry, X-ray diffraction, moisture content, and dissolution in artificial saliva. Salt crystallized at 150°C, 15 % initial salt concentration and from the small droplet size (17 μL) was selected because it had the highest D_{eq} and a low C . These microcrystals are hereafter called LC. Salt crystallized at 180°C, 26% of initial salt concentration and from a large droplet size (42 μL) was also selected because it resulted in a small D_{eq} and a higher C than the LC salt. These salt microcrystals are referred to hereafter as SC in the rest of the text.

4.3.2. Color of crystals

Color differences were found among samples (Table 4.2) The L^* parameter (luminosity) was significantly influenced by the volume of droplet, being lower when the droplet was small, meaning that these microcrystals were less white, or darker. The a^* parameter was significantly influenced by the temperature, i.e., a low temperature gave a lower a^* value or slightly less red. However, a^* values for microcrystals obtained under the different conditions of fast drying were similar to the a^* value of the original salt crystals. Lastly, the solution concentration and temperature had a significant impact on the b^* parameter, where the lower b^* value was found in the highest solution concentration. The temperature did not follow a clear tendency, the lower b^* value was found at 180°C, followed by 150°C and finally by 165°C. The b^* values of samples were significantly higher (more yellow) than b_0^* of original salt crystals.

Table 4.2. Color values of salt microcrystals.

Temperature (°C)	Solution (%)	Solution droplet	L	a	b	ΔE
150	15	Small	77.6 ± 0.4 ^b	0.8 ± 0.2 ^a	3.0 ± 0.3 ^{def}	3.5 ± 0.1 ^{abc}
		Large	81.0 ± 1.0 ^{cde}	0.9 ± 0.1 ^{ab}	3.6 ± 0.2 ^{ef}	4.3 ± 0.6 ^c
	26	Small	80.1 ± 1.6 ^{bcde}	1.1 ± 0.2 ^{abc}	1.4 ± 0.6 ^b	2.1 ± 1.1 ^a
		Large	79.7 ± 1.5 ^{bcd}	1.4 ± 0.1 ^{abc}	1.7 ± 0.3 ^{bc}	2.3 ± 0.2 ^{ab}
165	15	Small	77.7 ± 1.0 ^b	1.3 ± 0.4 ^{abc}	3.1 ± 0.4 ^{def}	3.6 ± 0.6 ^{abc}
		Large	79.0 ± 0.5 ^{bed}	1.2 ± 0.2 ^{abc}	2.2 ± 0.4 ^{bed}	2.4 ± 0.4 ^{ab}
	26	Small	72.9 ± 0.9 ^a	1.3 ± 0.7 ^{abc}	2.6 ± 0.5 ^{cde}	6.7 ± 0.7 ^d
		Large	78.1 ± 0.4 ^{bc}	1.8 ± 0.6 ^{bc}	3.7 ± 0.5 ^f	4.0 ± 0.5 ^{bc}
180	15	Small	70.7 ± 0.9 ^a	1.8 ± 0.3 ^c	1.3 ± 0.4 ^b	8.4 ± 0.9 ^d
		Large	78.6 ± 1.3 ^{bc}	1.6 ± 0.1 ^{abc}	2.7 ± 0.3 ^{cdef}	3.0 ± 0.4 ^{abc}
	26	Small	83.0 ± 0.2 ^e	0.9 ± 0.1 ^{abc}	1.8 ± 0.2 ^{bc}	4.5 ± 0.2 ^c
		Large	81.8 ± 0.8 ^{de}	1.4 ± 0.3 ^{abc}	1.4 ± 0.2 ^b	3.3 ± 0.6 ^{abc}
Original salt			78.9 ± 1.7 ^{bcd}	1.3 ± 0.1 ^{abc}	-0.1 ± 0.4 ^a	---

Different letters in a column are significantly different ($p < 0.05$) according to one way ANOVA and Tuckey's test.

As a consequence of the differences in L*, a* and b* values of the salt microcrystals with respect to the original salt crystals, differences in ΔE were found. These differences can be due to the fact that traces of olive oil could have remained occluded in the microcrystals (see below). The temperature and volume of droplet significantly influenced ΔE. The ΔE was higher at a higher temperature and at a lower volume of droplet. At higher temperatures and lower volume of droplet the salt microcrystals were agglomerated (low C), and these results could indicate that in agglomerated structures higher amount of oil could remain after acetone washing.

4.3.3. Thermogravimetric measurements, X-ray diffraction and moisture content of crystals of two selected fast drying conditions

Thermogravimetric measurements of microcrystals (Figure 4.4) showed that traces of occluded olive oil have remained in the structure. The weight loss between 350 and 500 °C was attributed to the degradation of the olive oil, as was confirmed with the thermogram of pure olive oil. Weight losses were $2.23 \pm 0.55\%$ for LC and $1.70 \pm 1.95\%$ for SC (Table 4.3). These values are not significantly different each other according to ANOVA ($p < 0.05$). It appears that there were no traces of the acetone used to remove the oil adhering to crystals. Acetone has a high vapor pressure at room temperature (20°C) and its boiling point is 56 °C (Sigma-Aldrich, 2015).

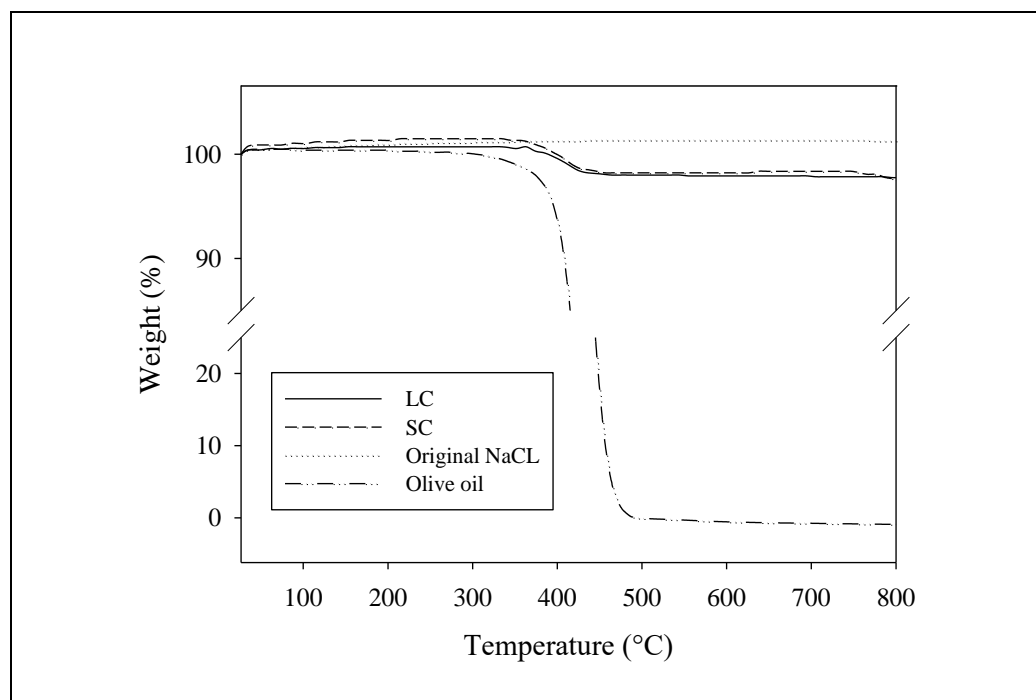


Figure 4.4. Thermograms from the TGA measurements of LC and SC microcrystals, original NaCl, and olive oil.

Table 4.3. Characteristics of LC and SC microcrystals, and original pure salt.

Sample	Remaining oil (%)	Crystallinity (%)	Moisture content (%)	K_1 (s ⁻¹)	$C_{90\%}$ (mS cm ⁻¹)	$DT_{90\%}$ (s)	C_{Max} (mS cm ⁻¹)	DT_{Max} (s)
LC	2.23 ± 0.55 ^a	90.82	2.37 ± 0.30 ^a	0.041 ± 0.009 ^b	29.01 ± 0.44 ^b	31 ± 13 ^a	32.24 ± 0.49 ^b	131 ± 27 ^{ab}
SC	1.70 ± 1.95 ^a	89.93	2.64 ± 0.06 ^a	0.040 ± 0.002 ^b	27.41 ± 0.00 ^a	29 ± 3 ^a	30.46 ± 0.00 ^a	118 ± 10 ^a
Original salt	-	98.82	3.01 ± 0.78 ^a	0.017 ± 0.002 ^a	28.81 ± 0.45 ^{ab}	144 ± 4 ^b	32.01 ± 0.51 ^{ab}	274 ± 56 ^b

Different letters in a column are significantly different ($p < 0.05$) according to one way ANOVA and Tuckey's test.

K_1 : Constant related to the dissolution velocity; C: Conductivity; DT: Dissolution time.

X-ray diffraction patterns of LC and SC microcrystals were 90.82% and 89.93%, respectively, and much lower than that of the original pure salt (98.82%, Table 4.3). The decrease in crystallinity could be attributed to the occluded oil and to the presence of some micro-amorphous regions or impurities. It has been shown that salt is a highly crystalline material, even when it is spray-dried. The crystallinity of spray-dried salt was higher at an inlet temperature of 210 °C than at 134°C (Langrish, 2009). It is well known that spray-dried organic materials are mostly amorphous because the water evaporation occurs within seconds or fractions of a second, giving not enough time to crystallize (Chiou, Langrish & Braham, 2008; Langrish, 2009). However, inorganic compounds have a fast rate of nucleation and crystal growth, and the crystallization rate becomes a function of operating conditions including temperature and supersaturation levels. This could explain to some extent why spray-dried organic materials are generally amorphous, but salt solutions become highly crystalline (Dombrowski, Litster, Wagner & He, 2007; Langrish 2009). Salt microcrystals obtained here showed only a slight difference (less than 1%) in degree of crystallinity among them.

It has been noted that a highly crystalline salt is quite stable. The presence of small quantities of amorphous material may lead under high humidity to recrystallization and formation of solid bridges between particles and caking (Aguilera, del Valle & Karel, 1995; Langrish, 2009; Tang, Chan, Tam, Gruyte & Chan, 2006). Conversely, amorphous particles dissolve faster than their crystallized counterparts (Hancock & Parks, 2000; Marabi et al., 2007). The moisture content of the microcrystals (Table 4.3) was similar to that of the original salt.

4.3.4. Salt dissolution in artificial saliva of crystals of two selected fast drying conditions

The dissolution curves of salt microcrystals had a similar behavior when compared to the dissolution curve of the original salt (Figure 4.5). Curves were fitted to a first order dissolution kinetic model (Costa & Sousa, 2001):

$$\ln (C_t / C_0) = K_I t \quad (4.4)$$

where C_t is the electrical conductivity (as a percentage of the initial electrical conductivity) at time t (s), C_0 is the initial electrical conductivity and K_I (s^{-1}) is a constant related to the dissolution velocity. The first order kinetics dissolution profile indicates that the release of ions is proportional to the amount of ions remaining in the non-dissolved crystals (Costa & Sousa, 2001).

K_I values (Table 4.3) were similar for both types of microcrystals and significantly higher than that of the original salt. The average D_{eq} of original crystals was 303 ± 83 μm ($n = 100$) and the size distribution together with the SEM image can be seen in Figure 4.6. Most probably, the high K_I values of microcrystals were due to the smaller sizes and the corresponding higher contact area of microcrystals with artificial saliva (Quilaqueo & Aguilera, 2015; Rama et al., 2013). Although the sizes of the two selected microcrystals were statistically different (Table 4.1), this was not sufficient to yield dissimilar K_I values.

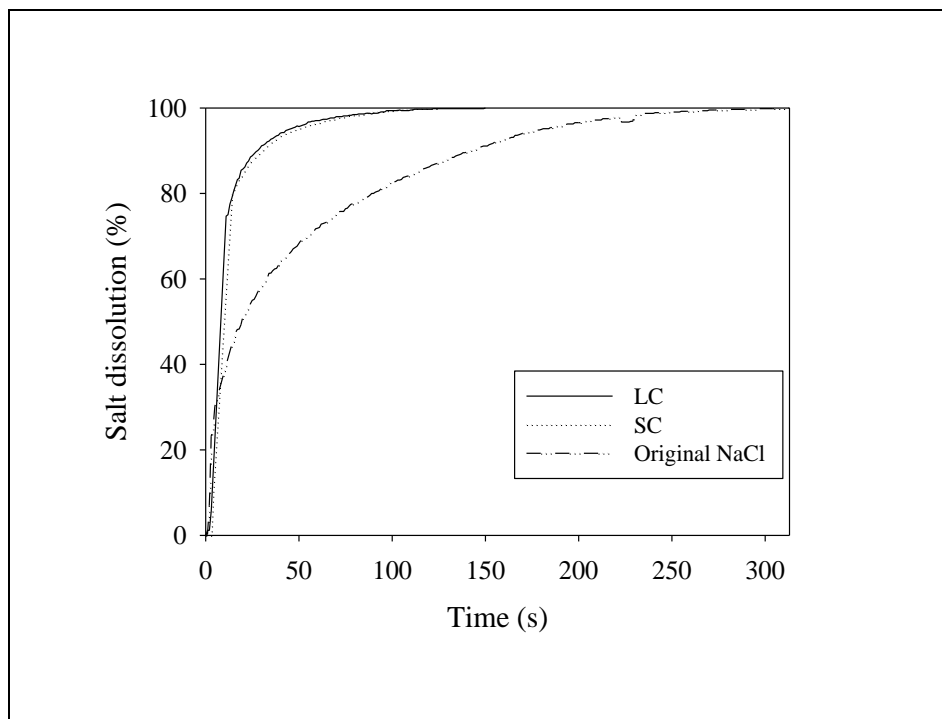


Figure 4.5. Dissolution in artificial saliva (20 °C) of LC and SC microcrystals and original salt.

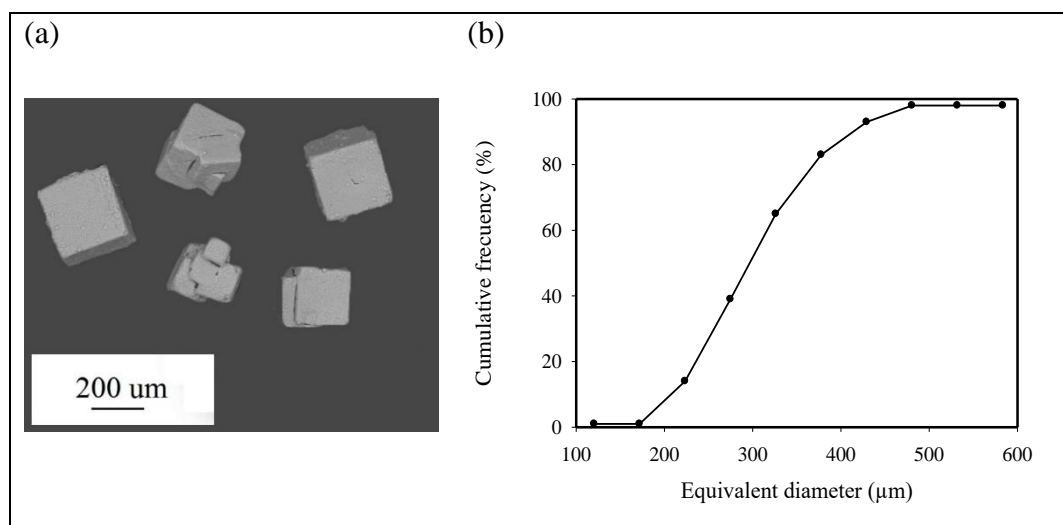


Figure 4.6. Original salt crystals: (a) SEM image, and (b) size distribution obtained from image analysis of 100 crystals.

Microcrystals dissolved much faster than the original salt crystals. Significant differences were found in dissolution time (DT) between the salts microcrystals and the original salt crystals. These differences changed over time being higher when the salt dissolution was around 90% ($C_{90\%}$). Table 4.3 exhibits that when 90% of salt was dissolved, the $DT_{90\%}$ of original crystals was around 5 times higher than that of microcrystals. At the end of dissolution DT_{Max} of original crystals was around 2 times higher than that of microcrystals.

The maximum conductivity (C_{Max}) of SC crystals was significantly smaller than LC crystals. Nevertheless, both values were similar to those of the original salt crystals. This indicates that the oil that remained in crystals (around 2% found by TGA) had no influence on conductivity.

The microcrystals obtained by fast water evaporation from droplets of salt solutions are a potential alternative for reducing sodium in surface-salted foods. The use of microsized salt crystals leading to an increase in the dissolution rate in saliva, makes the transfer of ions to salt receptors more efficient, and increases the saltiness perception of foods. It has been postulated that replacing regular salt (1500 μm of size) by microsized salt (from 1.5 to 15 μm of size) up to 50% of salt can be diminish in surface-salted foods as crackers (Moncada et al., 2015). Microsized salt can also be obtained by grinding of large salt particles, besides crystallization methods such as spray-drying and antisolvent crystallization (Langrish, 2009; Lee, Ashokkumar & Kentish, 2014). However, grinding of salt presents difficulties in obtaining particles with a narrow size distribution and uniform shape (e.g. from a grinding process cubic,

diamond and flaked crystals can be obtained) (Crowley & Zografi, 2002; Rama et al., 2013).

4.4. Conclusions

Salt crystal formation by fast water evaporation from droplets of NaCl solutions is an effective method of obtain microcrystals with mean sizes between 9 and 23 μm . The size of the microcrystals had a tendency to decrease with an increase of the oil bath temperature, initial solution concentration and droplet volume. The morphology of microcrystals was also a function of the process conditions. Circularity decreased with the increase of temperature, and with the decrease of the initial solution concentration and droplet volume.

Microcrystals with crystallinity of 90.82% (LC) and 89.93% (SC) were obtained and their crystallinity was lower than that of the original salt (98.82%). Traces of olive oil were detected in the microcrystals. Despite their variation in size, microcrystals did not exhibit differences among them in the dissolution rate in artificial saliva, which were more than double that of the original crystals.

The process reported here is a promising concept to design microcrystals for use mainly in surface-salted foods. However, the selected variables should be studied in a wider range of conditions and the possible effects of residual oil in microcrystals should also be investigated.

Acknowledgments

Author Quilaqueo acknowledges the financial support of a CONICYT doctoral fellowship (21110317).

References

- Aguilera, J.M., del Valle, J.M. & Karel, M. (1995). Caking phenomena in amorphous food powders. *Trends in Food Science & Technology*, 6, 149-155.
- Beck, M., Jekle, M. & Becker, T. (2012). Impact of sodium chloride on wheat flour dough for yeast-leavened products. II. Baking quality parameters and their relationship. *Journal of the Science of Food and Agriculture*, 92(2), 299-306.
- Bouchon, P. & Aguilera, J.M. (2001). Microstructural analysis of frying of potatoes. *Journal of International Food Science & Technology*, 36, 669-676.
- Braatz, R.D. (2002). Advanced control of crystallization processes. *Annual Reviews in Control*, 26, 87-99.
- Chen, J. (2012). Bolus formation and swallowing. In Chen, J., & Engelen, L. (Eds.), *Food oral processing: Fundamentals of eating and sensory perception* (pp. 139-155). Singapore: Wiley-Blackwell.
- Chiou, D., Langrish, T.A.G. & Braham, R. (2008). The effect of temperature on the crystallinity of lactose powders produced by spray drying. *Journal of Food Engineering*, 86, 288-293.
- Cho, H.Y., Kim, B., Chun, J.Y. & Choi, M.J. (2015). Effect of spray-drying process on physical properties of sodium chloride/maltodextrin complexes. *Powder Technology*, 277, 141-146.
- Costa, P. & Sousa, J.M. (2001). Modeling and comparison of dissolution profiles. *European Journal of Pharmaceutical Sciences*, 13, 123-133.
- Crowley, K.J. & Zografi, G. (2002). Cryogenic grinding of indomethacin polymorphs and solvates: Assessment of amorphous phase formation and amorphous phase physical stability. *Journal of Pharmaceutical Sciences*, 91, 492-507.
- Dombrowski, R.D., Litster, J.D., Wagner, N.J. & He, Y. (2007). Crystallization of alpha-lactose monohydrate in a drop-based microfluidic crystallizer. *Chemical Engineering Science*, 62, 4802-4810.
- El-Yafi, A.K.E. & El-Zein, H. (2015). Technical crystallization for application in pharmaceutical material engineering: Review article. *Asian Journal of Pharmaceutical Sciences*, 10, 283-291.
- Ferreira, A., Faria, N., Rocha, F., Feyer de Azevedo, S. & Lopes, A. (2005). Using image analysis to look into the effect of impurity concentration in NaCl crystallization. *Chemical Engineering Research and Design*, 83(A4), 331-338.

Ferreira, T. & Rasband, W. (2012). ImageJ User Guide. IJ 1.46r. <http://imagej.nih.gov/ij/docs/guide/>

Gupta, S., Pel, L., Steiger, M. & Kopinga, K. (2015). The effect of ferrocyanide ions on sodium chloride crystallization in salt mixtures. *Journal of Crystal Growth*, 410, 7-13.

Hancock, B. C. & Parks, M. 2000. What is the true solubility advantages for amorphous pharmaceuticals? *Pharmaceutical Research*, 17, 397-404.

He, F.J. (2012). Reducing salt intake to prevent hypertension and cardiovascular disease. *Revista Panamericana de Salud Pública*, 32(4), 293-300.

Kadota, K., Shirakawa, Y., Matsumoto, I. Shimosaka, A. & Hidaka, J. (2007). Formation and morphology of asymmetric NaCl particles precipitated at the liquid-liquid interface. *Advanced Powder Technology*, 18, 775-785.

Kim, Y.H.B., Liesse, C., Kemp, R. & Balan, P. (2015). Evaluation of combined effects of ageing period and freezing rate on quality attributes of beef loins. *Meat Science*, 110, 40-45.

Kloss, L., Meyer, J., Graeve, L. & Vetter, W. (2015). Sodium intake and its reduction by food reformulation in the European Union. A review. *Nutrition and Food Science Journal*, 1, 9-19.

Kuo, W. Y. & Lee, Y. (2014). Effect of food matrix on saltiness perception. Implications for sodium reduction. *Comprehensive Reviews in Food Science and Food Safety*, 13, 906-923.

Langrish, T.A.G. (2009). Assessing the relative tendency of different materials to crystallize in spray drying: A comparison between sodium chloride and lactose. *Journal of Food Engineering*, 91, 521-525.

Lee, J., Ashokkumar, M. & Kentish, S. (2014). Influence of mixing and ultrasound frequency on antisolvent crystallization of sodium chloride. *Ultrasonics Sonochemistry*, 21, 60-68.

Luna, M.P. & Aguilera, J.M. (2014). Kinetics of colour development of molten glucose, fructose and sucrose at high temperatures. *Food Biophysics*, 9, 61-68.

Marabi, A., Mayor, G., Raemy, A., Bauwens, I., Claude, J., Burbidge, A., Wallach, R. & Saguy, I. S. (2007). Solution calorimetry: A novel perspective into the dissolution process of food powders. *Food Research International*, 40, 1286-1298.

Mariscal, M. & Bouchon, P. (2008). Comparison between atmospheric and vacuum frying of apple slices. *Food Chemistry*, 107, 1561-1569.

Moncada, M., Astete, C., Sabliov, C., Olson, D., Boeneke, C. & Aryana, K.J. (2015). Nano spray-dried sodium chloride and its effects on the microbiological and sensory characteristics of surface-salted cheese crackers. *Journal of Dairy Science*, 98, 5946-5954.

Powles, J., Fahimi, S., Micha, R., Khatibzadeh, S., Shi, P., Ezzati, M., Engell, R., Lim, S., Danaei, G. & Mozaffarian, D. (2013). Global, regional and national sodium intakes in 1990 and 2010: a systematic analysis of 24 h urinary sodium excretion and dietary surveys worldwide. *British Medical Journal Open*, 3: e003733.

Quilaqueo, M. & Aguilera, J.M. (2015). Dissolution of NaCl crystals in artificial saliva and water by video-microscopy. *Food Research International*, 69, 373-380.

Quilaqueo, M., Duizer, L. & Aguilera, J.M. (2015). The morphology of salt crystals affects the perception of saltiness. *Food Research International*, 73, 675-681.

Rama, R., Chiu, N., Carvalho, M., Hewson, L., Hort, J. & Fisk, I. (2013). Impact of salt crystal size on in-mouth delivery of sodium and saltiness perception from snack foods. *Journal of Texture Studies*, 44, 338-345.

Rodríguez-Navarro, C. & Doehne, E. (1999). Salt weathering: influence of evaporation rate, supersaturation and crystallization pattern. *Earth Surface Processes and Landforms*, 24, 191-209.

Sigma-Aldrich Co. (2015). Chemistry. Solvent center. <http://www.sigmaaldrich.com/chemistry/solvents/acetone-center.html>

Tang, P., Chan, H.K., Tam, E., de Gruyter, N. & Chan, J. (2006). Preparation of NaCl powder suitable for inhalation. *Industrial & Engineering Chemistry Research*, 45, 4188-4192.

Tian, X. & Fisk, I. (2012). Salt release from potato crisps. *Food & Function*, 3, 376-380.

Vázquez, P., Thomachot-Schneider, C., Mouhoubi, K., Fronteau, G., Gommeaux, M., Benavente, D., Barbin, V. & Bodnar, J. (2015). Infrared thermography monitoring of the NaCl crystallisation process. *Infrared Physics & Technology*, 71, 198-207.

Vella, D., Marcone, M. & Duizer, L. M. (2012). Physical and sensory properties of regional sea salts. *Food Research International*, 45, 415-421.

WHO (2014). Salt reduction. Fact sheet N°393. World Health Organization (WHO). <http://www.who.int/mediacentre/factsheets/fs393/en/>

5. CONCLUSIONS AND FUTURE PROSPECTS

Strategies to reduce salt in foods are urgently needed but they should keep the sensory attributes and quality of products. This thesis is a contribution to this effort and some of the main conclusions are the following.

- Video-microscopy was instrumental to observe the dissolution in real time of salt crystals in water and artificial saliva. The analysis of images obtained by video-microscopy revealed that the dissolution profile of a single crystal depends on its morphology. Pyramidal, highly agglomerated and flat structures were fragmented during dissolution increasing their solubilization rate as a result of the increase of the surface area while cubic and slightly agglomerated crystals were not. The dissolution profile of pyramidal structures was well represented by a first order kinetics while that of cubic and agglomerated crystals followed a zero order kinetics. Amazingly, micro-CT revealed internal defects in salt crystals which may explain fragmentation during dissolution. The use of the micro-CT is recommended as a unique tool to characterize the internal structure of salt crystals in subsequent studies.
- The effect of viscosity of the dissolution media and its temperature depended on type of crystal. In cubic and slightly agglomerated crystals, the effect was negative, e.g., a higher viscosity resulted in a lower dissolution rate. The temperature had a positive effect on the dissolution rate of crystals, being faster at higher temperatures.

- As revealed by time-intensity analysis, the morphology of crystals influenced the saltiness perception, which in turn was positively correlated with the dissolution rate. Highly agglomerated, flat and pyramidal crystals had internal cavities and cracks, which facilitated crystal disintegration during dissolution, and had a higher maximum intensity of saltiness in time-intensity analysis which was detected at a shorter time compared to cubic and compact structures. This finding suggests that further work should be done on salt crystallization to control the shape and morphology of salt crystals.

- Microcrystals with average sizes between 9 and 23 μm were obtained by crystallization from droplets of salt solutions and fast water evaporation in hot oil. Smaller microcrystals were obtained at a high droplet volume and high initial concentration of salt solution. Although the effect of the temperature of the hot oil phase was not statistically significant, a clear tendency to decrease the microcrystal size with the increase of temperature was observed. The morphology of microcrystals could be controlled to a certain extent by adjusting the process variables (e.g., oil temperature, initial solution concentration, droplet volume, etc.). The microcrystals obtained contained traces of olive oil (about 2%) and their crystallinity was lower than that of the original salt crystals. Moreover, the dissolution rate of the microcrystals was over 2 times higher than that of the original crystals (average size 303 μm).

- The process reported above looks promising to design salt microcrystals for use in surface-salted foods. However, the selected variables should be studied in a wider range of conditions and the possible effects of residual oil in microcrystals should be investigated.

In perspective, future research should assess the effect of crystal microstructure on adhesion and subsequent delivery (considering the interaction between food matrix, saliva and crystals) in different surface salted foods.